EVALUATION OF MITRAL VALVE DIMENSIONS IN THE TERTIARY CARDIAC CENTRE OF KARACHI

DR MAHAIL KHAN

06-113222-002

BAHRIA UNIVERSITY ISLAMABAD

PAKISTAN

EVALUATION OF MITRAL VALVE DIMENSIONS IN THE TERTIARY CARDIAC CENTRE OF KARACHI

DR MAHAIL KHAN

(06-113222-002)

A thesis submitted in fulfillment of the
requirements for the award of the degree of
Master of Philosophy (Anatomy)

DEPARTMENT OF ANATOMY

BAHRIA UNIVERSITY HEALTH SCIENCES CAMPUS KARACHI

SEPTEMBER 2024

APPROVAL FOR EXAMINATION

Scholar's Name: Dr. Mahail Khan Registration No. 80421

Programme of Study: Anatomy- MPhil

Thesis Title: Evaluation Of Mitral Valve Dimensions In The Tertiary Cardiac Centre Of Karachi

It is to certify that the above scholar's thesis has been completed to my satisfaction and, to my belief, its standard is appropriate for submission for examination. I have also conducted plagiarism test of this thesis using HEC prescribed software and found similarity index 14% that is within the permissible limit set by the HEC for the MPhil degree thesis. I have also found the thesis in a format recognized by the BU for the MPhil thesis.

Principal Supervisor’s Signature: ____________________

Date: -08-2024

Name: Prof. Dr. Aisha Qamar

Senior Professor

Department of Anatomy

BUHSC

THESIS COMPLETION CERTIFICATE

Student's Name: Dr. Mahail Khan Registration No. 80421

Programme of Study: MPhil- Anatomy

Thesis Title: Evaluation Of Mitral Valve Dimensions In The Tertiary Cardiac Centre Of Karachi.

It is to certify that the above student's thesis has been completed to my satisfaction and to my belief. Its standard is appropriate for submission and evaluation. I have also conducted plagiarism test of this thesis using HEC prescribed software and found similarity index at 14% that is within the permissible limit set by HEC for the MPhil degree thesis. I have also found the thesis in a format recognized by the BU for the MPhil thesis.

Co-Supervisor's Seal & Signature: ___________________

Date: -08-2024

Name: Dr. Sabha Bhatti

Head of Cardiac Imaging, Professor of Cardiology

Department Cardiac Imaging, NICVD

AUTHOR’S DECLARATION

Dr. Mahail Khan hereby state that my MPhil thesis titled “Evaluation Of Mitral Valve Dimensions In The Tertiary Cardiac Centre Of Karachi” is my own work and has not been submitted previously by me for taking any degree from this university, Bahria University or anywhere else in the country/world.

At any time if my statement is found to be incorrect even after my graduation, the University has the right to withdraw/cancel my MPhil degree.

Name of scholar: Dr. Mahail Khan

Date: 06-08-2024

PLAGIARISM UNDERTAKING

I, solemnly declare that research work presented in the thesis titled "Evaluation Of Mitral Valve Dimensions In The Tertiary Cardiac Centre Of Karachi" is solely my research work with no significant contribution from any other person. Small contribution / help wherever taken has been duly acknowledged and that complete thesis has been written by me.

I understand the zero-tolerance policy of the HEC and Bahria University towards plagiarism. Therefore, I as an Author of the above titled thesis declare that no portion of my thesis has been plagiarized and any material used as reference is properly referred / cited.

I undertake that if I am found guilty of any formal plagiarism in the above titled thesis even after award of MPhil degree, the university reserves the right to withdraw / revoke my MPhil degree and that HEC and the University has the right to publish my name on the HEC / University website on which names of scholars are placed who submitted plagiarized thesis.

Scholar / Author's Sign: ________________

Name of Scholar: Dr. Mahail Khan

I would like to dedicate this thesis to my beloved parents and my loving husband

ACKNOWLEDGEMENT

ABSTRACT

Background: Current standards for assessing mitral valve dimensions are predominantly based on data from Western populations, which may not be applicable to diverse demographic settings. This study aims to establish normative data for mitral valve dimensions using Transthoracic 2D Echocardiography in the Pakistani population and to explore the variation of these dimensions with demographic variables such as age, gender, body surface area, and ethnicity and to assess the associations between mitral valve dimensions and left ventricle dimensions.

Methods: This cross-sectional study was conducted in the period of six months from March to August 2024, that constituted three hundred and eighty-five individuals who fulfilled the inclusion criteria coming to National Institute of Cardiovascular Diseases. Subject evaluation forms were used to note the measurements made by Transthoracic 2D Echocardiography. The mitral valve geometry was assessed based on parameters like age, gender, body surface area, ethnicity. The echocardiographic parameters included annular diameter (long axis and 4-chamber view), annular area, anterior leaflet length, anterior leaflet thickness, posterior leaflet length, posterior leaflet thickness, intercommissural distance, C-septal distance, interpapillary distance, left ventricle's systolic and diastolic dimensions, septal thickness and posterior wall thickness. Statistical analyses were performed using the Shapiro-Wilk test, Mann-Whitney U tests, Kruskal-Wallis and Spearman's correlation coefficient test.

Results: The echocardiographic measurements reveal significant variations across several factors. Males had a significantly longer posterior mitral valve leaflet compared to females and c-septal distance was found to be larger in males than in females. Similarly, both systolic and diastolic dimensions of the left ventricle were significantly larger in males compared to females. This also extended to left ventricular wall thickness, where males had thicker walls. The diastolic dimension of the left ventricle increased with advancing age and was found to be largest in individuals aged between 46-65 years and then decreased in individuals aged over 65 years. Both the septal thickness and posterior wall thickness increased with age, the walls of the left ventricles were thickest in individuals older than 65 years. Ethnic variations were significant in annular diameter measured in 4-chamber view and posterior wall thickness. Specifically, the Hindku and then Balochi ethnic groups show the largest annular diameter, followed by Pashtun, Punjabi, and Sindhi, while the Urdu-speaking group had the smallest annular diameter. The posterior wall of the left ventricle was significantly thicker in Punjabi, followed by Hindku and Balochi, Pashtun and Urdu-speaking had almost similar posterior wall thickness while Sindhi had the thinnest posterior wall. A family history of cardiac diseases was associated with a significantly larger annular diameter and area along with larger systolic and diastolic dimensions of the left ventricle in individuals. Smokers exhibited larger C-septal distances and larger systolic and diastolic left ventricular dimensions compared to non-smokers. Additionally, the majority of mitral valve parameters (annular diameter, area, leaflet lengths, and interpapillary distances) and left ventricular dimensions (systolic and diastolic) showed significant positive correlations with the body surface area, indicating that as the body surface area increases, these parameters also tend to increase. Importantly, these variations in mitral valve geometry were correlated with changes in left ventricular dimensions and wall thicknesses, suggesting that alterations in mitral valve structure could impact left ventricle structure.

Conclusion: In conclusion, this study highlights significant variations in echocardiographic measurements influenced by gender, age, ethnicity, family history of cardiac diseases, smoking status, and body surface area. Males exhibited longer posterior mitral valve leaflets and larger C-septal distances, alongside greater left ventricular dimensions and wall thicknesses compared to females. Age-related changes revealed that the diastolic dimension of the left ventricle peaked in individuals aged 46-65 years before decreasing in those over 65, while both septal and posterior wall thickness increased with age. Ethnic differences were notable, with the Hindku and Balochi groups showing the largest annular diameters and Punjabi individuals having the thickest posterior walls. A family history of cardiac diseases correlated with larger mitral valve annular diameter and area and left ventricular dimensions. Additionally, smokers demonstrated larger C-septal distances and left ventricular dimensions compared to non-smokers. The study found significant positive correlations between most mitral valve parameters and left ventricular dimensions with body surface area.

Keywords: Mitral valve dimensions, mitral valve variations, Transthoracic 2D Echocardiography, demographic variations, Pakistani population, personalized treatment

TABLE OF CONTENTS

CHAPTER	TITLE	PAGE
	APPROVAL FOR EXAMINATION	i
	THESIS COMPLETION CERTIFICATE	ii
	AUTHOR'S DECLARATION	iii
	PLAGIARISM UNDERTAKING	iv
	DEDICATION	v
	ACKNOWLEDGEMENT	vi
	ABSTRACT	vii
	TABLE OF CONTENTS	viii
	LIST OF TABLES	ix
	LIST OF FIGURES	x
	LIST OF ABBREVIATIONS	xi
	LIST OF ANNEXURES	xii
1	**INTRODUCTION**	1
	1.1 Background	1
	1.1.1 Heart Anatomy	1
	1.1.2 Left Ventricle Anatomy	12
	1.1.3 Mitral Valve Anatomy	15
	1.1.3.1 Mitral Valve Annulus	19
	1.1.3.2 Mitral Valve Commissures	24
	1.1.3.3 Mitral Valve Leaflets	24
	1.1.3.4 Subvalvular Apparatus	28
	1.1.4 Mitral Valve Diseases	32

	1.2 Research Gap	40
	1.2.1 Theoretical Gap	40
	1.2.2 Contextual Gap	40
	1.2.3 Methodological Gap	40
	1.3 Problem Statement	41
	1.4 Hypothesis	41
	1.5 Objectives of study	42
	1.6 Significance of study	42
2	**LITERATURE REVIEW**	44
	Operational definitions	57
3	**METHODOLOGY**	61
	3.1 Study Design	61
	3.2 Subjects	61
	3.3 Setting	62
	3.4 Inclusion criteria	62
	3.5 Exclusion criteria	62
	3.6 Duration of study	62
	3.7 Sample size calculation	63
	3.8 Sampling technique	63
	3.9 Human subjects and consent	63
	3.10 Materials	64
	3.11 Parameters of study	66
	3.12 Protocol of study	81
	3.13 Algorithm of study	82
	3.14 Statistical Analysis	83
4	**RESULTS**	84
5	**DISCUSSION**	122

5.1 Sequence of discussion experiment/hypothesis wise 124

5.2 Implications of the study 131

5.2.1 Theoretical implications 131

5.2.2 Practical implications 132

5.2.3 Policy implications 132

5.3 Limitations and strengths of study 133

5.4 Recommendations 134

5.5 Conclusion 135

REFERENCES 136

ANNEXURES 153

LIST OF TABLES

TABLE NO.	TITLE	PAGE
4.1	Tests of Normality	104
4.2	Measurement of Echocardiographic Parameter (mm) in the Study Population	105
4.3	Measurement of Body Surface Area (m^2) in the Study Population	106
4.4	Measurement of Body Surface Area (m^2) (Based on Gender)	106
4.5	Measurement of Echocardiographic Parameter (mm) (Based on Gender)	107
4.6	Measurement of Echocardiographic Parameter (mm) (Based on Age in Years)	108
4.7	Measurement of Echocardiographic Parameter (mm) (Based on Ethnicity)	110
4.8	Measurement of Echocardiographic Parameter (mm) (Based on Family Cardiac History)	113
4.9	Measurement of Echocardiographic Parameter (mm) (Based on Smoking)	114
4.10	Measurement of Echocardiographic Parameter (mm) (Based on Co-morbidities)	115
4.11	Correlation between BSA with Echocardiographic Parameters	120
4.12	Correlation between Mitral Valve Parameters with Left Ventricular Dimensions	121

LIST OF FIGURES

FIGURE NO.	TITLE	PAGE
1.1	Location of the heart in the middle of mediastinum between the lungs	4
1.2	Illustration demonstrating the oblique axis (acute angle) of the heart with respect to body's long axis	5
1.3	Borders and surfaces of the heart	6
1.4	Layers of the heart along with serous and parietal pericardium and pericardial cavity between them	8
1.5	Graphic image of heart's cross-section in the sagittal plane showing four cardiac chambers along with the flow of the blood through these chambers into the pulmonary and systemic circulation	8
1.6	Cardiac conduction system of the heart and its association with cardiac chambers	11
1.7	Lateral view of the heart showcasing the left ventricle and its boundaries, including the base, apex, and free wall	14
1.8	Illustration showing mitral valve complex	17
1.9	Diagram showing anterolateral and posteromedial commissures and also the relation between circumflex coronary artery (posterolateral) and coronary sinus (posteromedial) with posterior mitral annulus	18
1.10	Anatomical structure of mitral valve	20
1.11	A 3-D transesophageal echocardiogram of mitral valve in a healthy adult	22
1.12	Illustration showing the non-planar saddle shape of the mitral annulus along with the anterior-posterior diameter,	23

	anterolateral-posteromedial diameter, and intercommissural diameter	
1.13	Regions of mitral valve leaflets: clear (atrial zone) and rough zone (coaptation zone)	27
1.14	Illustration showing the attachment of chordae tendineae to papillary muscles and their types	30
1.15	A 2 – D echocardiography in a healthy adult	31
1.16	Echocardiographic images showing valve pathology	36
1.17	Image showing transthoracic echocardiographic windows: parasternal long-axis, parasternal short-axis, apical and subcostal	39
3.1	Height and weight scale from the current study	65
3.2	Echocardiographic machine from the current study	65
3.3	Echocardiography done in lateral left decubitus position	68
3.4	(A) Transducer position for parasternal long-axis (B) Echocardiographic image for parasternal long-axis view	69
3.5	Echocardiographic image measuring annular diameter in parasternal long-axis view from the current study	70
3.6	(A) Transducer position for 4 – chamber view (B) Echocardiographic image for 4 – chamber view	71
3.7	Echocardiographic image measuring annular diameter in 4 – chamber view from the current study	72
3.8	Echocardiographic image of PLAX view measuring (A) anterior (orange arrow) and posterior (blue arrow) leaflet length (B) Anterior (orange arrow) and posterior (blue arrow) leaflet thickness from the current study	74
3.9	(A) Transducer position for parasternal short-axis view (B) Echocardiographic image for short-axis view at the level of the mitral valve (C) Echocardiographic image for parasternal short-axis view at the level of the papillary	76

	muscles	
3.10	Echocardiographic image measuring intercommissural distance in parasternal short-axis view from the current study	77
3.11	Echocardiographic image measuring c-septal distance in parasternal long-axis view from the current study	77
3.12	Echocardiographic image measuring interpapillary distance in parasternal short-axis view from the current study	78
3.13	Echocardiographic image measuring systolic dimension of the left ventricle in the parasternal long-axis view from the current study	78
3.14	Echocardiographic image measuring interventricular septum (orange arrow), diastolic dimension of the left ventricle (blue arrow) and posterior wall thickness of the left ventricle (yellow arrow) in the parasternal long-axis view from the current study	80
4.1	Gender distribution of participants within the study population	100
4.2	Distribution of study participants into age groups (in years)	100
4.3	Gender distribution of participants within each age group (in years)	101
4.4	Distribution of study participants in ethnicities	101
4.5	Distribution of study participants based on family cardiac history	102
4.6	Gender distribution of participants based on smoking	102
4.7	Distribution of study participants based on co-morbidities	103

LIST OF ABBREVIATIONS

g	-	Grams
cc	-	Cubic centimeter
SA	-	Sinoatrial
AV	-	Atrioventricular
MV	-	Mitral Valve
LVOT	-	Left Ventricle Outflow Tract
T-T	-	Trigone-to-trigone
AMVL	-	Anterior Mitral Valve Leaflet
PMVL	-	Posterior Mitral Valve Leaflet
cm	-	Centimeter
mm	-	Millimeter
LA	-	Left Atrium
LV	-	Left Ventricle
AL	-	Anterior Leaflet
PL	-	Posterior Leaflet
PM	-	Papillary Muscle
PMPM	-	Posteromedial Papillary Muscles
ALPM	-	Anterolateral Papillary Muscles
VHD	-	Valvular Heart Disease
RHD	-	Rheumatic Heart Disease
MR	-	Mitral Regurgitation
MVP	-	Mitral Valve Prolapse
TTE	-	Transthoracic Echocardiography
TEE	-	Transesophageal Echocardiography
CMR	-	Cardiac Magnetic Resonance
CCT	-	Cardiac Computed Tomography
2D	-	Two-Dimensional
3D	-	Three-Dimensional
BMI	-	Body Mass Index

LAVC	-	Left Atrioventricular Valve Complex
NPA	-	Non-Planar Angle
TA	-	Tricuspid Annulus
MA	-	Mitral Annulus
MVA	-	Mitral Valve Annulus
TVA	-	Tricuspid Valve Annulus
AP	-	Anteroposterior
ECG	-	Electrocardiogram
SL	-	Septal-to-Lateral
LAV	-	Left Atrial End-Systolic Volume
LVED	-	Left Ventricular End-Systolic Volume
CT	-	Computed Tomography
TMVI	-	Transcatheter Mitral Valve Intervention
FMR	-	Functional Mitral Regurgitation
IC	-	Intercommissural
ARF	-	Acute Rheumatic Fever
MHz	-	Megahertz
IQR	-	Interquartile Range
LVEDD	-	Left Ventricular End-Diastolic Dimension
LVESD	-	Left Ventricular End-Systolic Dimension
IVSd	-	Septum Thickness at End-Diastole
IVSs	-	Septum Thickness at End-Systole
LVPWs	-	Posterior Wall Thickness at End-systole
USA	-	United States of America
UK	-	Unite Kingdom
BSA	-	Body Surface Area
SPSS	-	Statistical Package for Social Sciences
PLAX	-	Parasternal Long Axis
PSAX	-	Parasternal Short Axis
ALC	-	Anterolateral Commissure
PMC	-	Posteromedial Commissure
TB	-	Tuberculosis
IHD	-	Ischemic Heart Disease

ASD	-	Atrial Septal Defect
SD	-	Standard Deviation

LIST OF ANNEXURES

ANNEXURES	TITLE	PAGE
A	FRC Approval Letter	154
B	IRB Approval Letter	155
C	Subject Consent Form – English	156
D	Subject Consent Form – Urdu	158
E	Subject Evaluation Form	160
F	Hospital IRB Approval Letter	161
G	Turnitin Plagiarism Check Report	162

CHAPTER 1

INTRODUCTION

1.1 BACKGROUND:

1.1.1 Heart Anatomy:

Over decades, the gross anatomy of the human heart has progressively come to light. Deep diving into the structure of the heart, many known figures in history like Hippocrates, Galen, and Leonardo da Vinci along with artists, anatomists, and Philosophers have all made contributions to the discovery of the complex structure of the heart (Robert et al., 2019).

Many studies on the heart's function, characteristics, and anatomy have been conducted substantially since 3500 B.C. Even though their explanations were profoundly imbued with religious beliefs, the early Greek and Egyptian scientists managed to attain a basic understanding of the heart. Hippocrates and fellow scholars developed the scientific understanding of the circulatory system during the Hippocratic era, shifting from non-secular interpretations. The post-Hippocratic age featured an advancement in the description of the location, composition, and operation of the heart. Considerable progress was made during the Alexandrian, Roman, Medieval Islamic, and European eras, each contributing pivotal insights into cardiac anatomy. Further, researchers devoted their attention to the heart's connection with the lungs after they established its structure and function which led to the discovery of pulmonary circulation, accompanied by the identification of the conductive system of the heart with its innervation (Loukas et al., 2016; Robert et. al, 2019)

The human body's heart has a unique feature apart from other organs like the stomach (the cells in the heart are not rapidly repaired and divided). It is a pump made of muscles with independent electrical activity which is under the influence of central innervation and pumps blood every minute which is about 4 to 6 liters through the arteries, arterioles, and capillaries and returning to the heart employing veins and venules, thus forming a complex network between the vessels. The human tissue and major organs receive nutrients through this pumped blood that delivers oxygen and removes carbon dioxide and metabolic waste products. In a living heart, the typical weight of the heart is approximately 225 g for females and 310 g for males and it is about the size of a human's fist with dimensions of 6 cm in depth, 9 cm in width, and 12 cm in length (Bakose et al., 2023). The complex, three-dimensional, and spiral structure of the human heart does not precisely align with the planes of the human body. Conventionally used anatomical terms for the heart are constructed mainly based on the axial rotation of the cardiovascular tube during the early embryonic period. Further, it was difficult to comprehend the heart's vivo and surface anatomy when studies on isolated or dissected hearts outside the body were done. To dispel these misapprehensions, it is beneficial to visualize the heart's position in the chest as a contorted pyramid, with the apex pointing in a forward direction and to the left while the base faces backward. Moreover, this pyramid has some flat surfaces, while some are convex and have borders between them which are poorly defined. Thus, it is challenging to have precise descriptions of these surfaces and borders (Standring, 2021).

The hollow, asymmetrical cone-shaped, fibromuscular heart is positioned in the center of the mediastinum between the pleural sacs of both the right and left sides (Figure 1.1) It has a long axis that is oblique and encompasses the heart from front to back, that is, from the left mid-clavicular line to the mid-scapular line respectively. About one-third of the heart is located on the right side of the body's sagittal plane, while the remaining two-thirds are situated on the left (Figure 1.2). The heart can be described as having different borders and surfaces. It has a sternocostal surface and a diaphragmatic surface, forming the anterior and inferior surfaces of the heart respectively. Furthermore, it also has a left surface known as an ‘obtuse’ or left border, along with a rounded right border and inferior border also known as an ‘acute’ border. An acute border is formed where there is an intersection between the anterior and diaphragmatic surfaces (Figure 1.3) (Mahadevan, 2018).

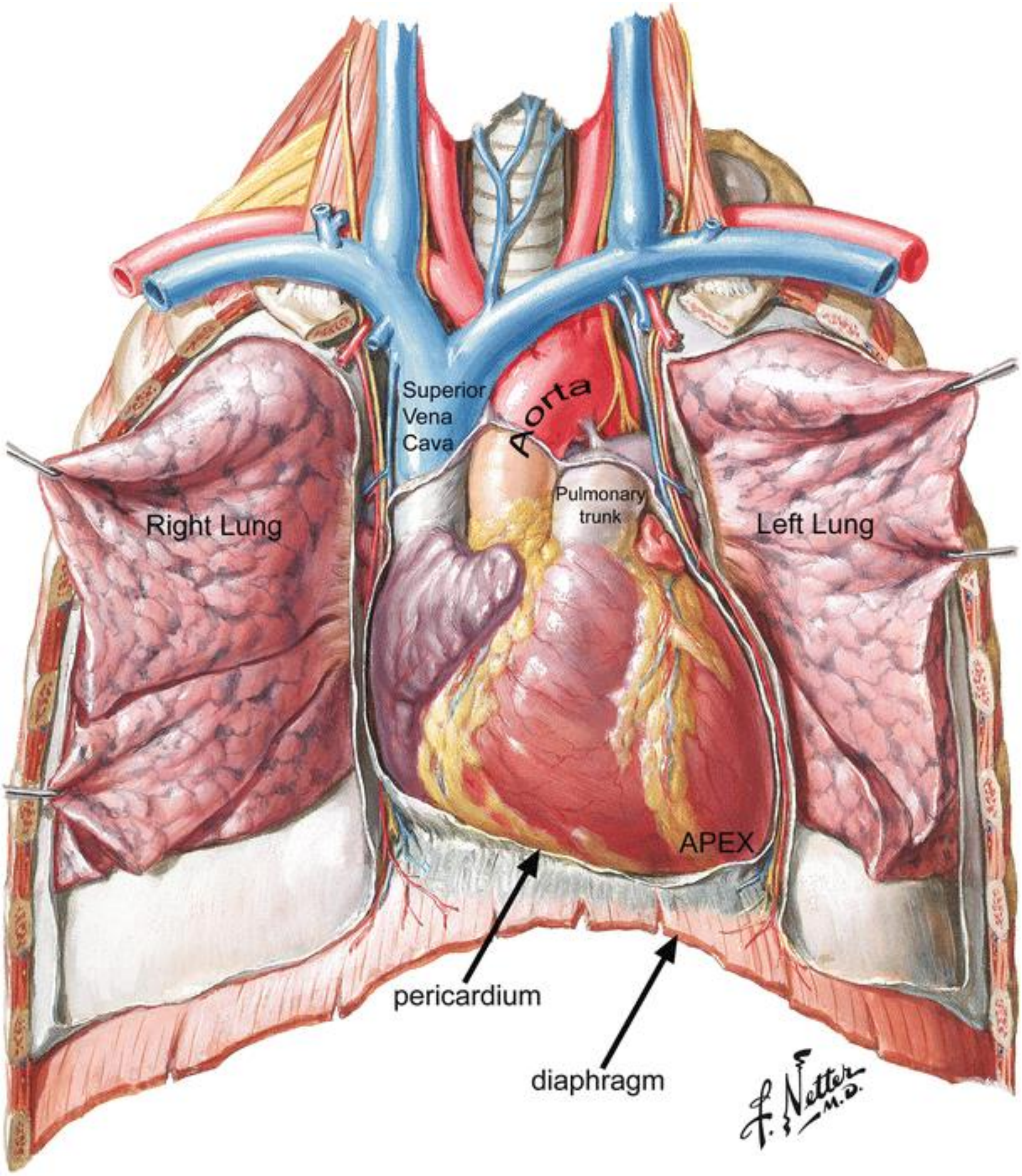

Figure 1.1: Location of the heart in the middle of the mediastinum between the lungs (Netter, 2022; 8th Edition)

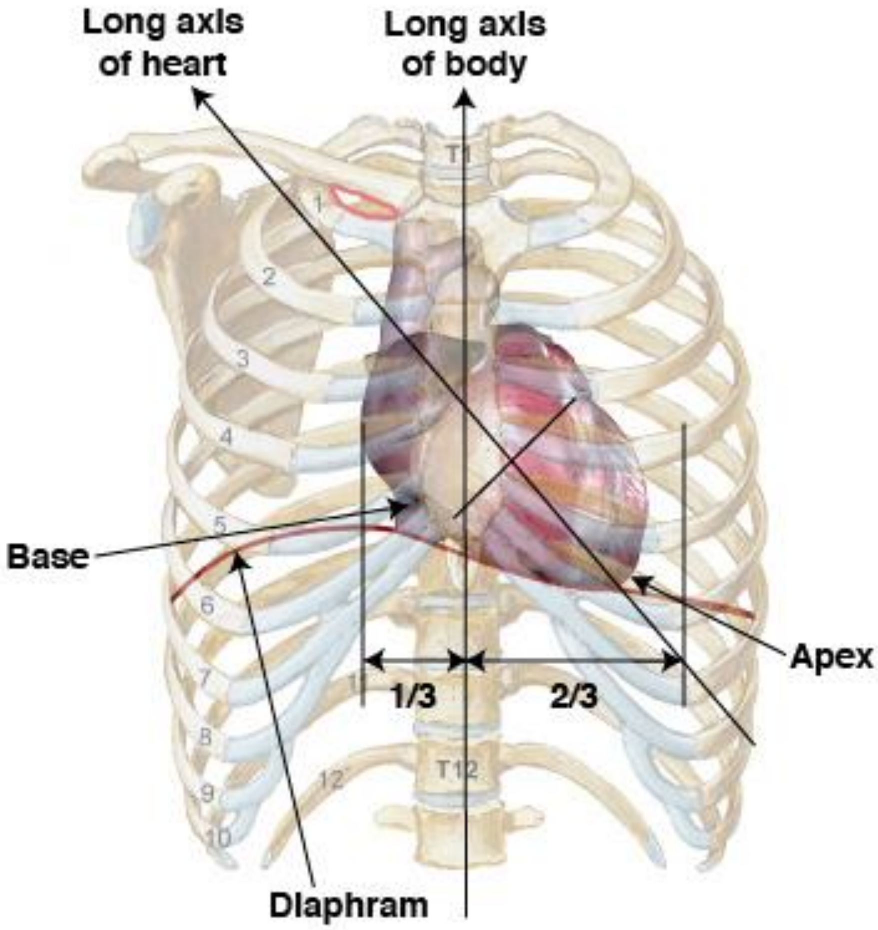

Figure 1.2: Illustration demonstrating the oblique long axis (acute angle) of the heart with respect to the body's long axis. Observe that in the thoracic cage two-thirds of the heart is placed left to the midline and one-third towards the right while resting on the diaphragm. The heart extends from the 2nd to the 5th intercostal cartilage with the apex pointing towards the left present in the 5th intercostal space in the midclavicular line (Iaizzo et al., 2012).

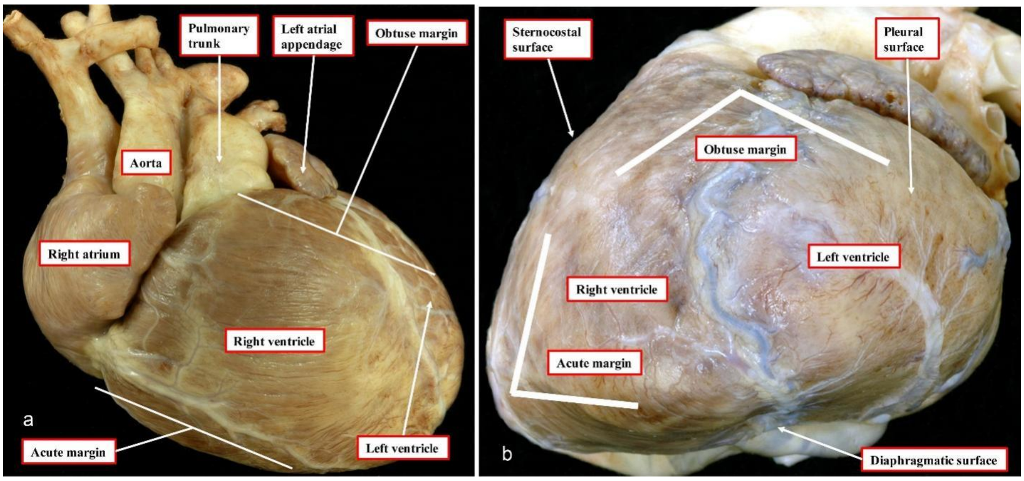

Figure 1.3: Borders and surfaces of the heart. (a) anterior view in anatomical position, (b) view from the cardiac apex (Spicer, Mill, and Anderson, 2023)

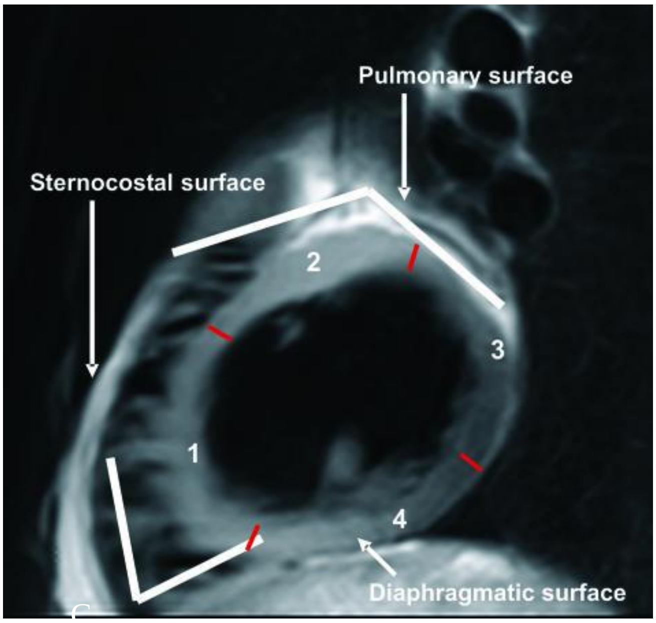

Figure 1.3 (c): Cardiac radiograph in short axis view of a section of left ventricle showing acute angle between sternocostal and diaphragmatic surfaces and obtuse angle between sternocostal and pulmonary surfaces. Red lines show the division of the left ventricle into segments (Anderson, Razavi, and Taylor, 2004).

The heart is sheathed by a pericardium (tough membrane) or enclosed in a pericardial sac, situated within the distinct space called a pericardial cavity inside the mediastinum (Soliyeva, 2022). Approximately 10 to 20cc pericardial fluid is present between two layers of the pericardium that serve as a shock absorber (Bakose, et al., 2023). Inside the pericardium, the heart has the thick striated muscular layer known as the myocardium, and then the innermost layer that lines the cardiac chambers is known as the endocardium while the epicardium is a part of the pericardium that forms the outermost protective layer of the heart (Figure 1.4) (Tran, Weber and Lopez, 2019). The anterior surface of the human heart is sited posterior to the sternum and costal cartilage, which extends from the second to the fifth intercostal space of the left side (Figure 1.2) (Bakose, et al., 2023). The vertebral bodies are close to the heart's dorsal surface and the upper surface, labeled as the base to which the aorta and pulmonary trunk, major arteries, superior and inferior venae cavae, and major veins of the heart are connected. The base is situated at the same level as the third costal cartilage while the apex, where the maximal pulse of the heart is felt is positioned to the most inferior and lateral part of the heart just to the left of the sternum in the midclavicular line at 5^{th} intercostal space between 4^{th} and 5^{th} ribs (Figure 1.2) (Bakose, et al., 2023; Soliyeva, 2022).

The intricate structure of the human heart is four-chambered which are distinct both functionally and morphologically comprised of two superior and two inferior chambers, known as atria and ventricles, respectively (Litviňuková et al., 2020; Tortora and Derrickson, 2018). The upper paired atria receive blood through the veins that bring back the blood from the entire body and the lungs to the heart while the lower paired ventricles eject blood through arteries to the lungs and different parts of the human body (Tortora and Derrickson, 2018). Interatrial and interventricular septa split the chambers of the heart and have valves between these chambers and their outlets, called atrioventricular and ventricular-arterial valves, respectively, that permit the unidirectional flow of the blood (Figure 1.5) (Litviňuková et al., 2020)

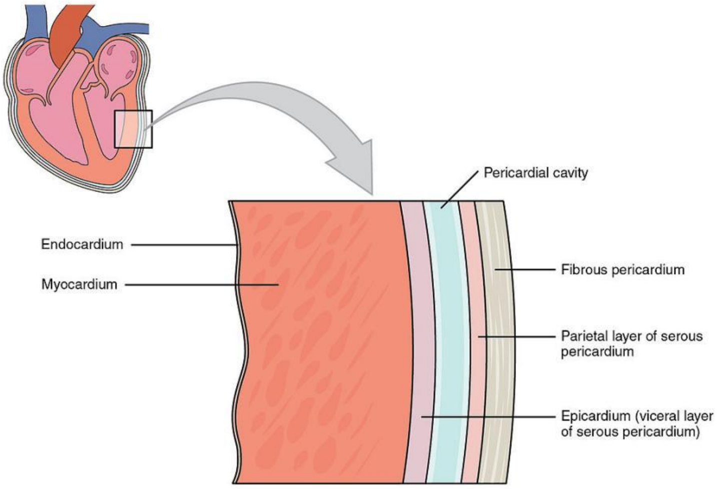

Figure 1.4: Layers of the heart along with serous and parietal pericardium and pericardial cavity between them (Soliyeva, 2022).

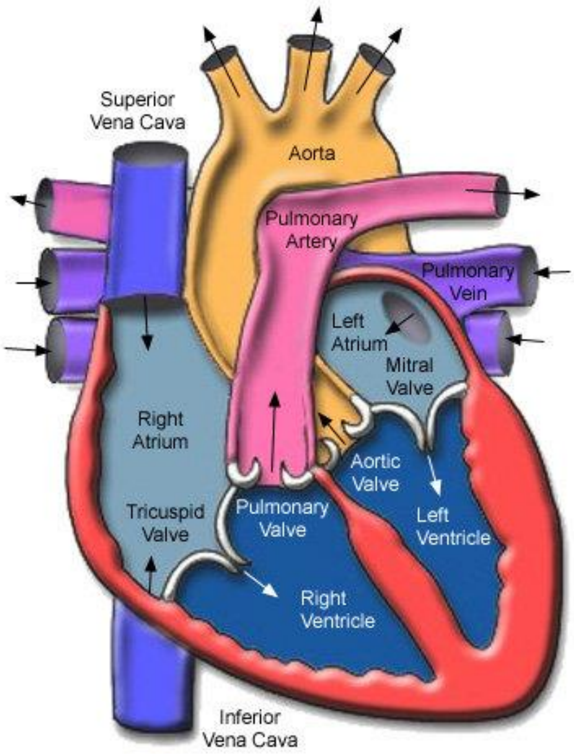

Figure 1.5: Graphic image of the heart's cross-section in the sagittal plane showing four cardiac chambers along with the flow of the blood through these chambers into the pulmonary and systemic circulation (Hammer, 2009)

The arrangement of the heart's chambers and the pressure difference between these chambers control the effectiveness with which the heart pumps blood throughout the body. Essentially, there are two integrated circuits connected to blood flow in the heart. First blood from the entire body returns to the right atrium guided through the superior or inferior vena cava, and then it is directed into the right ventricle through the tricuspid valve. During systole (period of muscular contraction of the heart chamber), the tricuspid valve closes, allowing the pulmonic valve to direct blood flow to the pulmonary circulation. Following pulmonary oxygenation, blood flows into the left atrium, where it transits through the mitral valve and empties into the left ventricle. Eventually, the blood enters the systemic circulation by way of the aortic valve as a result of high-pressured ventricular contraction (Rehman, Nassereddin and Rehman, 2023).

The system that regulates the heart's pumping and contractions of heart chambers, known as the electrical conduction system of the heart, follows electrical impulses generated throughout the framework of the heart due to the muscular contractions. The electrical impulses are generated first at the sinus node or SA node (also known as a primary pacemaker) placed at the intersection between the superior vena cava and the right atrium at a rate of about 70 beats per minute. This impulse is then transmitted by way of Bachmann's bundle to the left atrium and then to the atrioventricular node or AV node via the striated branched involuntary cardiac muscles. The atrioventricular node is sited in the triangular area, a triangle of Koch (area enclosed by coronary sinus ostium's lip, the tendon of Todaro, and the tricuspid valve). After receiving the electrical signals, there is a minor postponement before it passes to the bundle of His from the atrioventricular node. This postponement is vital because before the electrical signal causes ventricular contractions, atria copiously empty blood into the ventricles (Figure 1.6) (Rehman and Rehman, 2023; Ripa et al., 2023).

The complex and detailed anatomy of the heart necessitates its meticulous coordination to guarantee contraction and relaxation in each chamber which is synchronized amidst the heart's varied cell population. The His-Purkinje system (bundle of His splits into two branches, right and left, that further give out several branches to form Purkinje fibers), assists swift electrical impulse transmission throughout the right and left ventricles, leading to synchronized contraction and thus providing evidence of this particular orchestration of the heart that assures competent cardiac pumping (Litviňuková et al., 2020; Rehman et al., 2023).

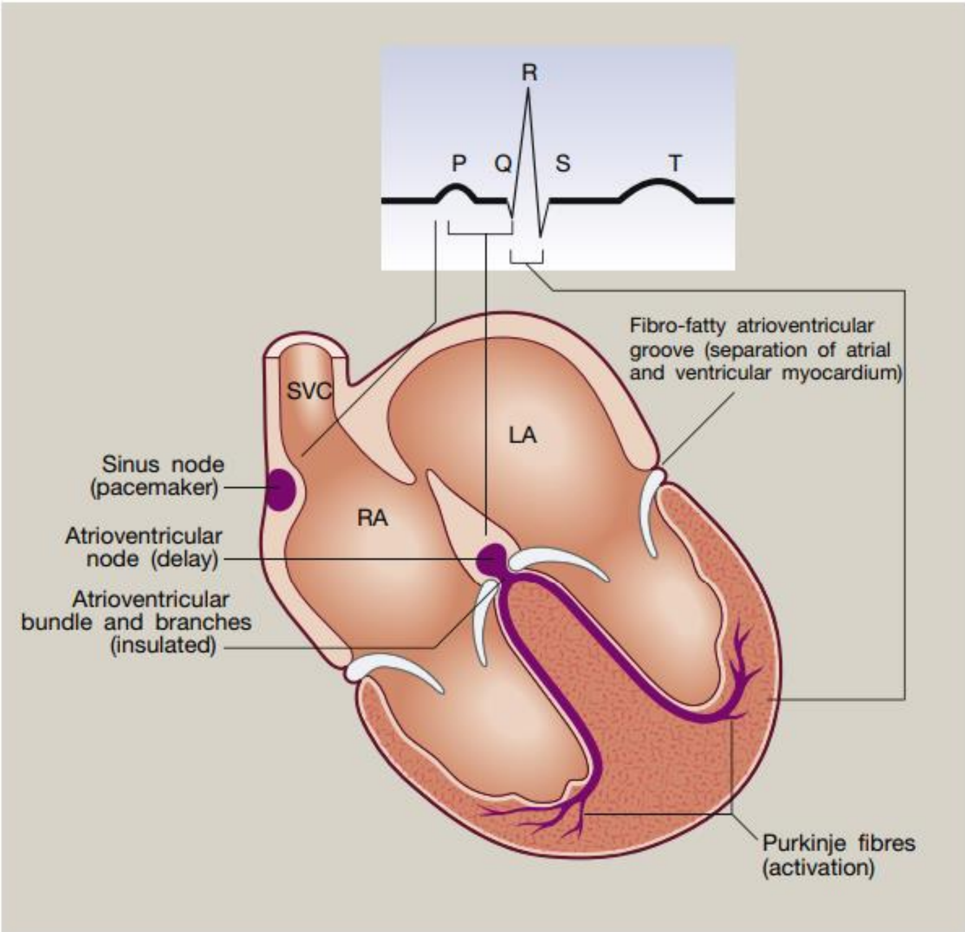

Figure 1.6: Cardiac conduction system of the heart and its association with cardiac chambers (Mahadevan, 2018).

1.1.2 Left Ventricle:

For ages, researchers have meticulously examined the left ventricle. Hippocratic doctors and researchers defined it as having thick walls having the most atypical interior gross structure when compared to the right ventricle. These findings led to the theory that the left ventricle was where heat was produced and where the "pure air of life" was confined (Loukas et al., 2016).

The cone-shaped left ventricle is wide-ranging and more constricted than the right ventricle and it is limited by the demarcations marked by the anterior and posterior or inferior interventricular grooves that signify ventricular septum's attachment to the heart (Whiteman et al., 2021). The left ventricle of the heart extends in the forward direction and constitutes the larger part of the sternocostal surface of the heart (the front surface of the heart facing the chest), diaphragmatic surface (bottom surface lying on the diaphragm) and left side of the heart. It is also remarkably visible at its lower end towards the back of the heart (Standring, 2021). The heart's left ventricle slants toward the apex from its base along the atrioventricular groove plane (Figure 1.7) (Whiteman et al., 2021). This apex that is directed downward, forward, and to the left is generally epitomized as the vortex of the left ventricle (Ho, 2020), and this site is significant as it provides access to surgeons for various valvular interventions (Standring, 2021). As the myocardium is comparatively thin at the apex, it allows surgeons to insert catheters or support devices for the left ventricle, tubes for drainage, and even electrodes but this also makes the left ventricle more prone to perforation while operating (Anderson et al., 2013).

The left ventricle encompasses an inlet (entrance), apical trabeculae, and an outlet (exit) analogous to the right ventricle structurally and positioned behind the right ventricle (Anderson et al., 2013). The mitral valve (MV) apparatus integrates as a left ventricular inlet (Ho, 2009), from where oxygenated blood is transmitted from the left atrium to the left ventricle and blood exits the left ventricle into the ascending aorta via an aortic orifice. Therefore, the region known as the aortic vestibule, which is situated exactly inferior to the aortic orifice, signifies the left ventricular outflow tract (LVOT) (Wineski, 2024). Further, the trabeculae are the organization of muscular extensions and protrusions crisscrossed in all directions in the internal surface of the ventricles, that project from the atrioventricular junction to the apex, and these trabeculae at the apex of the left ventricle are more intricate and fragile as compared to the ones present in right ventricle (Standring, 2021; Whiteman et al., 2021). The ventricular walls are generally thick except for the areas where trabeculae carneae are located. These trabeculae grant extra strength to the left ventricle without making the ventricular walls thick (Whitaker, 2010).

The left ventricle is undoubtedly stronger and more resilient than the right ventricle to withstand the most significant pressure variations between both the right and left atrium and ventricle (the difference of pressure should be between 120 and 160 mmHg) as the forceful ejection of oxygenated blood from the ventricle to the systemic circulation occurs. Consequently, compared to the right side of the heart, the left ventricle has six times greater blood pressure and three times thicker walls (Meschini et al., 2018; Wineski, 2024).

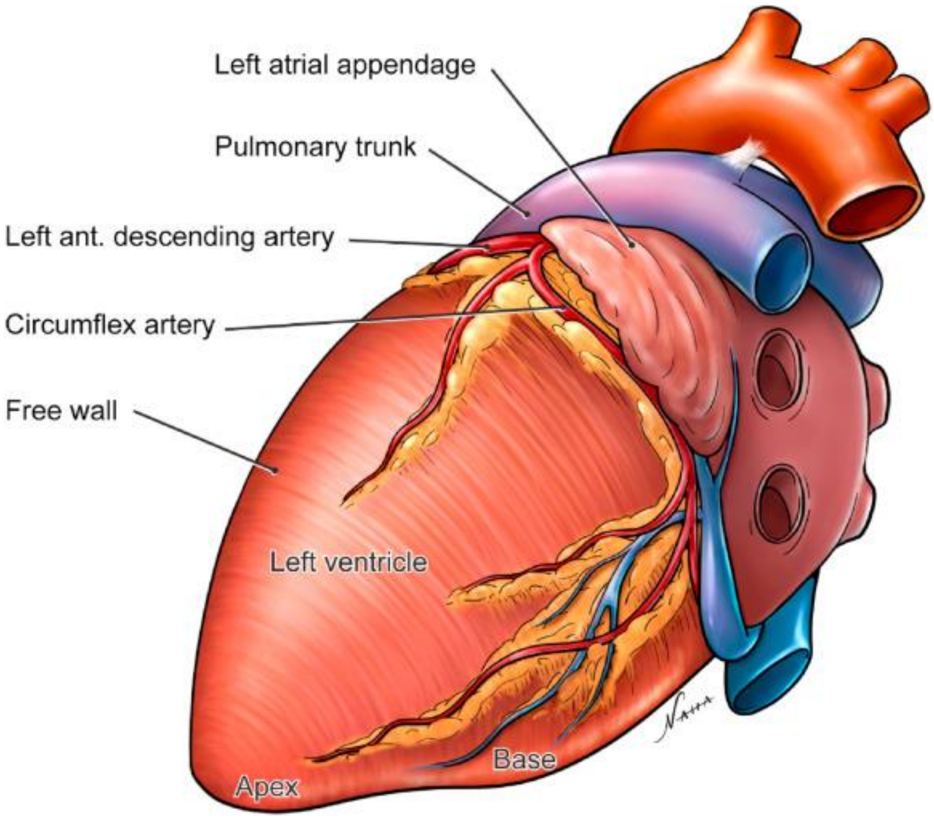

Figure 1.7: Lateral view of the heart showcasing the left ventricle and its boundaries, including the base, apex, and free wall (Whiteman et al., 2021)

1.1.3 MITRAL VALVE ANATOMY:

The living pump of the human body, the heart, is dynamic and functions as an integrated unit, as it can acclimate itself to the constant variance in the blood pressure and blood flowing through the heart. For efficient working of this pump, unidirectional or one-way valves are the most vital structures, as they are naturally modified in such a way that they can endure extreme pressures of the heart and are capable of sustaining the framework stability of the muscular cardiac chambers. The mitral valve among all the valves of the heart has the greatest challenge of enduring the utmost pressure of closing the powerhouse of the heart, the left ventricle. (Moorjani, Rana, and Wells, 2018).

The mitral valve (MV) is named after a ceremonial headdress called a mitre, which resembles the structure of the valve. The name was given by Andreas Vesalius, and it refers to the folding cap consisting of two similar parts sewn together, which resembles the structure of the left ventricular inflow valve (Omran, Arifi, and Mohamed, 2010). This resemblance is most perceived when observed from a ventricular viewpoint with valves being closed. (Anderson and Wells, 2021).

The unidirectional blood flow into the ventricle from the atrium of the left side of the heart during the diastole is guarded by the mitral valve positioned between the left atrium and left ventricle, having much greater surface area compared to another heart valve on the left side of the heart, that is aortic valve, and during systole withstands the peak difference in the transvalvular pressure. (Gao et al., 2017). Thus, the functioning of the mitral valve is twofold: firstly, during diastole aids the one-way flow of blood from the left atrium to the left ventricle, and secondly, during systole resists the blood reflux into to left atrium. The right atrium and pulmonary arteries, which form the low-pressure areas of the heart, and the left ventricle and the aorta that constitute the high-pressure region, the mitral valve serve as a terminal barrier between these two systems. (Levine et al., 2015).

The mitral valve is beyond being a merely simple tissue flap, it’s a dynamic valve (Muresian, 2009). The tissue of the mitral valve contrasts mainly in structure and composition, having a non-uniform surface due to the bundle of fibers which are large, visible, and running in all directions, so that the thickness of the mitral valve varies across the surface. This organization of fibers and varied thickness at each area of the valve's surface, not only differ on the same valve but between humans and even entities of similar species. (Kaiser, McQueen, and Peskin, 2019). The interstitial cells of the mitral valve certify the equilibrium between structural and biochemical properties; thus, these cells are mechanotransducers, responsive to mechanical stimuli, and contribute to the remodeling of the valve. These cells also interact with the endothelial cells, abundantly present on the surface of the valve that provide contour and resilience of the valve (Vaca and Bordoni, 2023).

The three-dimensional structure of the dynamic mitral valve is remarkable despite its intricate functions in a healthy individual (Dal-Bianco and Levine, 2013). According to Faletra et al., Perloff and Roberts aptly specified the mitral valve as having complicated architecture in 1972 consisting of multiple components. (Faletra et al., 2013). The intricate mechanical arrangements of the mitral valve complex consist of the annulus, two leaflets, commissures, chordae tendineae, papillary muscles, and walls of the left atrium and ventricle as shown in Figure 1.8 (Krawczyk-Ożóg et al., 2017). Thus, the mitral valve apparatus which is crucial for the structural integrity of the heart and fundamental for its architecture comprises two main elements, the first being the mitral valve leaflets and commissures and the second component involves the subvalvular apparatus, chordae tendineae and papillary muscles (Krawczyk-Ożóg et al., 2018; Tumenas et al., 2021).

The unidirectional and unhindered blood flow into the left ventricle is due to the spatial and temporal kinetics of the elements constituting the mitral valve complex. (Donal, and Panis, 2021). Failure of even one element of this complex can result in valvular malfunction and serious damage to the heart pump (Krawczyk-Ożóg et al., 2017). During the cardiac cycle, all parts undergo significant changes in position, shape, angulation, and size (Standring, 2021). Each component within the mitral valve complex works together to ensure the proper functioning of the valve including blood passage from the left atrium to the left ventricle at the right time, tight closing of MV during systole to prevent blood from flowing back into the atrium, and accommodating and competent ejection of blood into the aortic root through the left ventricular outflow tract (Muresian, 2009).

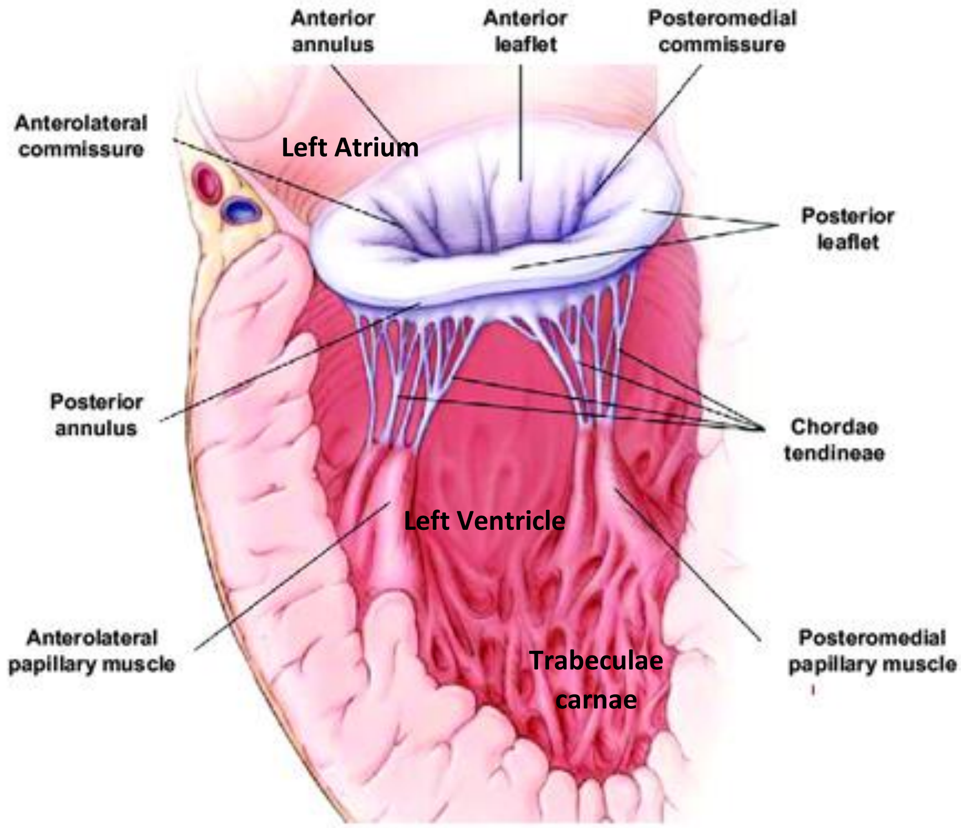

Figure 1.8: Illustration showing mitral valve complex (Huang et al., 2023)

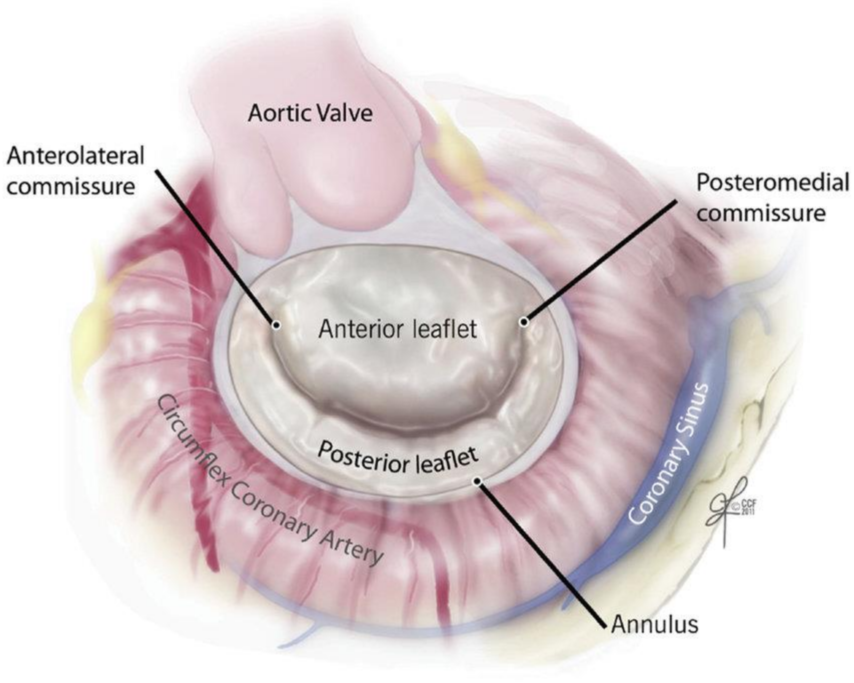

Figure 1.9: Diagram showing anterolateral and posteromedial commissures and also the relation between a circumflex coronary artery (posterolateral) and coronary sinus (posteromedial) with a posterior mitral annulus (Gentry III et al., 2018)

1.1.3.1 MITRAL VALVE ANNULUS:

The annulus of the mitral valve is an ovoid ring like structure composed of fibrous tissue, that encircles the edge of the valvular opening along with the valve's base and operates as a sphincter by reducing the mitral valve dimension during systole to maintain the appropriate closing of mitral valve leaflets when they approach each other as shown in the Figure 1.9, thus, anchoring the valve to the framework of heart (Dal-Bianco and Levine, 2013; Schubert et al., 2017). The aortic valve is present in front of the mitral valve annulus in cohesion along with the left coronary and non-coronary aortic leaflets which are separated from the mitral annulus by the presence of right and left trigone (Figure 1.10 A) (Oliveira et al., 2020). The annulus having the bandlike framework has two peaks: anterior (higher peak) and posterior (lower peak) while the commissures or trigones form the deepest areas of the mitral annulus, which participate in the formation of the fibrous architecture of the heart as shown in Figure 1.10 B (Saremi et al., 2017). So, three-dimensional structure of the dynamic mitral annulus which is shaped like a saddle has the highest peak in the center of the annulus anteriorly also known as the aortic peak forming aortomitral continuity, a link between the aorta and mitral valve, and posteriorly the maximum peak is where the posterior leaflet is inserted (Asgar, 2016; Blanke et al., 2014).

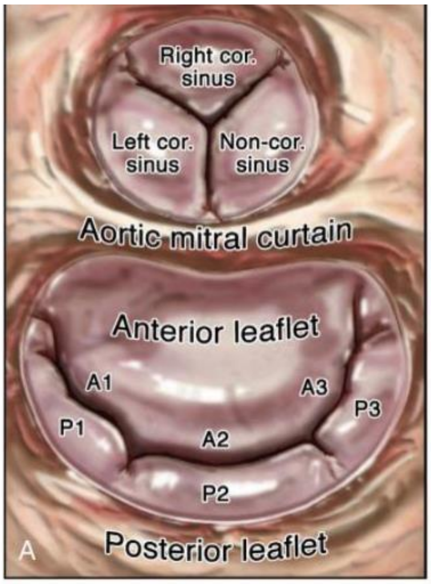

Figure 1.10: Anatomical structure of the mitral valve. (A) The anterior leaflet and posterior leaflet are shown, represented as segments A1, A2, and A3 (anterior) and P1, P2, and P3 (posterior) as classified by Carpentier. The aortic mitral curtain is indicated, along the leaflets of the aortic valve are also labeled (Tsang, Freed, and Lang, 2020)

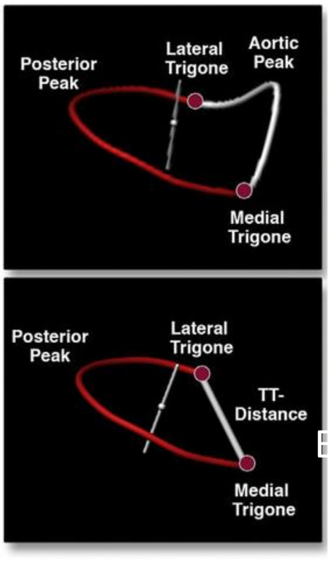

Figure 1.10: (B) Illustrations show the anterior and posterior peaks with the deepest areas of the mitral annulus (commissures and trigones). The annulus is restricted by trigone-to-trigone (TT) distance apart from aortomitral continuity (Blanke et al, 2015)

The mitral annulus constitutes two distinguishable segments: anterior and posterior segments having straight and curved margins respectively as shown in Figure 1.11. The anterior segment is continuous while the posterior segment is a thinner area of the annulus which is a fragmented fibrous string scattered among adipose tissue, where the integration of four elements occurs, including muscular walls of ventricle and atrium, cardiac adipose tissue, and hinge line (attachment line) of leaflets. The annulus attaches posteriorly directly to the myocardium of the ventricle and atrium where it is deficient (Faletra et al., 2021). This structure of the posterior segment makes it vulnerable to incomplete closure of the leaflets due to dilatation of the annulus, leading to mitral regurgitation (Schubert et al., 2017), also because of the direct attachment to the ventricle muscular walls' crest, so this portion of the leaflet become more prone to calcification due to friction abrasions as left ventricle contract and relax continuously (Faletra et al., 2021). Further, the circumflex coronary artery is present posterolateral to the posterior mitral annulus, and on the posteromedial side it is near the coronary sinus (Figure 1.9) (Omran et al., 2010).

The structure of the annulus is dynamic as there is variation in its diameter and shape during the cardiac cycle. (Jiang et al., 2014). The shape is more likely circular during diastole while saddle-shaped (non-planar) during systole in unison with the closure of the valve (Figure 1.11) (Oliveira et al., 2020). The mitral annulus is presented as a D-shaped configuration when aortomitral continuity is eliminated in two-dimensional cross-sectional imaging (Maggiore et al., 2020), having two dimensions: anteroposterior and medial-lateral dimension (Fig 1.12) (Omran et al., 2010).

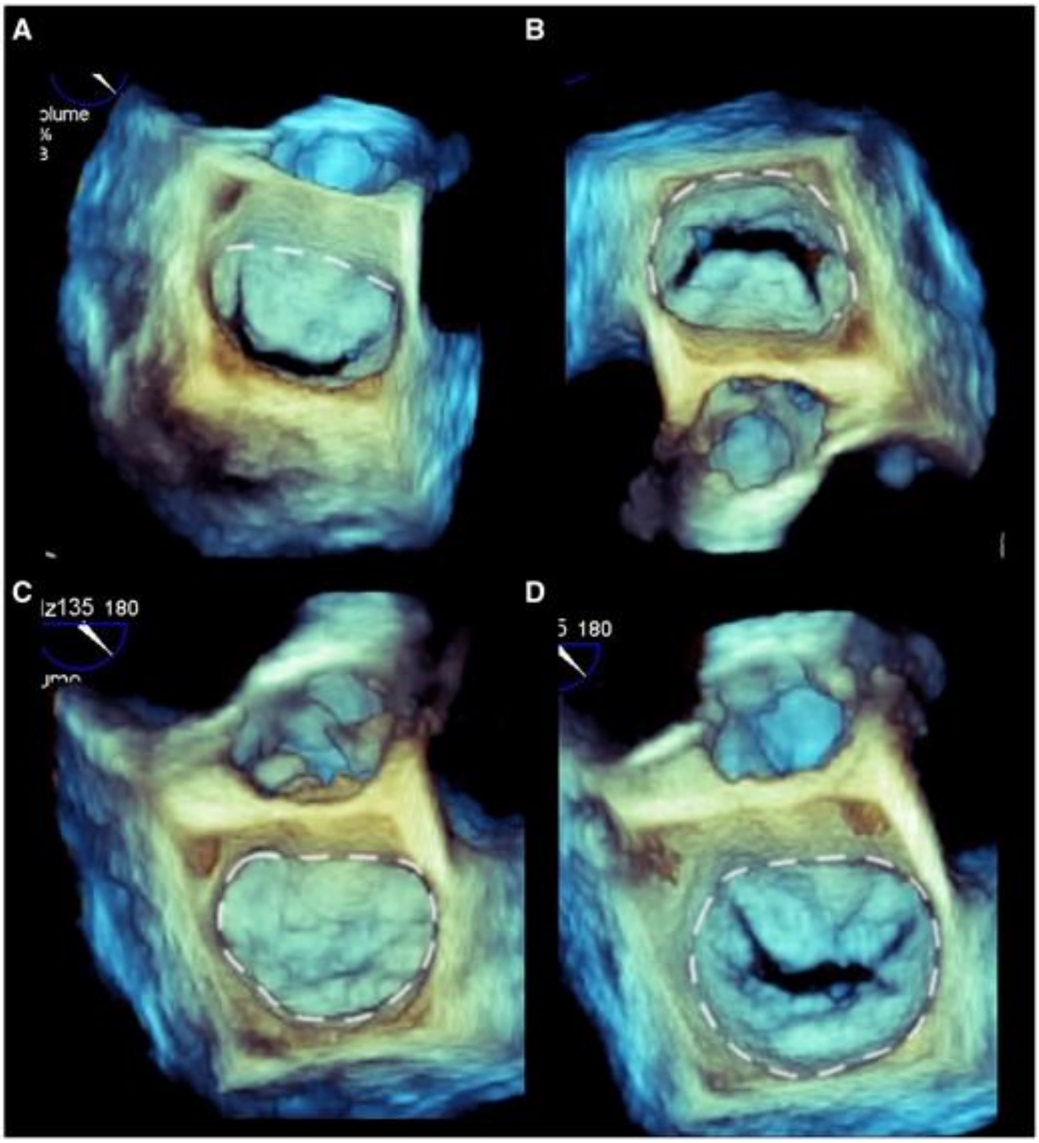

Figure 1.11: A 3-dimensional transesophageal echocardiogram of mitral valve in a healthy adult. (A) The surgical view shows a dotted line that is straight anterior mitral annulus. (B) The C-shaped posterior mitral annulus is marked by a dotted line when viewed from an anterior angle. (C) Surgical view during mid-systole exposes a D-shaped annulus. (D) The circular appearance of the mitral annulus in mid-diastole (Faletra et al., 2019)

.

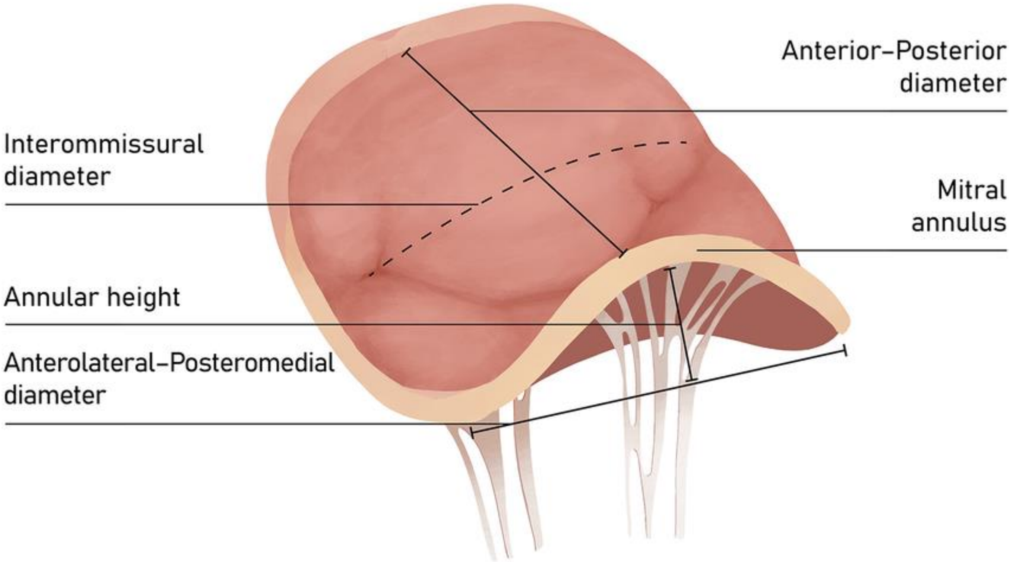

Figure 1.12: Illustration showing the non-planar saddle shape of the mitral annulus along with the anterior-posterior diameter, anterolateral-posteromedial diameter, and intercommissural diameter (Gasior et al., 2019)

1.1.3.2 MITRAL VALVE COMMISSURES:

The commissures of the mitral valve demarcate a distinguishable area where the two leaflets of the valve come in contact with each other. Carpentier in 1983 further separated them into two divisions: posteromedial and anterolateral commissures as shown in Figure 1.9 (Tsang et al., 2020). Commissures are differentiated from indentations based on certain characteristics, including, tendinous cords which are fan-shaped are present in commissures unlike indentations and also scallop-shaped commissures are recognized as having wrinkles on leaflets surface facing the atrium (Krawczyk-Ożóg et al., 2017).

1.1.3.3 MITRAL VALVE LEAFLETS:

The mitral valve or the bicuspid valve, is regarded as having two leaflets starting from the period of Andreas Vesalius, and this practice of naming the mitral valve was followed by successive researchers. However, in the last few years, different interpretations of the structural attributes and number of leaflets have been unfolded (Deopujari, Sinha, and Athavale, 2013). There are two principal leaflets: anterior and posterior (Figure 1.9), while there are small tissue flaps between these two main leaflets, that are recognized as distinct commissural leaflets by some researchers thus proposing the mitral valve to be a four-leaflet organization (Kaiser et al., 2019). The two leaflets are tethered to a saddle-shaped annulus base or ring that encircles the valve's aperture as seen in Figures 1.9 and 1.10 (demarcation between the left atrium and left ventricle) and the leaflets' free edges are affixed by the chordae tendineae (a network of strings), like a parachute, to the muscular walls of the left ventricles (Figure 1.8) (Kaiser et al., 2019; Munafò et al., 2024). Due to the discrete mitral annulus shape, the two leaflets that are anterior mitral valve leaflet (AMVL), also known as an aortic leaflet, and the posterior mitral valve leaflet (PMVL), also known as a mural leaflet, are of different sizes and even shapes (Figure 1.10). The anterior leaflet covers about one-third, the posterior leaflet covers two-thirds of the annular ring and the posterior leaflet also constitutes a portion of LVOT supported by subvalvular apparatus (Morris et al., 2010; Saremi et al., 2017; Weir-McCall et al., 2018).

The AMVL appears like a sail in shape situated anteriorly close to the non-coronary cusp, which is bigger in size, thicker, and more robust than PMVL and divided into three segments: lateral, central, and medial designated as A1, A2, and A3 respectively as shown in Figure 1.10 A. The PMVL on the other hand is crescentic shaped as it attaches to the two-thirds of the mitral annulus posteriorly and is also divided into three scallops in opposition to the AMVL counterparts by two indentations between them. These indentations in normal valve anatomy do not reach the annular orifice. The three scallops of PMVL according to the nomenclature of Carpentier are lateral, larger central, and medial designated as P1, P2, and P3 respectively. These divisions of the posterior leaflet are anatomical unlike the anterior leaflet, which are not anatomically divided and considered as segments as seen in Figure 1.10 A (Dal-Bianco et al., 2016; Maréchaux et al., 2017; Marsit et al., 2020). These leaflets are separated from each other by two commissures, anterolateral and posterolateral, at each end, having two zones: smooth and rough (Maréchaux et al., 2017). The smooth zone is referred to as the leaflets' atrial surface while the rough zone which is a protein-rich area, hydrophilic in nature, ranges about 1 cm from the terminal part of the tip of leaflets and aids the ideal closure of the valve, this is known as coaptation zone, which is about 0.3cm to 0.5cm measured area (Figure 1.13) (Moorjani et al., 2018; Topilsky, 2020) and where the leaflets meet at both the commissures, a line is formed that resembles semilunar arc, is known as coaptation line (Maggiore et al., 2020).

Throughout one's lifetime, mitral valve leaflets open and close three billion times approximately (Topilsky, 2020). During the diastole phase of normal cardiac functioning, the blood enters the left ventricle by opening the mitral valve and aids in the efficient filling of blood to maintain the configuration of blood flow and during the systole the ventricle contracts, the leaflets of the mitral valve are pushed towards the atrium due to pressure difference and prevent the regurgitation of the blood into the left atrium. This is achieved by the efficient working of all parts of the mitral valve to seal the leaflets and these sealed leaflets have specific shapes that assist in reducing the stress of the valve tissue when the blood streams out of the left ventricle into the aorta and improves the flow (Munafò et al., 2024). Thus, the leaflets of the mitral valve resemble the leaflets of the door and its movement is vital, either its opening or closing. Malfunctioning of these leaflets can either lead to mitral regurgitation when there is incomplete closure of the valve or the opening of the leaflets is constrained which results in stenosis (Moorjani et al., 2018).

A

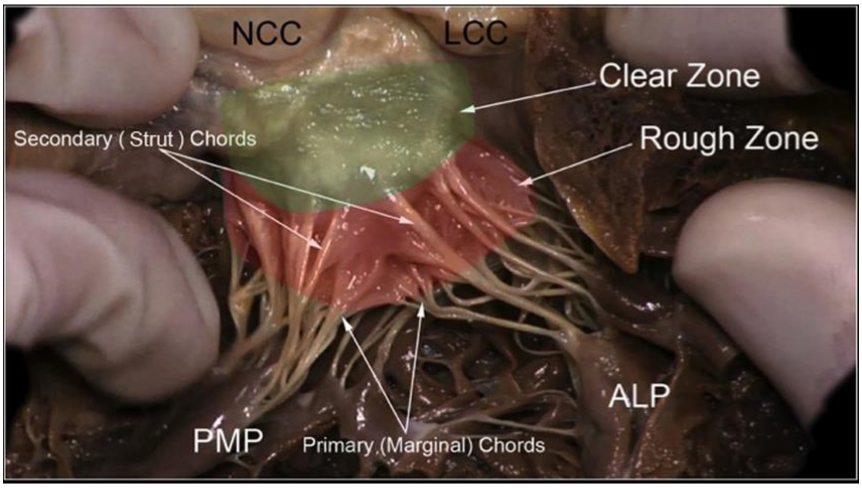

Fig 1.13: Regions of mitral valve leaflets: clear (atrial zone) and rough zone (coaptation zone). (A) Dissected mitral valve showing clear zone (green) and rough zone (red) from where several chordae tendineae originate and attach the leaflets to the papillary muscles (Pozzoli, Zuber, and Reisman, 2018)

B

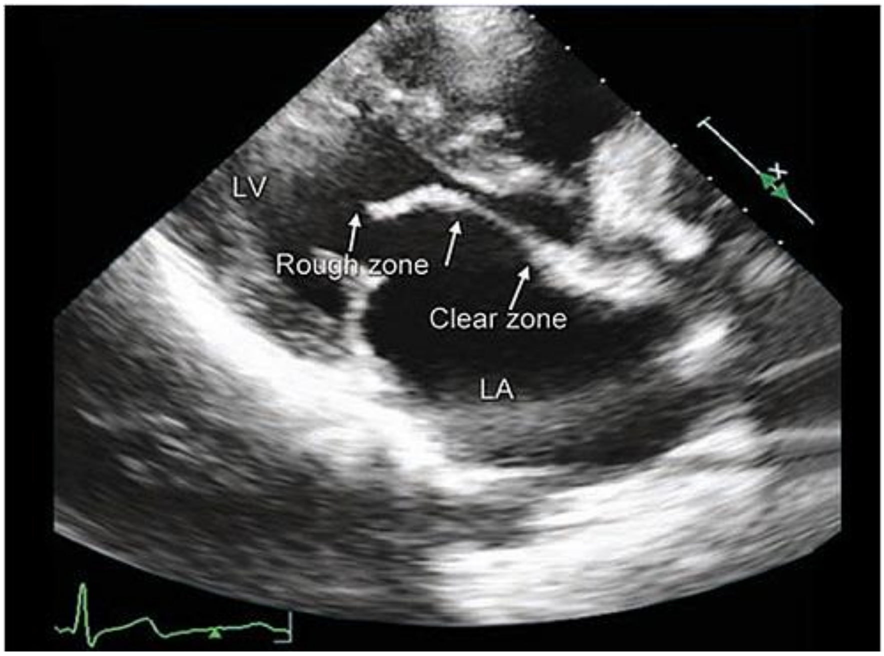

Fig 1.13: (B) 2-dimensional echocardiographic image shows the atrial zone at the base of the leaflet and the coaptation zone at the tip of the leaflet (Mohan, 2014).

1.1.3.3 SUBVALVULAR APPARATUS:

The leaflets of the atrioventricular valve (AV) have a tension apparatus comprising chordae tendineae and papillary muscles (Figure 1.8). This distinguishes the AV from the semilunar valves (Goodwin, and Biechler, 2019). The fundamental purpose of this apparatus is to facilitate accurate sealing of the valve's leaflets and during ventricular systole to prevent prolapse of the valve (Krawczyk-Ożóg et al., 2018)

The fibrous extensions, resembling a network of strings, come off from the leaflets of the valve and unite with two discrete papillary muscles present at the apex of the left ventricle, known as chordae tendineae (Figure 1.14) (Goodwin, and Biechler, 2019; Spicer et al., 2014). These are attached to the free edges of the valve's leaflet and at the site of attachment they divide and smoothly blend with the tissue of the leaflet. Many twigs of the chordae tendineae unite under the leaflets and form a few sturdier cords that fuse with papillary muscles that bulge out of the walls of the left ventricle (Kaiser et al., 2019). Thus, the attachment of the chordae is majorly at the site of coaptation making it to share the leaflets' mechanical stress. This permits coaptation and prolapse of the leaflets in the left atrium is prevented. Between the leaflets, if there is insufficient coaptation, it will not only result in mitral regurgitation but have higher chances of rupture of chordae tendineae due to anomalous traction (Capoulade et al., 2017; Leo et al., 2020). Chordae tendineae can be divided into three subtypes derived from their level of insertion, that are, primary, secondary and tertiary chordae. Primary chordae, also called as marginal as they attach to the leaflets' free margin and sustain coaptation; secondary chordae, also known as basal, insert on the rough zone of the AMVL edges and also cover the entire body of PMVL; tertiary chordae provide structural support as it attaches PMVL base to the left ventricular myocardium as seen in Figure 1.14 (Capoulade et al., 2017; Harb, and Griffin, 2017).

The papillary muscles are the part of the ventricles that are earliest to contract as it is embedded within conductive tissue that is firmly linked with the bundle branch, thus gearing up the valve and its structures to endure the pressure difference created during systole by firming the leaflets (Goodwin, and Biechler, 2019). The papillary muscles are of two types based on their position of attachment: anterolateral and posteromedial papillary muscles (Figure 1.15) (Harb and Griffin, 2017). The papillary muscles are not directly adhered to the wall of the left ventricle apex, but rather several fine delicate trabeculations which are muscular bridges that unite the muscles to the ventricular wall. Anterolateral and posteromedial papillary muscles are linked with both AMVL and PMVL, thus injury to any of the papillary muscles will detriment both the leaflets. The former group of the papillary muscle, that is, anterolateral receives its blood supply from two sources: the left anterior descending artery and branches of the left circumflex artery. On the other hand, posteromedial is supplied by a single artery, right coronary artery, or sometimes left circumflex artery determined by the dominant blood flow pattern of the heart. As the posteromedial papillary muscle gets its supply from a single artery it is more prone to ischemia during myocardial infarction that can damage the PMVL and result in mitral regurgitation (Morris et al., 2010; Rajiah, Fulton, and Bolen, 2019).

Any impairment of the subvalvular apparatus (chordal attachment or the papillary muscles) can lead to dysfunction of the mitral valve’s normal activity and failure of the heart to pump blood competently. Thus, it is essential for the mitral valve to properly function, and therefore, during the replacement of the valve surgically, the subvalvular apparatus is retained as it is pivotal after surgery for the heart to function optimally (Moorjani et al, 2018).

Now it has become essential for cardiac healthcare professionals to understand the functioning of the atrioventricular valves, especially the mitral valve. This detailed knowledge will aid them in accurate diagnoses and tailored treatment to get the best results for patients going through specific valve surgery (Moorjani, et al., 2018).

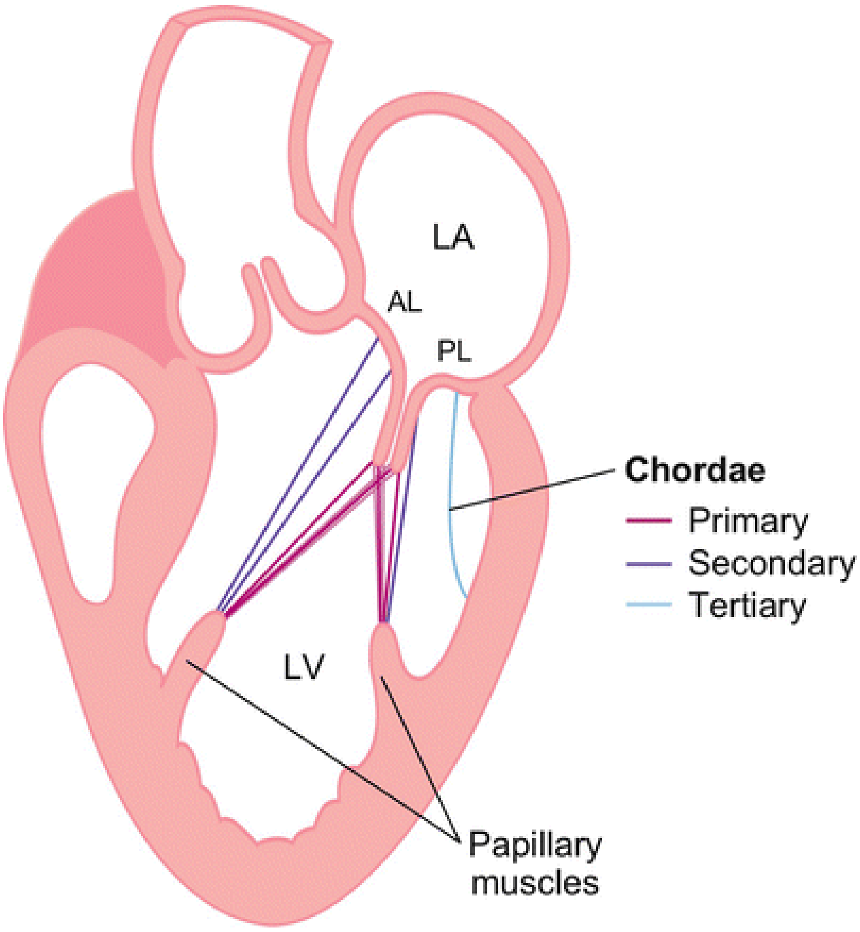

Figure 1.14: Illustration showing the attachment of chordae tendineae to papillary muscles and their types. LA= Left Atrium; AL=Anterior Leaflet; PL=Posterior Leaflet; LV=Left Ventricle. (Jellis, 2015)

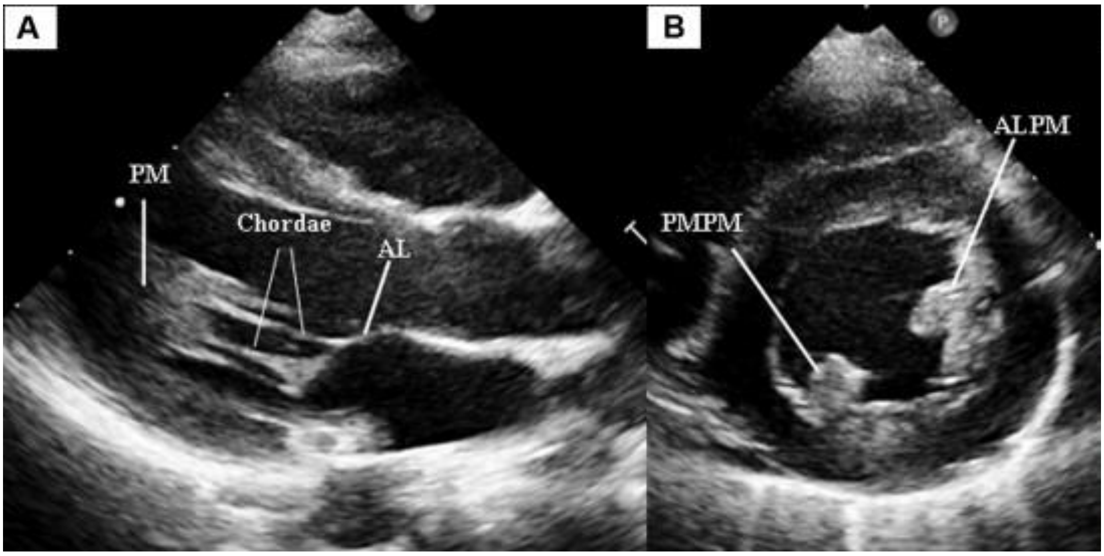

Figure 1.15: 2-dimensional echocardiography in a healthy adult. (A) Parasternal long-axis view showing subvalvular apparatus anchored to the anterior mitral valve leaflet. (B) Parasternal short-axis view showing anterolateral and posteromedial papillary muscles. AL: anterior leaflet; PM: papillary muscle; PMPM: posteromedial papillary muscle; ALPM: anterolateral papillary muscle (Séguéla, Houyel, and Acar, 2011)

1.1.4 MITRAL VALVE DISEASES:

Valvular heart diseases (VHD) have a prevalence of about 0.7% in people of ages between 18 to 44 years and 13.3% in people with age 75 years and above (Rostagno, 2019). From 1990 to 2019, Pakistan's non-rheumatic VHD prevalence grew by 14.1%, from 6.4 to 7.3/100,000, and a 12.9% increase in age-standardized death rate per 100,000 population was observed (Ahmed et al., 2022). Diseases of the mitral valve frequently occur in all groups of age but become more prevalent with age, approximately 5.1% of patients aged 65 and older are affected (Harky et al., 2021).

The mitral valve due to its varied components, its cellular composition, and its continuous motion within the heart, is considered a highly detailed and exceedingly complicated structure. Mitral valve diseases are of two types, congenital or acquired, and can be further classified into mitral stenosis, mitral valve regurgitation, and mixed valve diseases. Among these, congenital mitral valve diseases are infrequent, including about 0.005% of the general population and 0.4% of patients suffering from congenital heart defects. Around 60% of congenital heart diseases are linked with most of the congenital mitral valve disorders. However, among acquired disorders, rheumatic mitral disease is most prevalent globally, but infrequent in developed countries (Walsh et al., 2023). Worldwide, patients who are suffering from rheumatic heart disease (RHD) are greater than 30 million in number, which results in about 10 million impairments leading to disabilities and around three hundred thousand deaths occurring every year due to RHD (Watkins et al., 2017). RHD is a global strain because of elevated mortality and morbidity, specifically in developing countries having limited financial resources, and the progression of this disease, leads to regurgitation or stenosis of the mitral valve (Fu et al., 2021). In Pakistan, rheumatic heart accounts for about 15.8 per 1009 patients obtained from echocardiography in young patients and has been mostly observed with unhygienic conditions, overcrowding, poor housing, and malnutrition. (Kumar et al., 2022; Maken et al., 2016).

In Western nations, diseases of the mitral valve after aortic valve is the most prevalent valvular heart disease (Omran et al., 2010). Among them, mitral regurgitation (MR) and stenosis are the two predominant representatives of mitral valve pathology. The excessive thickening of the mitral valve, which frequently results from rheumatic heart disease, causes mitral stenosis (Harb and Griffin, 2017). Mitral stenosis, a complication of rheumatic fever in up to 95% of patients (advances years later after the first occurrence of rheumatic carditis), is considered to be a condition in which there is reduced opening or narrowing of the valve due to restriction created by mitral valve leaflets, as they become stiff (Figure 1.16 A) (Gomadam et al., 2014; Vaca and Bordoni, 2023). The normal measurement for a mitral valve orifice is around 4 to 6 cm^2, while this area is narrowed to 2.5 cm^2 or below in mitral stenosis or even less than 1 cm^2 in severe stenosis (Oehler, Sullivan, and Mansoor, 2017; Vaca and Bordoni, 2023). Mitral valve degenerative diseases are also the most common cause of mitral stenosis after rheumatic fever, which occurs as a result of mitral apparatus calcification while rheumatic mitral stenosis is mainly due to the fusion of commissures (de Hemptinne et al., 2015). Furthermore, congenital mitral stenosis, inflammatory and metabolic storage diseases, connective tissue defects, drug abuse, exposure to radiation, and even abnormal formation of myxoma, thrombi, and other structures, are other causes of mitral stenosis (Tumenas et al., 2021). In mitral stenosis, due to the narrowing of the orifice, the pressure in the left atrium rises and ultimately leads to the exudation of fluid into the interstitium of the lungs. This accumulation of fluid leads to shortness of breath at rest and even at exertion (Vaca and Bordoni, 2023). Mitral valve stenosis is primarily treated by taking preventive measures against group A β-hemolytic streptococci as in rheumatic fever the antibodies formed against streptococcal antigens intermingle with the tissue of the valve (Tumenas et al., 2021; Vaca and Bordoni, 2023) and most effective way to treat it is with percutaneous balloon mitral valvuloplasty. This intervention involves expanding the valve area with a balloon to decrease the difference in pressure gradient between the left atrium and left ventricle (Harb and Griffin, 2017).

Mitral regurgitation (MR) is characterized by the unusual retrograde current of blood into the left atrium through the mitral valve from the left ventricle, whose main cause is a rheumatic disease in underdeveloped countries and ischemic coronary disease in developed countries (Vaca and Bordoni, 2023). Among the general population of the United States, MR is present in 1.7% of patients approximately (Capoulade et al., 2017). Alain Carpentier was the one who originally described the phenomena of MR based on the activity of leaflets of the mitral valve (Donal and Panis, 2021). MR triggers excessive volume load of the left ventricle and thus pressure within the left atrium is elevated (Figure 1.16 B). In critical conditions, the ventricular cavity expands and surplus preload stress on the fibers of the myocardium occurs. This happens in extreme situations when MR goes unaddressed in patients and leads to the impairment of the optimal contraction, as stated by the Starling law, and eventually leads to heart failure (Munafò et al., 2024). Depending on the underlying cause, mitral regurgitation can be categorized as primary or secondary. Primary mitral regurgitation may occur because of degenerative disorders including mitral prolapse, flail leaflet, or endocarditis, per the European Society of Cardiology (Habib et al., 2015). The condition known as functional MR or secondary MR, is brought on by an imbalance between the mitral valve's closing and tethering forces. It is associated with structural changes like dilated cardiomyopathy, ischemic cardiomyopathy, and annular dilation, which expand mitral valve annular diameter of the heart. The different therapeutic strategies for primary and secondary mitral regurgitation highlight the significance of thoroughly examining (Yandrapalli, Biswas and Kaplan, 2021).

The most commonly diagnosed and second prevalent heart valve disease is mitral regurgitation and in patients aged over 75 years it accounts for about 9.3% of mitral valve diseases (Harky et al., 2021; Munafò et al., 2024). Mitral valve prolapse is primarily occur due to mitral regurgitation and is marked by the protrusion of the mitral valve leaflets into the left atrial chamber and approximately 2 to 3% of the population is affected by it (de Groot-de Laat et al., 2016). Mitral valve prolapse (MVP) when viewed on echocardiography in the parasternal long-axis during systole, is typically a 2 mm or more dislocation of mitral valve leaflets' edges or the entire body which is superior to the mitral annulus plane as shown in Figure 1.16 C (Levine et al., 2015). MVP is a benign progressive disease, that leads to MR and is exacerbated by supraventricular arrhythmias and eventually heart failure. It is also commonly associated with other syndromes like Marfan's syndrome but is frequently found in non-syndromic diseases (Le Tourneau et al., 2018). Classically MVP is classified into two types: one that occurs in older people known as fibroblastic degeneration and the second one occurring in early life is myxomatous degeneration or Barlow's disease (Delwarde et al., 2023)

For mitral valve diseases to be treated, the gold standard intervention is surgery either to repair or replace the mitral valve, and transcatheter therapies, which are demonstrated as the most reliable procedures, are performed if surgically the valve cannot be treated (Harky et al., 2021).

A

B

C

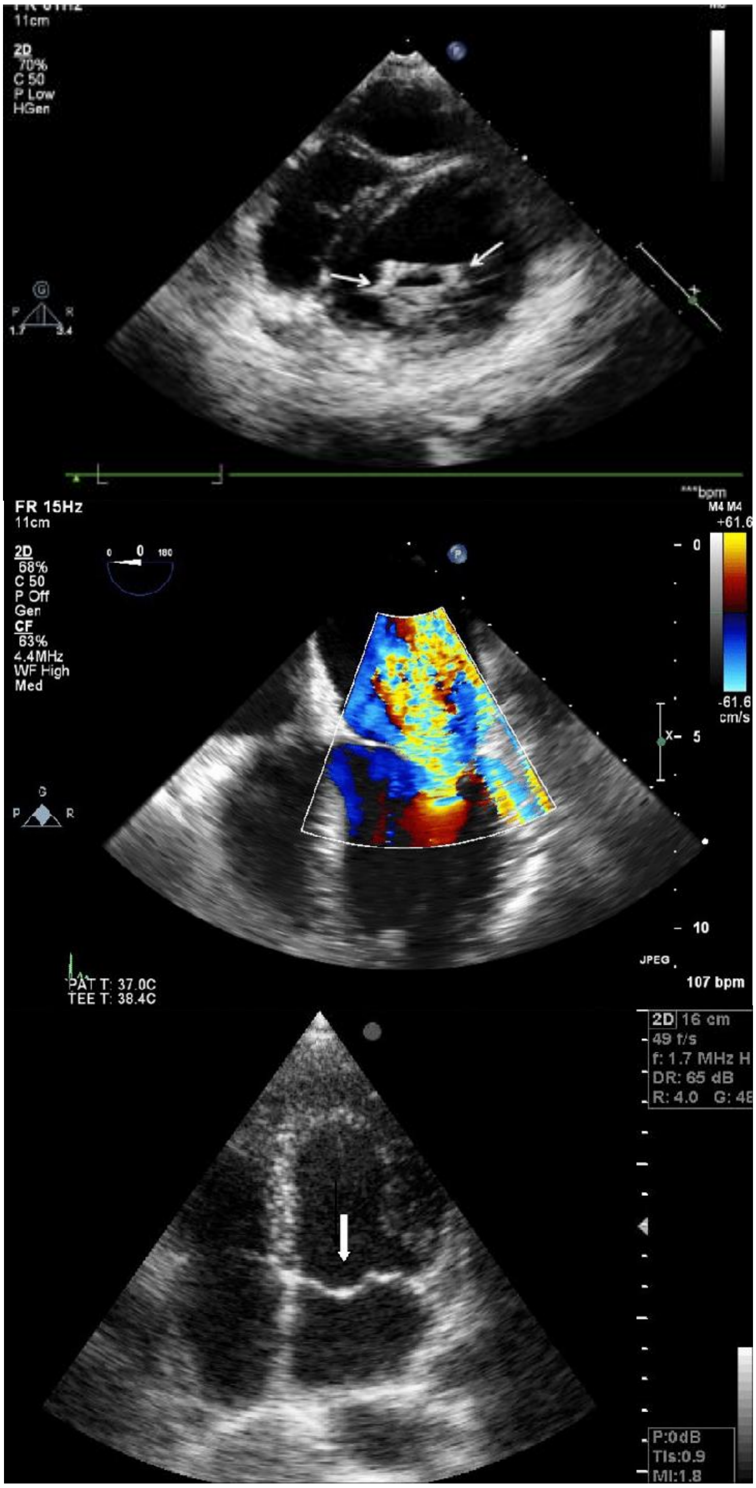

Fig 1.16: Echocardiographic images showing valve pathology. (A) severe mitral stenosis with fusion of commissure (arrows); (B) mitral regurgitation; (C) mitral valve prolapse (arrow) (Saxena, 2013; Mujtaba, and Clark, 2018; Arinc, Gunduz, and Tamer, 2004).

Understanding the emblematic structure and function of the MV is crucial for recognizing abnormalities and determining appropriate treatment strategies to reduce patient injury and mortality, to direct mitral valve repair surgeries, or to preserve a valve and its attachments, like its connection with the papillary muscles (Nordblom and Bech-Hanssen, 2007). Currently, cutting-edge imaging techniques are present that are non-invasive and provide images of high resolution of the heart and its movement, which has markedly boosted the ability to notice the elaborated complexity of morphological defects in heart diseases. These techniques include 2-dimensional and 3-dimensional transthoracic echocardiography (TTE), transesophageal echocardiography (TEE), cardiac magnetic resonance (CMR), and cardiac computed tomography (CCT) (Faletra et al., 2019)

The mitral valve has long been a focus for researchers in echocardiography because of its position that is perpendicular to the echo beam in the parasternal view, which permitted Edler and Hertz in 1953 to identify it first. At present, echocardiography remains the primary method for evaluating the mitral valve anatomy and its function, using advanced techniques to guide medical and surgical interventions based on the obtained structural and hemodynamic information (Omran et al., 2010). It has developed from using M-mode to using two-dimensional and now three-dimensional imaging techniques to provide a thorough investigation of mitral valve structure and motion. (Dal-Bianco and Levine, 2013). Transthoracic echocardiography (TTE) has appeared as the preferred method for assessing MV geometry due to its uncomplicatedness, consistency, and extensive approachability (Henry et al., 2022). Three-dimensional echocardiography augments two-dimensional and thus should be used whenever accessible as it delivers extra valued information (Gonzalez-Gomez et al., 2015).

TTE is chiefly used to assess mitral valve and its defects. Multiple views are taken to evaluate the mitral valve as seen in Figure 1.17, which are as follows: firstly, the parasternal long-axis view is seen to determine the thickness and movement of the leaflets during the cardiac cycle long with it the size of the left atrium is assessed in MV disorders. In this view, a Doppler study can be done to evaluate blood flow during the phase of relaxation through the mitral valve. Second, is the parasternal short-axis view that can detect movement of the mitral valve, chordal attachment, and commissure splitting, also mitral valve area can be measured by using planimetry at the leaflets' tip level. This view also demonstrates the presence of papillary muscles, the number of papillary heads, and their alignment. The third view is the apical 4-chamber, which illustrates leaflets and their orientation around the annulus of the mitral valve. Also, by using pressure half time, the "area of the mitral valve" can be determined and the mitral inflow Doppler study gives insight into parameters of the left ventricle during diastole. Lastly, a 3-chamber or apical long-axis view is essential to assess mitral valve leaflets segments and the extent of MR can be calculated (Omran et al., 2010).

The interface between each valvular element, along with the left atrial, and the left ventricle forms the intricate anatomical structure of the mitral valve. Each of these components is crucial to the mitral valve's function in one way or another. One must be well-versed in anatomy and comprehend the normal functioning of the mitral valve structure to evaluate valve failure and its mechanism. Consequently, improved clinical case implementation and longer-lasting mitral valve restoration (valvuloplasty) procedures will be made possible by this understanding.

.

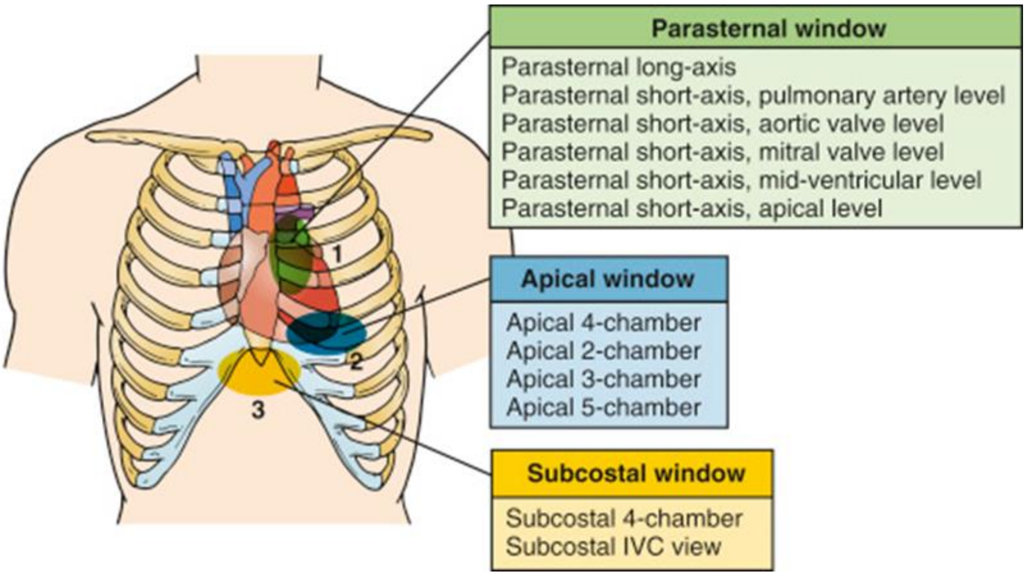

Figure 1.17: Image showing transthoracic echocardiographic windows: parasternal long-axis, parasternal short-axis, apical, and subcostal (Millington, 2014).

1.2. RESEARCH GAP

1.2.1 Theoretical Gap: Currently, there is limited literature present after searching Google Scholar, PubMed, and PakMediNet on the detailed assessment of mitral valve within the Pakistani population. As the people of Pakistan belong to diverse cultures and ethnicities with unique characteristics, the study seeks to understand the influence of various factors on the normal anatomy of the mitral valve and to determine the underlying mechanisms and etiological factors that contribute to its variations.

1.2.2 Contextual Gap: As no study has been conducted to examine mitral valve anatomy, this study will provide insights into the specific characteristics of variation in mitral valve in the Pakistani population and provide a foundation for future research for the development of specific guidelines and interventional strategies tailored according to patients with mitral valve condition within Pakistani population.

1.2.3 Methodological Gap: The assessment of multiple parameters by 2-dimensional echocardiography, including mitral valve and its components and also left ventricular measurements, provides a holistic view of cardiac structure. Comprehensive correlation analyses between echocardiographic parameters and demographic factors (age, gender, family history, smoking status, and body surface area) clarify underexplored relationships. By including diverse ethnic groups such as Sindhi, Punjabi, Balochi, Pashtun, Urdu-speaking, and Hindku, the research enhances understanding of ethnic variations in mitral valve and left ventricular parameters, filling gap in previous studies.

1.3 PROBLEM STATEMENT:

For gaining insights into the underlying mechanisms leading to failure of mitral valve functioning it is crucial to understand normal measurements and variations of mitral valve geometry among people of different descents within Pakistani Population.

1.4 RESEARCH QUESTION/ HYPOTHESIS OF STUDY:

A) Null Hypothesis

- Mitral valve parameters do not vary in relation to age, gender, body surface area, smoking, family history of cardiac diseases, co-morbidities and ethnicity in the subset of Pakistani population
- Variations in mitral valve parameters do not have an impact on the left ventricular dimensions and its wall thickness in the subset of Pakistani Population.

B) Alternate Hypothesis

- Mitral valve parameters vary in relation to age, gender, body surface area, smoking, family history of cardiac diseases, co-morbidities and ethnicity in the subset of Pakistani population
- Variations in mitral valve parameters do have an impact on the left ventricular dimensions and its wall thickness in the subset of Pakistani Population.

1.5 OBJECTIVES OF THE STUDY

To,

1. Determine the normal values of mitral valve parameters in a subset of Pakistani population by Transthoracic 2D Echocardiography
2. Determine the association of variations in mitral valve parameters with age, gender, body surface area, smoking, family history of cardiac diseases, co-morbidities and ethnicity in the subset of Pakistani population by Transthoracic 2D Echocardiography
3. Evaluate the impact of variations of mitral valve parameters on left ventricular dimensions and wall thickness in the subset of Pakistani population by Transthoracic 2DEchocardiography

1.6 SIGNIFICANCE OF THE STUDY

As the Pakistani population boasts people with genetic, ethnic, and cultural diversity, it is imperative to determine the anatomic variations of the mitral valve parameters for an enhanced understanding of the factors that may contribute to the development and progression of mitral valve diseases in Pakistan. This will add to the literature as no study has been conducted so far on the detailed evaluation of the mitral valve and its components specific to the population of Pakistan and it can also provide the foundation for baseline research values of these parameters that would enhance the accuracy of diagnosis and can improve patient management. Researchers can also identify the factors that may impact the outcome of different surgical techniques involving mitral valve repair and replacement, that require proper sizing and positioning of repair devices or prosthetic valves thereby enabling them to develop new technologies or interventions for mitral valve disorders. Hence, the precise knowledge of mitral annular dimensions and its leaflets along with papillary muscles not only ensures optimal functionality but also minimizes complications.

CHAPTER 2

LITERATURE REVIEW

Kunzelman et al., 1994 were the first to conduct a study to examine the structure of a mitral valve and determine the measurements of its dimensions, including the length and height of the valve ring and leaflets, as well as the arrangement of the chordae tendineae. This study used human and porcine mitral valve samples that were removed for analysis. Further, Espino, Shepherd, and Buchan (2007) investigated the effect of the mitral valve geometry on the valve's functional competence. They carried out the study on the mitral valve in a lab setting on porcine and assessed the effect on the ability of the mitral valve to operate under pressure following the changes occurring in the mitral valve's shape and size during the cardiac cycle. The investigators altered the annulo-papillary length (length from the annulus to the papillary muscles), mitral annulus area, and left ventricle diameter where papillary muscles are attached. For each change, they used six valves and the results showed that the minimum annulo-papillary length is essential for the appropriate functioning of the valve, and valve closure additionally improved when this length was increased, however, no significant effect was seen with changing the diameter of the left ventricle where papillary muscles arise to withstand the pressure by the mitral valve. Meanwhile, it was seen around 149mmHg pressure was endured by the normal-sized annulus before failing, 117mmHg by medium-sized, and only 50 mmHg by a larger-sized mitral valve annulus. Hence, as the size of the mitral valve annulus increased, the ability of the valve to withstand the pressure decreased and the valve became frailer. Thus, this study concluded mitral valve’s components and its geometry are vital for the valve's proper functioning as the failure of any of them can easily lead to valve disorders.

Over the following years, autopsied studies of the mitral valve have been conducted vastly worldwide. Gupta, Shetti, and Manju (2017) studied the mitral valve in specimens of the human heart of adults preserved in formalin to measure the mitral valve diameter along with its orifice. They measured the mitral valve's inner circumference, the leaflets' surface areas, the free margin's length, and the area of each leaflet. The findings revealed that the anterior leaflet's free margin was 5-7 cm long, the posterior leaflet's free margin was 7-9 cm long, the area of the anterior leaflet and the area of the posterior leaflet was 1-3 cm^2 and 2-4 cm^2 respectively. The mitral valve annulus was also 8–10 cm in diameter. In the same year, Krawczyk-Ożóg et al. (2017) measured mitral valve parameters along with its associated structures in 200 autopsied human hearts. The mitral annulus (MA) diameter was found to be 485.4 ± 171.4 mm^2 and MA circumference was 89 ± 12.6 mm along with the inter-commissural diameter was measured to be 28.0 ± 4.8 mm^2. The aorto-mural diameter was found to be 19.7 ± 4.8 mm, and the ratio of inter-commissural/ aorto-mural diameter was 1.49 ± 0.38. Significant differences were observed between both genders, with decreased values in women. Furthermore, they studied the variations in the mitral valve leaflets. Approximately 34.5% ± 4.8% of the mitral annulus circumference was occupied by the anterior mitral leaflet, whereas the posterior leaflet accounted for approximately 50.7% ± 5.1%. The posterior mitral leaflet showed accessory scallops between various sections other than typical P1, P2, and P3 scallops with the rare existence of accessory scallops in the anterior mitral valve leaflet which was commonly uniform in structure. BS and Varsha (2019) measured the annular diameter, area, and circumference of the mitral valve on 50 autopsied adult cadaveric human hearts of both males and females aged between 20 to 70 years using a measuring scale and vernier calipers conducted at the Department of Anatomy, Vydehi Institute of Medical Sciences and Research Centre, Bangalore, India. The mitral valve annular diameter was measured to be 3.26 ± 0.48 cm in females and 3.10 ± 0.40 cm in males, the mitral valve circumference was 8.19 ± 1.01 cm in males and 7.76 ± 0.99 cm in females, while the area was 5.45 ± 1.34 cm^2 and 4.89

± 1.20 cm² in males and females respectively. It was exhibited in the study that except for the diameter of the annulus which was larger in females, all other parameters were greater in males than females, however, the differences were not statistically significant.

Mishra et al. (2014) studied different parameters of the annulus and leaflets of the mitral valve on the 120 specimens of the human heart fixed with formalin. These parameters included cross-sectional area, circumference of the mitral annulus, and height and length of the leaflets of the mitral valve. It was presented in the study that in about 55.83% of the specimens, the cross-sectional area of the valve ranged between 5.1 to 7.5 cm² and the circumference was between 7.5 cm to 10 cm. The length and height of the anterior leaflets or cusps were wide-ranging between 0.73 cm to 5.71 cm and 1.11cm to 3.74 cm respectively. The length and height of the posterior cusps were about 2.15 cm to 9.31 cm and 0.61 cm to 2.55 cm. The results also showed accessory cusps in three specimens, which were about 2cm and in length and height ranged between 0.76 cm to 1.02 cm. Mohtaj et al. (2018) conducted a study in Iran on 120 hearts obtained from deceased patients with no cardiac disorders within 24 hours after death. Out of 120, only 88 were included in the study as 32 hearts had various cardiac disorders, and these individuals with healthy hearts aged between 25 to 86 years. The results showed average mitral valve area was 5.14 cm², ranging between 2.12 to 8.7 cm²; the average valve perimeter was about 8.3 cm, ranging between 5.77 to 10.76 cm²; and the inter-commissural distance was about 2.7 cm and ranging between 1.79 to 3.82 cm. The researchers also measured distances between different points on the mitral valve and areas of the valve segments and concluded the result based on gender, age, and BMI. The anatomic areas and perimeters of the valve were larger in men than in women and even between both genders, the distances between A2 to P1 and A2 to P3 of the mitral valve leaflets were significantly different. There was also a significant difference in distances from A2 to P2 and A2 to P1 among different age groups and a significant difference among different BMI groups in the distance measured from the base of P2 of the mitral valve's posterior leaflet. Overall, this study provided thorough morphometric data of the mitral valve parameters based on gender, age, and BMI in the healthy Iranian population. Similarly, Lama et al. (2018) conducted a morphometric study at the Anatomy Department of Nepal Medical College and Teaching Hospital on 50 heart valves of cadavers, having no gross morphological anomalies or no calcified valves. The heart was dissected from the left auricle to the apex along the left border, which opened the left ventricle, and the mitral valve was exposed. The researchers measured mitral annular circumference and diameter by using tools like thread, ruler, and digital vernier caliper. The annular circumference was measured as 7.5 cm to 11.0 cm (most common range 7.5 – 8.5 cm: 40%) with a mean of 9.22 ± 1.49 cm and the annular diameter ranged between 1.61 cm to 2.72 cm (most common range 1.89 – 2.16 cm: 48%) with mean of 2.01 ± 0.27 cm.

Gumpangseth et al. (2020) conducted a study at Forensic Medicine and Anatomy, Chiang Mai University in Thailand on 60 fresh human hearts derived from cadavers aging between 20 to 90 years that showcases the applicability of heart valves' morphometric parameters as an age indicator. The circumference of the mitral valve was 173.4 mm within the range of approximately 132.5 mm to 214.3 mm with a correlation coefficient of 0.455, which suggested a statistically significant moderate positive correlation between age and circumference of the mitral valve. Thus, with increasing age, the mitral valve's circumference shows a tendency to increase. Similar significant findings were seen with the mitral valve leaflets' length and the area of the posterior leaflet that increases with age having a correlation coefficient of 0.393 and 0.336 respectively representing weak to moderate correlation between the area of the posterior leaflet and age. These parameters can potentially be used to estimate the age of an individual based on the dimensions of the heart valve. Savalgi et al. (2022) examined 50 embalmed human hearts aged between 20 to 60 years dissected from cadavers and studied the mitral valve. They measured mitral valve leaflets' width and length, and also commissures and zones of the valve by using calipers and magnifiers. It was also exhibited from this study that in comparison to women, larger dimensions were found in men in most aspects of the mitral valve but had one exception, the posterior leaflet width to a small extent was larger in females. The investigators also noticed discrete rough and clear zones of both mitral valve leaflets, with the anterior leaflet having smooth edges and a triangular shape while the posterior leaflets presented with several indentations and clefts. The measured parameters of the mitral valve were as follows: the mean length of the anterior mitral leaflet in males and females was 2 cm and 1.98 cm respectively, mean length of the posterior mitral leaflet in males and females was 1.29 cm and 1.2 cm respectively while the anterior and posterior leaflet breath in males was 2.85 cm and 3.99 cm respectively and in females 2.83 cm and 4.01 cm respectively. The mean length of the anterior commissure was 0.65cm in males and 0.60 am in females while that of the posterior commissure was 0.64 cm in both genders. The mean length of the leaflet's free edge was 9.42 cm in males and 9.41cm in females. Recently, Çandır et al. (2024) measured and examined various parameters of the left atrioventricular valve complex (LAVC) or mitral valve in 120 hearts of humans who died in less than 24 hours before the study was conducted on them. These people were 30 years or older in age and had a body mass index over 26.7. The heart weighed over 414 grams and the height/ width ratio of 1.24 or less. The mitral valve width was over 99.96 mm with over 30.71 mm of mediolateral diameter of the mitral annulus and over 619.37 mm^2 annular area. The left ventricular wall thickness was over 15.08 mm.

Advancements in medical imaging techniques have enabled the use of non-invasive procedures like echocardiography. Sonne et al. (2009) conducted a study in which real-time 3-dimensional transthoracic echocardiography (TTE) was performed on 120 individuals with normal function of the left ventricle and minimal mitral regurgitation. Using specialized software, the images were analyzed to determine the annular area, height, and tenting parameters of the mitral valve. Significant variations were observed within subjects, in which the annular area which was found to be 8.6 ± 2.2 cm^2 was most influenced by body surface area. It was followed by the interpapillary distance which was 17.7 ± 4.8 mm among the participants. However, age did not significantly impact the measured parameters, except for a slight correlation with the angle between the papillary muscles. Another study (Mihăilă et al., 2014) collected data from 30 patients who were indicated for 3D TTE and 3D TEE clinically. Additionally, 3D TTE data was also gathered from 224 healthy individuals between the ages of 18 to 76 years. The study concluded that the measurements of the mitral annulus taken by 3-dimensional TEE and 3-dimensional TTE were similar. Further, the study showed that men had higher measurements involving areas, diameters, and circumferences of the mitral annulus (MA) along with anterior leaflet length than women and these measurements were significantly correlated with body surface area. Both genders had similar MA sphericity and non-planar angle (NPA). The anteroposterior diameter of MA, the angle located in the anterior-posterior direction between the mitral annulus and aortic valve, and MA sphericity showed significant correlations with age. It was found that during systole, due to shortening of the anteroposterior diameter, the mitral annulus area was decreased by 29.6 ± 5%.

Dwivedi et al. (2014) measured normal ranges of MA along with tricuspid annular dimensions using transthoracic echocardiography. They included 480 participants in the study after excluding patients with pathological valve conditions having age above 60 years. Similarly, dimensions were found to be larger in men compared to women and were generally larger at end-diastole than at end-systole. Similarly, Kapadia, S. (n.d.) conducted a study at the Cleveland Clinic which was oriented to compare dimensions of mitral annulus and tricuspid annulus between 50 normal participants and 50 patients with severe mitral regurgitation using cardiac computed tomography software, Aquarius Terarecon. This study found significant differences between mitral annulus (MA) and tricuspid annulus (TA) dimensions, with the TA generally being larger in area, perimeter, and linear dimensions but as compared to the MA, TA was smaller in height. Both MA and TA dimensions were correlated, this means that as one dimension increased, the other also showed the tendency to increase. MA dimensions were influenced by body surface area and gender, but not strongly by age or BMI. These findings provide imperative insights into the anatomical variations of the annulus of the tricuspid and mitral valve, which are pivotal for understanding cardiac function and pathology. Makaryus et al. (2017) compared the measurement between the tricuspid valve annulus (TVA) and mitral valve annulus (MVA) dimensions in terms of circumference, area, height, anterolateral-posteromedial axis, and anteroposterior (AP) axis. This study was conducted in 49 patients (45% were males) with comorbidities like hypertension, diabetes mellitus, coronary artery disease, and dyslipidemia but no valve pathology and an average age of 61 ± 14 years of the participants. The circumference of the MVA was measured 27.9 ± 16.8 mm and the area was 1103.7 ± 307.8 mm^2. The MVA and TVA were similar in circumference, area, and even shape (oval). The anterolateral-posteromedial axis and AP axis were also similar between the two valves with MVA having an anterolateral-posteromedial axis and AP axis of about 37.9 ± 6.4 mm and 34.8 ± 5.7 mm, respectively. The ratio between the anterolateral-posteromedial and AP axis was significantly different, which was 1.08 ± 0.33 in MVA and 1.09 ± 0.28 in TVA. Similarly, the height of the MVA was significantly greater than that of the TVA, which was measured to be 9.23 ± 2.11 mm in MVA and 4.37 ± 1.48 mm in TVA.

Jolley et al. (2017) involved 250 participants entitled to 3-dimensional scans of the heart out of which only 100 people were suitable for analysis due to clear images having normal cardiac function during a scan. Both neonates and young adults, 1 day to 22 years of age with a 9.4 median age, suggested that the mitral valve's so-called saddle shape or the ratio of its annular height to commissural width remained constant across different age groups. With age, the dimensions of the mitral valve increased but no differences were seen with some parameters related to the shape of the valve. A linear relationship was seen between the patient's body surface area and measured parameters of the mitral valve that included valve area, length, and surface area. An increase in the ratio of the lengths of the anterior and posterior mitral valve leaflets along with the angle of the posterior mitral valve leaflet occurred with an increase in body surface area, indicating a displacement of the coaptation line posteriorly. No significant difference was found between both genders. This study showed that 2-dimensional measurements although being lesser than 3-dimensional measurements, were strongly associated with each other.

Ring et al. (2018) assessed normal values for mitral annular and leaflet parameters in 103 patients with no significant cardiac problems using 3D transesophageal echocardiography (TEE). They found that, except annulus height, annulus height to inter-commissural ratio, tenting height, and tenting volume, all mitral annular parameters including mitral valve area, anteroposterior diameter, inter-commissural diameter, and leaflet surface area were higher in men as compared to women. Nevertheless, when adjusting for body surface area (BSA), not one of the parameters that was measured between males and females showed any significant difference. The normal size of the area of the mitral valve was found to be 5.00 cm^2/m^2, and they established an upper limit of 6.86 cm^2/m^2 for a range of normal levels. The size of the mitral valve area was associated with body size, left atrium, and the left ventricle volume during systole. Factors like gender, age, left ventricle mass and diastolic volume, ejection fraction, and right ventricle size did not independently influence the mitral valve area. The leaflet area was measured about 10.59 ± 2.15 cm^2 for both males and females. Ricci et al. (2021) established reference values for the size and dimensions of the mitral valve as well as the tricuspid valve using cardiovascular magnetic resonance. They examined 5065 healthy Caucasian individuals without any cardiovascular disease or conditions. Age and gender-specific strata for the measurements were used. The findings demonstrated that some metrics, including mitral and tricuspid valve diameters, were bigger in men than in women. With increasing age, they also noticed alterations in the dimensions. In the 3-chamber view, both end-diastolic and end-systolic mitral annular diameters were measured which were 2.9 ± 0.4 cm and 3.3 ± 0.4 cm in men, and 2.6 ± 0.4 cm and 3.0 ± 0.4 cm in women, respectively. According to the study's findings, these reference ranges can be utilized to distinguish between normal and abnormal states, facilitating the assessment and planning of interventions for valve-related problems.

Blanke et al. (2015) measured the annular dimensions of the mitral valve of 136 patients without any mitral valve anomaly using ECG-gated cardiac Computed Tomography Scans retrospectively to establish the normative values and to understand the impact of gender, body surface area, and sizes of the heart chamber on these dimensions. The age of the involved patients was 58.3 years on average consisting of 75 men and using semi-automated segmentation, the mitral valve's annular dimensions were measured at end-diastole. These dimensions included the perimeter and area projected by the annulus, trigone-to-trigone (TT) distance, and septal-to-lateral (SL) distance. The authors also measured left atrial end-systolic volume (LAV) and end-diastolic left ventricle volume (LVEDV). The mitral valve annular area was measured to be 9.1 ± 1.6 cm², the distance across the valve ring was about 28mm, a TT distance of 27.8 ± 3.2 mm, an SL distance of 28.3 ± 3.0 mm, and a 2-dimensional anticipated perimeter of PMVL insertion of 82.3 ± 8.0 mm. While an extensive range was observed in all parameters, the measurements were normally distributed. There was a strong relationship between body surface area, LAV, LVEDV, and larger mitral annulus. Additionally, the study showed that higher body surface area was a strong predictor of larger annular size along the male gender, higher LAV and higher LVEDV (larger heart chambers) were also predictors of larger mitral annulus. In conclusion, the study found that mitral annular dimensions measured by CT vary widely among individuals. Key factors influencing these dimensions include gender, body surface area, left atrial volume, and left ventricular end-diastolic volume. Naoum et al. (2016) conducted a case-control study using cardiac computed tomography to determine mitral annulus dimensions in patients who were considered for transcatheter mitral valve intervention (TMVI) having moderate to severe mitral regurgitation. They included 32 patients diagnosed with mitral valve prolapse (MVP) and 27 with functional mitral regurgitation (FMR) and compared the findings with the healthy participants. The findings revealed that the control group's MA dimensions varied widely, with men typically having bigger diameters while patients with mitral regurgitation (MR) had greater MA dimensions. In contrast to controls, MR patients had reduced inter-commissural (IC)/septal to lateral (SL) ratios but larger IC and SL distances. Additionally, the morphology of the annulus was altered in MR patients, with anteroposterior expansion. Remarkably, there were differences between MR subgroups, MVP and FMR. There was a positive link between annular size and both the left atrial and left ventricular systolic volumes in MVP patients, whereas in FMR patients, annular size was mainly associated with increasing size of left atrium. These findings have implications for determining the appropriate device size before TMVI, according to the specific characteristics of the mitral annulus in patients with different types of MR. Similarly, van Wijngaarden et al. (2018) recruited 123 patients with MR and 29 individuals as controls. They studied mitral annular dynamics in different types of MR, including FMR, fibroelastic deficiency, and Barlow’s disease, and compared it with healthy individuals using 3-dimensional transesophageal echocardiography. The study found patients had larger mitral annular dimensions as compared to control along variation in the annular shape among different types of MR. Mitral annular dynamics and parameters were reduced in FMR patients but fibroelastic deficiency and Barlow’s disease showed increased measurements. The study concluded that the mitral annulus undergoes distinct changes in size and dynamics in different types of MR, and these changes impact the assessment and quantification of MR using 3D TEE.

Webb et al. (2017) conducted a study that provided baseline measurements for normal valve thickness in children, which is crucial for identifying abnormalities related to conditions like rheumatic heart disease. It took place in South Auckland, a region with a high incidence of Acute Rheumatic Fever (ARF) and Rheumatic Heart Disease (RHD) in New Zealand, which recruited 288 normal children devoid of any congenital valve disease or RHD or mitral regurgitation with ages between 10 to 13 years. 2-dimensional Doppler images in parasternal and apical 4-chamber views were taken by using a 2–3 MHz variable frequency probe attached to Vivid e (GE Healthcare) portable cardiac ultrasound machines. The thickness at the tip of the anterior mitral valve leaflet and midpoint was measured from the parasternal long axis (PLAX) view in both diastole and systole of the cardiac cycle at the midpoint of the leaflets from the apical 4-chamber view, while, the posterior mitral valve leaflet was measured in diastole at midpoint. The results showed thickness for the mitral valve's anterior leaflet at both tip and midpoint was 2.0 mm (Interquartile Range (IQR) 1.7–2.4 mm) with the maximum measurement for both tip and midpoint being 2.9 mm, thus no significant difference in measurements between the tip and midpoint or between different views was seen. The midpoint thickness of the posterior mitral valve leaflet was about 2.2 mm (IQR 1.9–2.5 mm) showing the posterior being thicker than the anterior mitral valve leaflet.

Henry et al. (2022) published their study in the European Heart Journal which aimed to evaluate the normal values of mitral valve apparatus and its variation across both genders, male and female, and various age groups by employing data from the World Alliance of Societies of Echocardiography study. The study consisted of 618 normal participants, 301 men, and 311 women, and they were divided into different age groups: 18-40 years, 41-65 years, and >65 years to identify differences correlated with gender and age. Three-dimensional full-volume datasets were taken from the transthoracic echocardiography of the participants and these were analyzed using TOMTEC, mitral valve analysis software commercially available. Gender-related differences showed larger mitral valve annular dimensions in both the anterior-posterior and anterolateral-posteromedial planes in males and also annular area, annular circumference, tenting size parameters, and even valve leaflet area and length were larger in males. The anterior-posterior diameter was measured to be 3.4 ± 0.4 cm and 3.1± 0.4 cm in males and females respectively while the anterolateral-posteromedial diameter was 3.8 ± 3.8 cm in males and 3.5 ± 0.4 cm in females. The 2D area was 10.4 ± 2.4 cm^2 in males and 8.8 ± 2.2 cm^2 in females while the 3D area was about 11.2 ± 7.6 cm^3 and 9.2 ± 2.2 cm^3 in males and females respectively. The anterior and posterior mitral valve leaflets' length was 2.7 ± 0.3 cm and 1.6 ± 0.4 cm in males respectively while in females 2.5 ± 0.4 and 1.4 ± 0.4 respectively. Various parameters showed statistically significant differences across age groups, anterolateral-posteromedial diameter was slightly larger in the middle-aged group (3.7 cm) as compared to young and older age groups while anterior-posterior diameter was similar across all age groups which was about 3.2- 3.3 cm. The circumference was also slightly larger in the middle-aged group as well as the 2D area while 3D was similar across all age groups. The non-planar angle and tenting volume were larger in the middle-aged group, unlike the height of the annulus which decreased slightly with age. The anterior leaflet area of the mitral valve was larger in the younger and middle-aged group while the posterior leaflet area was slightly larger in the oldest group. The anterior leaflet was found to be longer in the youngest and middle age groups while the length of the posterior leaflet was slightly longer in middle age group only. The results highlighted the variations of the mitral annular and leaflet measurements among gender and variations with age, with certain parameters being significantly different across these categories. In the same year, Henry et al. (2022) determined mitral annular and leaflet areas and dimensions in 748 normal individuals by obtaining 3-dimensional images from transthoracic echocardiography and this study was published in the Journal of the American Society of Echocardiography. They divided the participants according to age, gender, and race. The study concluded that men had larger mitral valves than women. This was observed across all measured parameters, including mitral annular shape, size, and leaflet measurements. However, the sphericity index, non-planar angle (NPA), and annular height did not show significant differences between both genders. Mitral valve size and shape also decreased with age, except for tenting and leaflet size measurements, and NPA did not show a significant decrease. However, the anterior leaflet area in the elderly population was found to be smaller than in younger and middle-aged individuals, also the elderly population showed a significantly larger anteroposterior diameter of the mitral annulus, making it flatter than in young and middle-aged individuals. In the middle-aged group, the NPA and annular height were significantly larger than in the young and elderly groups. This suggested that the middle-aged group had more spherical mitral annulus than the young and elderly groups. Mitral annular size measurements in both Asian men and women were compared with the black and white population, which exhibited lower values significantly. All these differences between men and women, different age groups, and races were largely attributed to the variations in body surface area.

Majonga et al. (2018) from various studies analyzed and compared the sizes of the left atrium and left ventricle adjusted for body surface area (mostly measured by the Dubois method followed by the Haycock method for calculating body surface area) by using M-mode or two-dimensional echocardiography (92%) while three-dimensional echocardiography and other techniques were used in small numbers. Initially, 4398 articles were screened spanning from 1975 to June 2017, with 130 assessed in full, leading to the inclusion of 36 studies based on relevant echocardiographic measurements of dimensions of the left atrium and left ventricle in the healthy pediatric population. These studies were majorly from North America and Europe while a few were from Asia, and a single study from Africa (Zimbabwe), and South America (Brazil). The reported dimensions include the left ventricular end-diastolic diameter (LVEDD), end-systolic diameter (LVESD), interventricular septum thickness at end-diastole (IVSd), interventricular septum thickness at end-systole (IVSs), left ventricular posterior wall thickness at end-diastole (LVPWd) and left ventricular posterior wall thickness at end-systole (LVPWs). There were notable racial and geographic differences in LV and LA sizes. Significant variations in LV dimensions existed across different ethnic populations, as evidenced by studies from India, Italy, Zimbabwe, the USA, Germany, and the UK. India reported LVEDD of 35.02 mm and LVESD of 21.32, and Italy reported slightly larger LVEDD of 37.86 mm and LVESD of 22.97. In the children of Zimbabwe, the LVEDD was found to be 37.10 mm and LVESD 25.29 mm, in Americans the LVEDD and LVESD were 39.09 mm and 25.1 mm respectively, while the UK reported LVEDD of 38.27 mm and LVESD of 24.428mm. In German children, the LVEDD was found to be 38.50 mm and LVESD was 24.4 mm which showed similar LVEDD in children of USA. Further results showed Zimbabwean children had a thicker interventricular septum compared to German children. Although the findings showed similar ranges but overall, the measurements specified variability in left ventricle dimensions across different populations. The study emphasized the necessity of standardized echocardiographic methods and BSA normalization techniques considering demographic differences to establish accurate reference values for the size of heart chambers.

These studies collectively boost our understanding of the mitral valve's anatomy, its variability, and the factors influencing its dimensions and function. This knowledge is indispensable for improving diagnostic accuracy and guiding clinical interventions for mitral valve disorders. These studies provide baseline data for mitral valve dimensions, which is valuable for cardiologists and surgeons in assessing valve conditions and designing prosthetic valves. The significant variation in the size and shape of mitral valves highlights the importance of personalized approaches in the design and implementation of replacement valves.

OPERATIONAL DEFINITIONS

1. Mitral valve:

The mitral valve is a complicated anatomical structure located where the left atrium and left ventricle unite. It is made up of a fibro-muscular annulus, two leaflets, tendinous chords, and papillary muscles that are all separate but connected (Rana and Robinson, 2020).

2. Mitral valve annulus:

The mitral annulus is a fibrous ring that serves as an attachment point of the mitral valve leaflets separating the left atrium from the left ventricle that changes shape during the cardiac cycle, thus marked as a flexible and dynamic structure that resembles a kidney bean from above but in 3-dimension it has a saddle shape. It comprises of anteroposterior dimension along with three-quarters of the medial-lateral dimension The posterior mitral annulus is closely located to the circumflex coronary artery on the posterolateral side and the coronary sinus on the posteromedial side. The mitral annulus is connected to the aortic and tricuspid valves through the aortomitral fibrosa and the right and left fibrous trigons. The maximum normal diameter of the mitral annulus along the medial-lateral axis is approximately 3.0 cm (Issa, Miller, and Zipes, 2019; Omran et al., 2010).

3. Mitral valve leaflets:

The mitral valve is commonly comprised of two leaflets: a shorter posterior leaflet attached to a wider surface and a longer anterior leaflet with a narrower base. The anterior mitral valve leaflet covers approximately 45% of the mitral annulus circumference, while the posterior mitral valve leaflet occupies the remaining 55%. The normal thickness of the mitral valve leaflets ranges from 3 to 5 mm (Omran et al., 2010; Shah, 2010).

4. Anterior mitral valve leaflet (AMVL):

The AMVL is markedly longer than the posterior mitral valve leaflet which is trapezoid in shape and segmented into three parts from lateral to medial that correspond to the posterior leaflet scallops, which are, A1, A2, and A3. It is linked with left and non-coronary aortic valve leaflets through aorto-mitral curtain (Karagodin, Singh, and Lang, 2020).

5. Posterior mitral valve leaflet (PMVL):

PMVL as compared to AMVL, has a greater circular base and shorter radial length giving it a crescentic shape. It is divided into three scallops with indentations between them, which are, lateral, central, and medial scallops designated as P1, P2, and P3 respectively. (Bahiraie et al., 2024).

6. Chordae tendineae:

The chordae tendineae are the strong fibrous attachments that link leaflets of the valve to papillary muscles of the ventricles to prevent the leaflets from inverting into the atrial chamber during systole. These chordae can be classified into three types according to their point of insertion. The primary chordae attach to the free edge of the leaflets, the secondary chordae attach to the rough surface of the leaflets, and the tertiary chordae attach solely to the base of the posterior leaflet. (Gunnal, Wabale, and Farooqui, 2015; Harb et al., 2017).

7. Papillary muscles:

The papillary muscles of the heart are anchored to the walls of the ventricles where they originate. These pillar-shaped muscles through chordae tendineae are linked to leaflets of the tricuspid and mitral valve ensuring proper cardiac functioning. They are two in number, anterolateral muscle, and posterolateral muscle. The anterolateral papillary muscle emerges from the sternocostal wall, while the posteromedial papillary muscle emanates from the diaphragmatic wall of the ventricle (Rich, and Khan, 2020; Saha, and Roy, 2018).

8. Commissures:

Commissures are regions where the anterior and posterior leaflets join together as they attach to the annulus (Carpentier, Adams and Filsoufi, 2010).

9. C-septal distance:

C-septal distance is the shortest distance between the septum and the coaptation of leaflets which is the point where the leaflets of the valve come together (Makhija et al., 2019).

10.Left ventricle:

The left ventricle is structured as a half-ellipsoid or cone-shaped structure and is longer and narrower than the right ventricle because it functions as a strong pump for carrying blood under high pressure. It commences from the atrioventricular groove as its base and extends up to the apex of the heart. It has an inlet protected by the mitral valve and an outlet protected by the aortic valve (Standring, 2020).

CHAPTER 3

METHODOLOGY

3.1 Study design:

A cross-sectional study design.

3.2 Subjects:

Both males and females aged between 18 to 75 years, fulfilling the inclusion criteria and allied with different ethnic backgrounds (Sindhi, Punjabi, Balochi, Pashtun, Urdu speaking, and Hindku) were included in the study. The participants undergoing routine echocardiography with minor complaints at NICVD were selected for the study.

3.3 Setting:

The study was conducted at the National Institute of Cardiovascular Diseases (NICVD), Karachi. It is the leading government-funded cardiac centre in Karachi, which is well-equipped with advanced facilities, cardiologists having specialized knowledge in cardiac imaging, and well-trained technicians.

3.4 Inclusion criteria:

- Both male and female
- Ages between 18 to 75 years
- Different ethnicities (Sindhi, Punjabi, Balochi, Pashto, Urdu speaking, and Hindku).

3.5 Exclusion criteria:

- History of previous mitral valve surgery and intervention
- Known structural abnormalities like mitral valve prolapse, Rheumatic heart disease, or congenital mitral valve malformation
- Pregnant women
- Athletes
- Physical limitations like severe obesity or chest wall deformation
- Poor imaging by 2D Transthoracic Echocardiography.

3.6 Duration of study:

- Individual study period: 1 hour per subject
- Total period of study: 6 months

3.7 Sample size estimation:

The sample size of 385 for the current study, "Evaluation of Mitral Valve Dimensions in the Tertiary Cardiac Centre of Karachi" was calculated based on the population size of 1,000,000. For this estimation, a maximum variation of 50% with a 95% confidence interval and a ±5% margin of error was considered to ensure statistical significance and generalizability and it was determined by the open-source calculator available at www.openepi.com, version 3.01-SSPropor.

Sample size n = [DEFF*Np(1-p)]/ [(d2/Z21-α/2*(N-1)+p*(1-p)]

3.8 Sampling technique:

Purposive sampling was employed in this study. Recruiting participants for this non-probability sampling was based on characteristics, like, age (18-75 years), gender, and ethnicity (Sindhi, Punjabi, Balochi, Pashto, Urdu-speaking, and Hindku) along with the health conditions appropriate to evaluate mitral valve and it subvalvular apparatus parameters. Participants coming to NICVD with minor cardiac problems undergoing echocardiography were selected while individuals with severe cardiac diseases, past mitral valve intervention, or structural abnormality were excluded. This approach ensured that the sample for evaluating the mitral valve and its subvalvular apparatus and its association with the demographic factors was significant and representative.

3.9 Human subjects and consent:

The study parameters and its rationale were explained in either English or Urdu by the principal investigator to each participant and then informed consent was obtained from all the participants by either signing or by inked thumb impression on the printed informed consent form. The research participants were free to discontinue being part of the study at any moment or to choose not to participate at all. Ethical approval was taken from the Institutional Review Board of NICVD and also from Bahria University Health Sciences (BUHS).

3.10 Materials:

Participants' consents were taken on the informed consent form available in both English and Urdu. The height and weight of the individuals were measured by using a weight and height scale (Figure 3.1). The study's parameters were all recorded on the subject evaluation form. For capturing cardiac measurement Cannon Aplio i600 CV echocardiography machine, frequency range 1-22 Mhz, iBeam, ApliPure+, CEUS: Quad view, Display modes 2D, 3D was used (Figure 3.2). SPSS software version 23.0 was used for statistical analysis.

Figure 3.1: Height and weight scale from the current study conducted at National Institute of Cardiovascular Diseases, Karachi (NICVD).

Figure 3.2: Echocardiographic machine from the current study conducted at NICVD, Karachi.

3.11 Parameters of the study:

The demographic parameters included age, gender, body surface area (m^2), and ethnicity. The body surface area was calculated using the Mosteller formula (Schmidt, and Schmidt, 2019), which is as follows:

$$BSA\ m^2 = (\sqrt{[(\text{height in cm} \times \text{weight in kg})/3600]})$$

The echocardiographic parameters included:

- Annular diameter (long-axis view):

  The parasternal long-axis view (PLAX) on echocardiography was obtained in the left lateral decubitus position (Figure 3.3) by placing the transducer perpendicular to the left sternal border at the third or fourth intercostal space on the chest wall. The probe was adjusted in a way that the transducer orientation marker was pointing toward the patient's right shoulder to visualize the left atrium and left ventricle (Figure 3.4 A). The PLAX view showed the left atrium, left ventricle, and mitral valve from the base of the heart to the apex along with the aortic valve, left ventricular outflow tract (LVOT), and parts of ascending and descending aorta (Figure 3.4 B). The annular diameter of the mitral valve in the PLAX view was measured where the leaflets of the mitral valve are attached to the annulus (seen as a round or elliptical structure) in end-diastole by using the caliper tool on the echocardiographic machine. First, the caliper was placed on the inner edge of the annulus at the septal aspect, and second at the lateral aspect on the inner edge of the annulus (Figure 3.5).

- Annular diameter (4-chamber view):

  The apical or 4-chamber view is obtained on echocardiography, first by positioning the patient in the left lateral decubitus position. The transducer was placed on the chest oriented towards the left flank at the point of maximal impulse just below the left nipple that signifies the apex of the heart in the 5^{th} intercostal space in midclavicular line (Figure 3.6 A). This view gave excess to all four heart chambers, the right and left atrium and right and left ventricle along with the tricuspid and mitral valve (Figure 3.6 B). The annular diameter of the mitral valve was measured in the 4-chamber view in the end-diastolic phase between the hinge points of both leaflets at the annulus along the coaptation line (the line where the anterior and posterior leaflet come together to close the ventricle during systole) as seen in Figure 3.7.

- Annular area:

  According to the study (Sadeghpour, et al., 2008), the annular area was calculated by the formula:

  $$(\text{MA area} = d1 \times d2 \times \pi/4)$$

  where d1= annular diameter (long-axis view) and d2 = annular diameter (4-chamber view).

Figure 3.3: Echocardiography done in the lateral left decubitus position for the current study conducted at NICVD, Karachi.

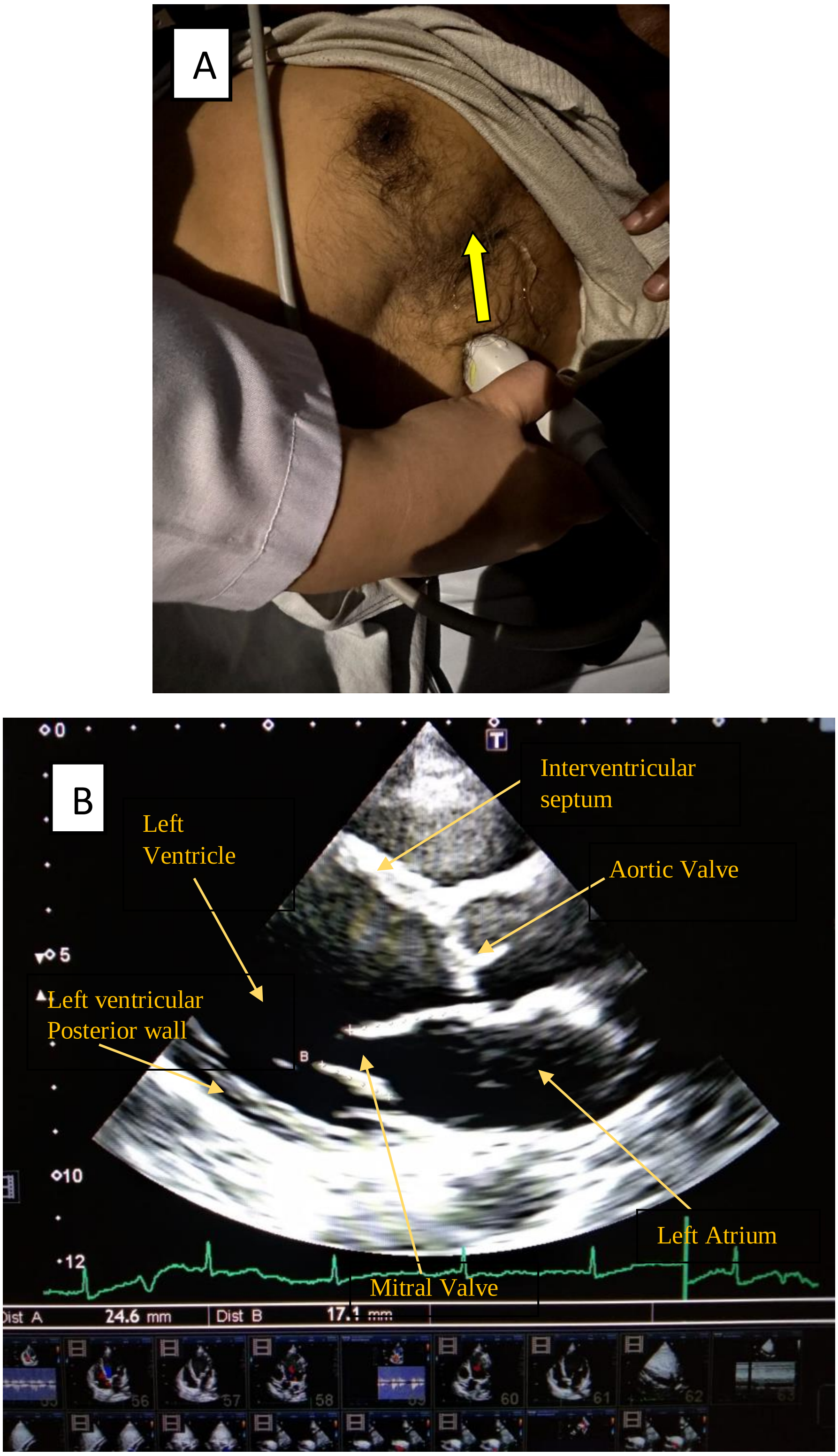

Figure 3.4: (A) Transducer position for parasternal long-axis view. (B) Echocardiographic image for a parasternal long-axis view from the current study conducted at NICVD, Karachi.

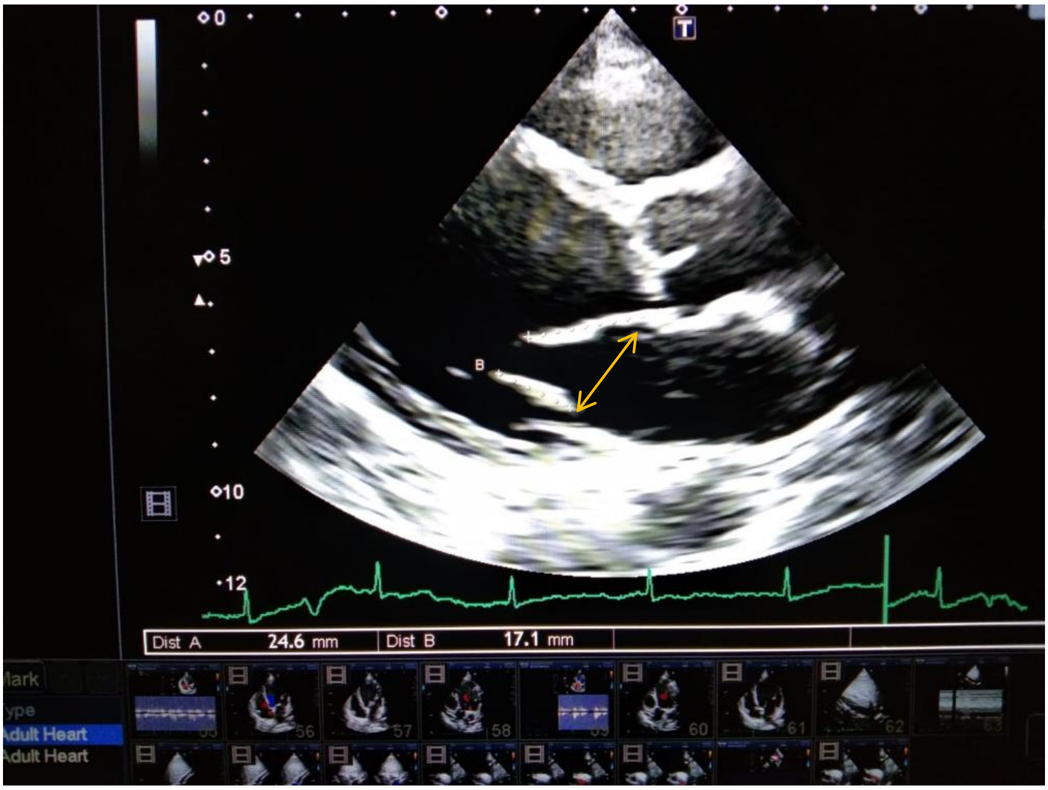

Figure 3.5: Echocardiographic image measuring an annular diameter in the parasternal long-axis view from the current study.

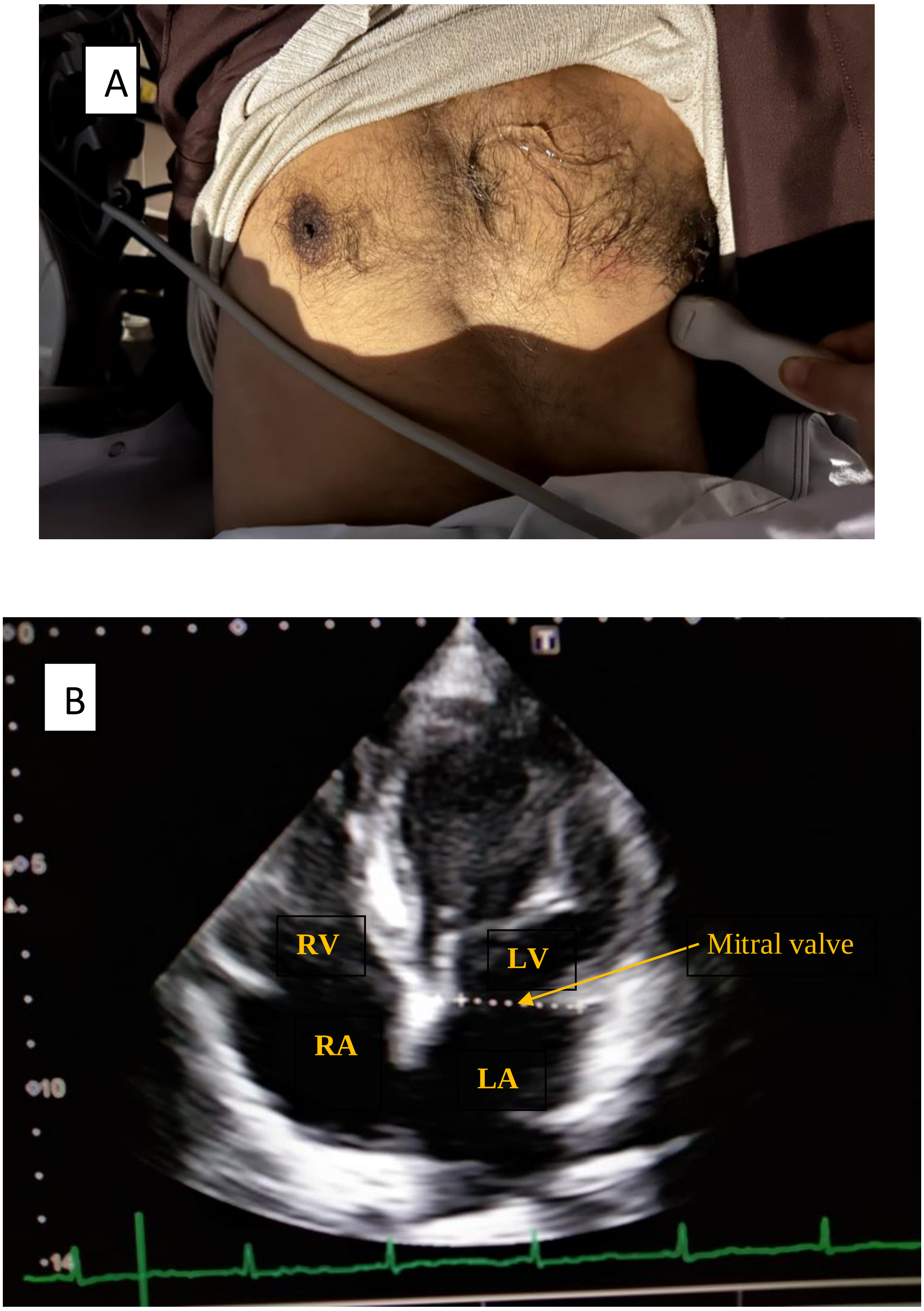

Figure 3.6: (A) Transducer position for 4-chamber view. (B) Echocardiographic image for a 4-chamber view from the current study conducted at NICVD, Karachi. RV=right ventricle; RA=right atrium; LV=left ventricle; LA=left atrium.

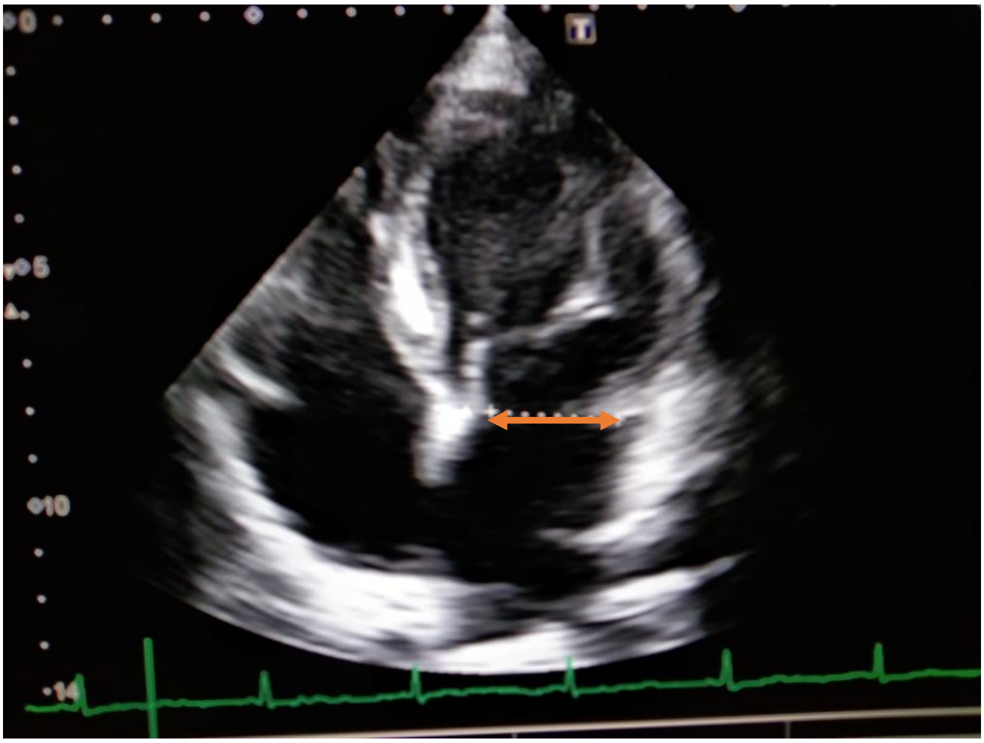

Figure 3.7: Echocardiographic image measuring an annular diameter of mitral valve in a 4-chamber view from the current study conducted at NICVD, Karachi.

- Anterior leaflet length:

  The anterior leaflet length of the mitral valve was measured in PLAX view in the end-diastolic phase (valve is relaxed and open) with the caliper extending from the hinge point of the leaflet at the annulus to its free edge (Figure 3.8 A).

- Anterior leaflet thickness:

  The anterior leaflet thickness of the mitral valve was also measured in PLAX view in the end-diastolic phase perpendicular to the surface of the leaflet at the midpoint (Figure 3.8 B).

- Posterior leaflet length:

  The posterior leaflet length of the mitral valve was also measured in the PLAX view from the attachment of the leaflet at the annulus to its free edge in the end-diastolic phase of the cardiac cycle (Figure 3.8 A).

- Posterior leaflet thickness:

  The posterior leaflet of the mitral valve thickness is measured in the end-diastole phase in the PLAX view at the midpoint of the leaflet (Figure 3.8 A).

A

B

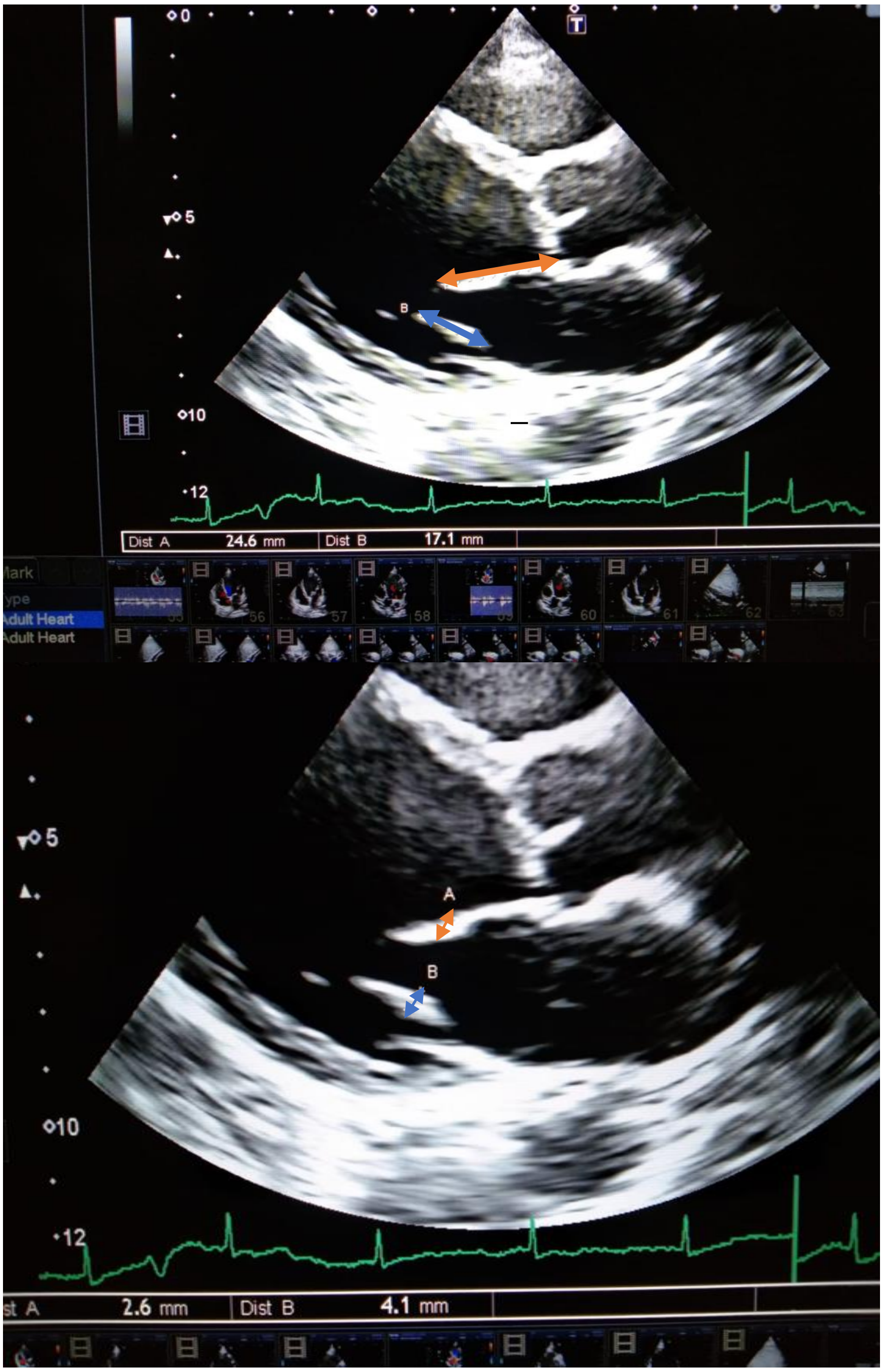

Figure 3.8: Echocardiographic image of PLAX view measuring (A) anterior (orange arrow) and posterior (blue arrow) leaflet length (B) anterior (orange arrow) and posterior (blue arrow) leaflet thickness from the current study conducted at NICVD, Karachi.

- Intercommissural distance:

  The distance between two commissures was measured in parasternal short-axis (PSAX) view which was obtained in the left lateral decubitus position by rotating the transducer 90 degrees clockwise from the position of the transducer on the chest after acquiring the PLAX view so that the transducer is indicated towards the left shoulder (Figure 3.9 A). This view gave excess to the left ventricle with papillary muscles, both anterior and posterior leaflet of the mitral valve when closed and open, other than these, the aortic valve, tricuspid valve, right ventricular outflow tract, and left atrium (Figure 3.9 B and C). The intercommissural distance was measured from anterior to posterior commissures between two leaflet attachments to each other laterally in the diastole phase in which the mitral valve resembles an open fish mouth (Figure 3.10).

- C-septal distance:

  The c-septal distance was measured in PLAX view at systole when the leaflets of the mitral valve were closed and the caliper was extended from the interventricular septum to the coaptation point of the mitral valve (Figure 3.11).

- Interpapillary distance:

  The interpapillary distance was measured in PSAX view when the transducer was set at the level of papillary muscle between the tips of both papillary muscles in the end-systolic phase (Figure 3.12).

- Systolic dimension of the left ventricle:

  The systolic dimension is measured in PLAX view from the inner side of the interventricular septum to the inner side of the posterior wall of the left ventricle (Figure 3.13).

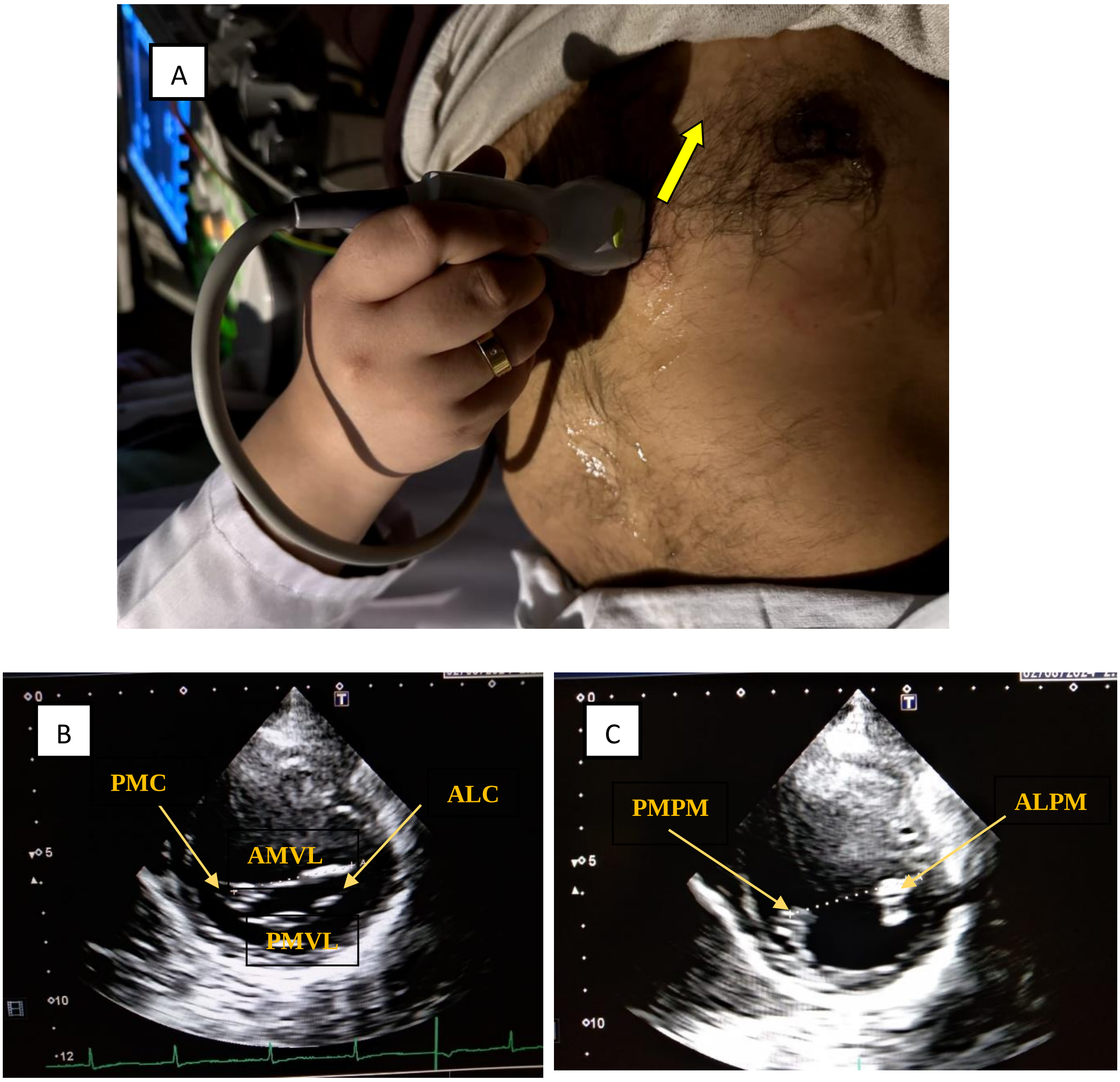

Figure 3.9: (A) Transducer position for a parasternal short-axis view. (B) Echocardiographic image for parasternal shot-axis view at the level of the mitral valve. (C) Echocardiographic image for parasternal shot-axis view at the level of the papillary muscles from the current study conducted at NICVD, Karachi. ALC=anterolateral commissure, PMC=posteromedial commissure; AMVL=anterior mitral valve leaflet, PMVL=posterior mitral valve leaflet, ALPM=anterolateral papillary muscle, PMPM=posteromedial papillary muscles.

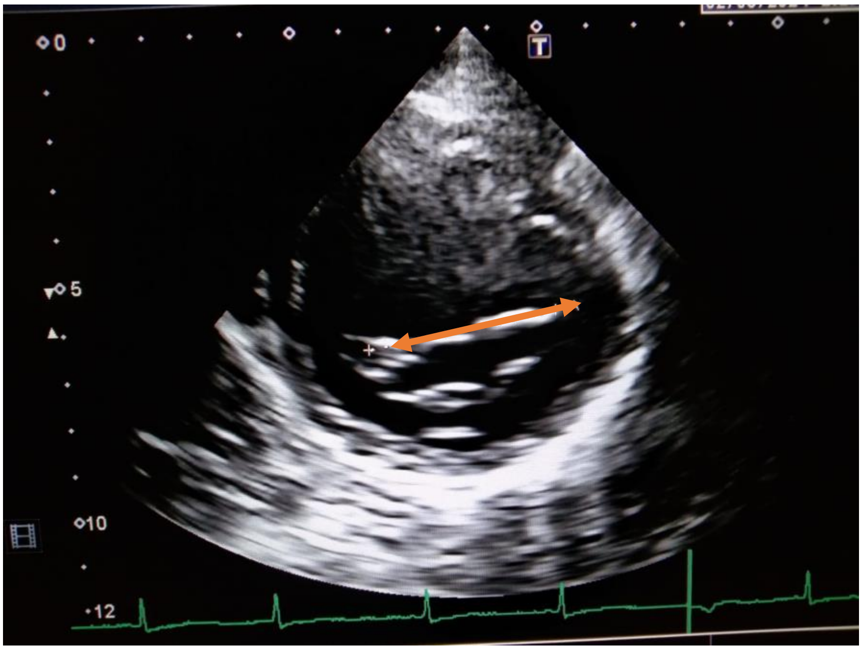

Figure 3.10: Echocardiographic image measuring intercommissural distance in parasternal short-axis view from the current study conducted at NICVD, Karachi.

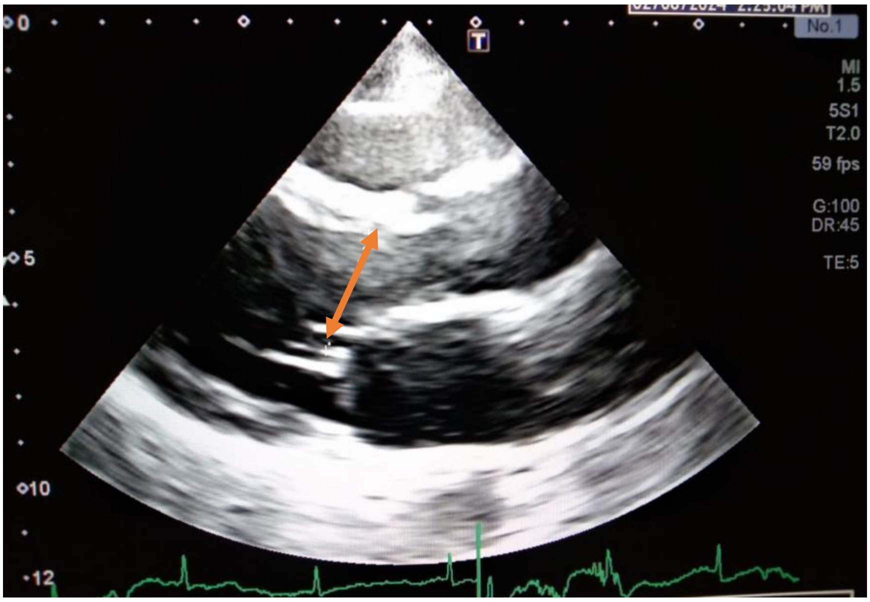

Figure 3.11: Echocardiographic image measuring c-septal distance in the parasternal long-axis view from the current study conducted at NICVD, Karachi.

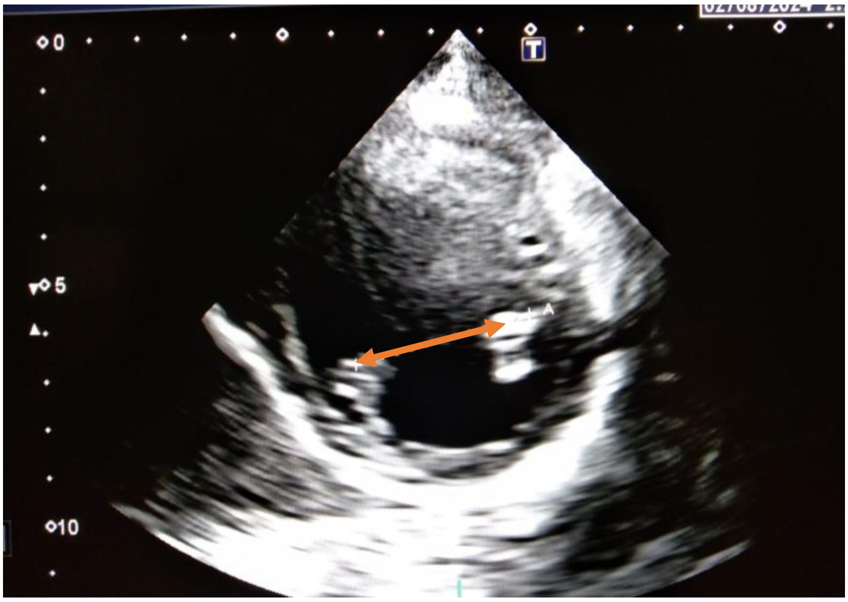

Figure 3.12: Echocardiographic image measuring interpapillary distance in parasternal short-axis view from the current study conducted at NICVD, Karachi.

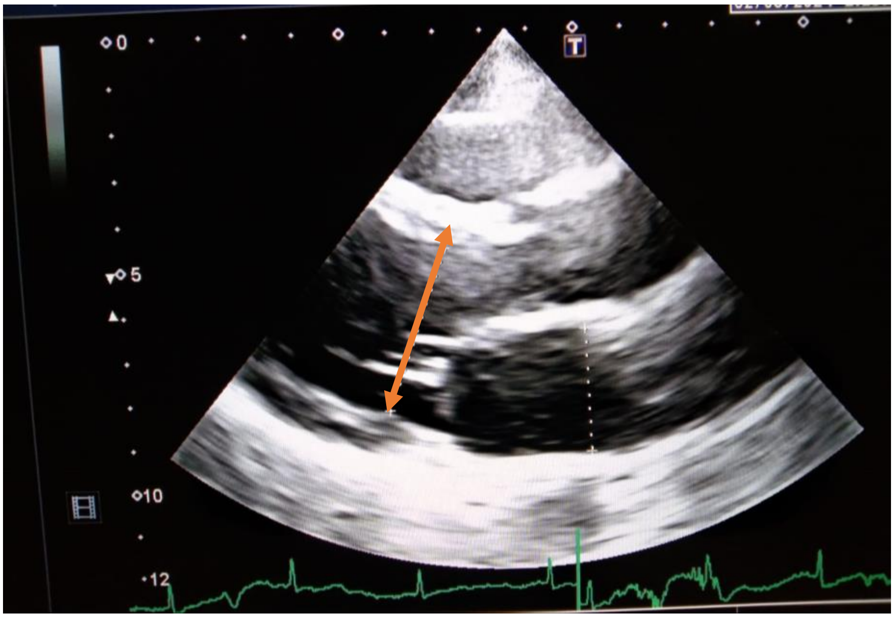

Figure 3.13: Echocardiographic image measuring systolic dimension of the left ventricle in parasternal long-axis view from the current study conducted at NICVD, Karachi.

- Diastolic dimension of the left ventricle:

  Similar to the systolic dimension, measured in PLAX from the atrioventricular septum to the posterior wall of the left ventricle but in the end-diastolic phase (Figure 3.14).
- Septal thickness:

  The septal thickness was measured in PLAX in the end-diastolic phase as shown in Figure 3.14.
- Posterior wall thickness of Left Ventricle:

  The posterior wall thickness was also measured at the end-diastole phase in the PLAX view, shown in Figure 3.14.

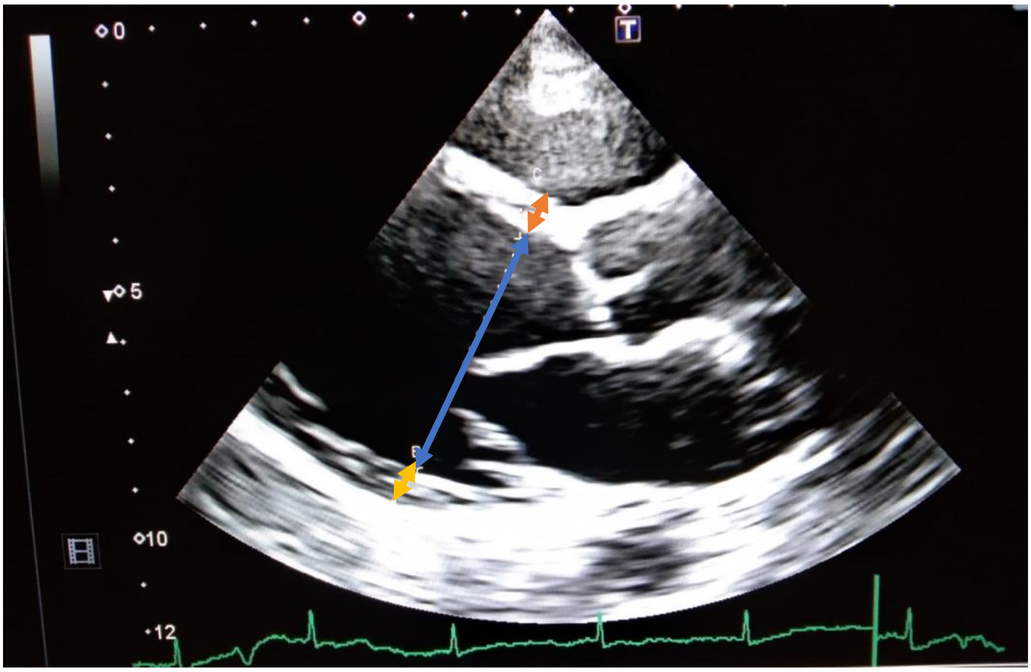

Figure 3.14: Echocardiographic image measuring: interventricular septum (orange arrow), diastolic dimension of the left ventricle (blue arrow) and posterior wall thickness of the left ventricle (yellow arrow) in the parasternal long-axis view from the current study conducted at NICVD, Karachi.

3.12 Protocol of the Study:

Participants fulfilling the inclusion criteria, undergoing routine 2D transthoracic echocardiography with minor complaints at NICVD were included in the study. After explaining the procedure, rationale, risks, and benefits of the study, informed consent was obtained on a consent form. Height and weight were measured using the height and weight scale as seen in Figure 3.1.

The participant was then asked to lie in a left lateral decubitus position on an examination bed to achieve maximum access to the heart so that good-quality views were obtained. Three ECG electrodes were placed in the direction of the right arm, left arm, and left leg to monitor the electrical activity of the heart during the echocardiography. A transducer was placed at various positions on the chest after applying conductive gel to obtain heart images from various angles. A cardiologist with expertise in Advanced Cardiac Imaging performed the Transthoracic Echocardiography and measured the following parameters: annular diameter both in long-axis and 4-chamber view, anterior and posterior mitral valve leaflet lengths and thicknesses, intercommissural distance, C-septal distance, and interpapillary distance. Additionally, systolic and diastolic dimensions of the left ventricle, septal thickness, and posterior wall thickness of the left ventricle were also measured. Three readings of each parameter were taken for accuracy. These readings were documented on the subject evaluation form along with demographic factors. All the results were incorporated and analyzed using SPSS version 23.0.

3.13 Algorithm of study:

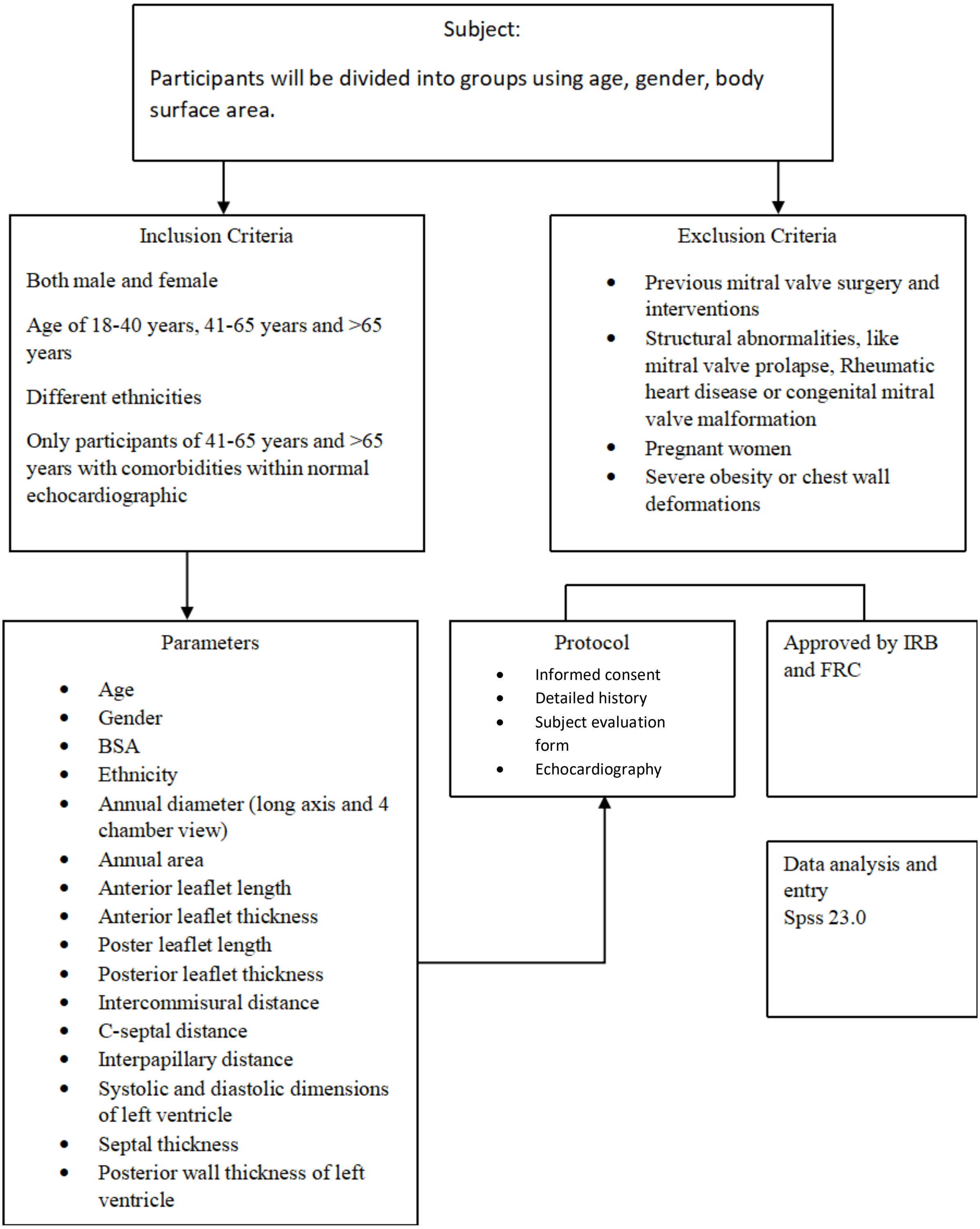

3.14 Statistical analysis:

SPSS version 23.0 was used to analyze all of the data. To check the normality of the data Kolmogorov-Smirnov and Shapiro-Wilk test was applied. Descriptive statistics were generated and due to the non-normality of the data non-parametric tests were applied. Mann-Whitney U test and Kruskal-Wallis test were applied to compare two independent and more than two independent tests respectively. To determine the correlation between mitral valve parameters and left ventricle parameters Spearman's correlation coefficient test was applied. The level of statistical significance (p-value) was set at < 0.05.

CHAPTER 4

RESULTS

For the current cross-sectional study, the selected sample size was 385 in total, in which gender was divided into a way that men were 182 and female were 203 (Figure 4.1). The study participants were classified into 4 groups according to age:18 -30 years, 31- 45 years, 46 –65 years, and >65 as young adults, middle-aged adults, older adults, and elderly respectively (Figure 4.2). In the age group of 18-30 years, a total of 38 participants were included making up for 9.9% of the entire sample population out of which 20 were men (11 %) and 18 were females (8.9%). There was a marked difference in gender distribution in the age group of 31 - 45 years, having 37 males (20%) and 71 females (35.0%) and overall it accounted for about 28.1% (N=108) of the sample size. The largest number of participants were included in the 46 - 65 years age group, which constituted a total of 190 individuals accounting for about 49.4% of the entire sample with uniform distribution among males and females which was 95 individuals for each gender. In the elderly age group (>65 years), 49 (12.7%) individuals were included out of which 30 were males and 19 were females accounting for about 16.5% of males and 9.4% of females for the total sample (Figure 4.3). This analysis of the division of participants by age and gender showed diversity in the age distribution with differing gender proportions across distinct age groups, such as, the majority of individuals were included in the 46 – 65 years age group with a uniform gender distribution; a majority of females were included in the age group of 31 -35 years which also showed significant representation while the other two groups 18 -30 years and >65 years exhibited lower representation than other in the study population. The Pearson Chi-Square test was applied and showed a p-value of 0.007 indicating that across the participants of the study, the association between gender and age was significant.

Moreover, as shown in the Figure 4.4, the distribution of the males and females across different ethnicities was also analyzed. The different ethnicities included Sindhi (N=48), Punjabi (N=53), Balochi (N=16), Pashtun (N=53), Urdu speaking (N=198), and Hindku (N=17). Among Sindhi, 24 (13.2%) participants were males while 24 participants with a percentage of 11.8% were females, making a total of 13.5% of the study population. Punjabis accounted for about 13.8% of the entire sample with 30 (16.5%) males and 23 (11.3%) females. In Balochi, 6 (3.3%) males were included with 10 (4.9%) females, constituting a total of 4.2%. Among all the ethnicities, Urdu-speaking represented the largest proportion of the study population constituting 51.4% of the total sample of which 91 (50%) were males and 107 (52.7%). And lastly, Hindku (4.4%), included 9 (4.9%) male and 8 (3.9%) female participants. No statistically significant association was observed between ethnicity and gender when the Chi-Square test was conducted.

The current study also analyzed the distribution of the participants between the genders with a family history of cardiac diseases as shown in the Figure 4.5, among which 85 males reported having a family cardiac history accounting for 46.7% of the study sample while 53.3% of males (N=97) were devoid of any cardiac history. 68 (33.5%) female participants declared having a family cardiac history while 135 (66.5%) had no history. This concluded that the majority of men presented with a family history of cardiac disease as compared to females but an overall greater proportion of both males and females revealed no cardiac history among family members. Thus, 153 individuals had a family history of cardiac diseases making up 39.7% and 232 participants were free of any family cardiac history accounting for about 60.3% of the entire study population. Pearson's Chi-Square test showed a significance of 0.008, representing a significant association between gender and a family history of cardiac diseases.

Smoking status among males and females was also analyzed. Out of 182 male participants, 76 (41.8%) males testified as smokers while 106 (58.2%) were non-smokers, and out of 203 female participants 7 (3.4%) were smokers while non-smokers among females were 196 (96.6%) showing higher prevalence of smoking among males as compared to women whose larger proportion comprises of non-smokers. On the whole, 83 (21.6%) individuals were smokers while 302 (78.4%) individuals included non-smokers (Figure 4.6).

As shown in the Figure 4.7, the study also identified the distribution of male and female participants according to their comorbidities. A total of 248 (64.4%) of the study population documented having no comorbidities, among these 128 (70.3%) participants were reported to be males with a higher percentage than females who were 120 in number with a percentage of 59.1%. Diabetes mellitus was diagnosed in 2.2% of males and 3.9% of females, with a total of 3.1% of the sample population; hypertension was documented in 15.4% of males and 20.2% of females, constituting 17.9% of the entire sample and the combination of diabetes and hypertension was recorded in 7.7% of the male participants and 9.9% of females, making up 8.8% of the entire sample. Other comorbidities included hypothyroidism, tuberculosis (TB), ischemic heart disease (IHD), chronic kidney disease, asthma, liver transplant, and atrial septal defect (ASD). The data specified that the majority of respondents registered no comorbidities hypertension being the most common comorbidity indicated among the participants, then diabetes and hypertension combined concurrently.

The Kolmogorov-Smirnov and Shapiro-Wilk tests were conducted to evaluate the normality of continuous variables of the data. Significant deviation was observed among most of the variables, especially the posterior wall thickness of the left ventricle which exhibited severe deviation from a normal distribution. The significant p-values of less than 0.05 (especially Kolmogorov-Smirnov p-values) for most of the continuous variables were documented for both tests which did not fulfill the criteria of normality thus non-parametric tests were applied as shown in Table 4.1.

Further Table 4.2, presents a detailed rundown of the statistical analysis for the measured echocardiographic measurements of the mitral valve and left ventricle in the 385 participants included in the current study. The table comprises metrics of central tendency and distribution of all the parameters for understanding the variability associated with these parameters. The body surface area (BSA) being the continuous variable was also analyzed and showed a mean of 1.753 with a standard deviation of 0.203, a minimum BSA of 1.17 and a maximum of 2.52, and a median of 1.75 in the entire study sample (Table 4.3) and Table 4.4, presents measurement of body surface area based on gender with males having mean rank of 221.29 larger than female that showed mean rank of 167.63.

The results for echocardiographic parameters were as follows:

1. Annular diameter long axis: The mean of the annular diameter in the parasternal long-axis view was found to be 27.7 mm with a standard deviation of 4.38 mm, a minimum measurement of 15.0 mm, and a maximum measurement was 49.0 mm. The median was estimated to be 28.0 mm with IQR (Interquartile Range) of 5.50 mm. The Q1 (25^{th} percentile) shows that 25% of the annular diameter measured in the study sample was equal to or less than 24.5 mm while Q3 (75^{th} percentile) indicated that measurements were less than or equal to 30 mm. The central value, median (Q2), which is 50^{th} percentile was 28.0 mm which means that the 50% values of the measurements were below 28.0 mm and 50% above this value. This result reflected moderate variability in annular diameter in long-axis view measurements among the study participants.
2. Annular diameter (4-chamber): The mean of 30.02 mm was measured for the annular diameter in the study participants with a standard deviation of 4.501 mm, spanning from a minimum value of 17.0 mm to a maximum of 46.0 mm. The results showed a wider range of measurements as the median was calculated to be 30.0 mm with IQR (6.00 mm) extending from 27.0 mm to 33.0 mm when compared with the measurements of the annular diameter in the long-axis view.
3. Annular area: The mean of the annular area measurement was 655.346 mm^2 with a standard deviation of 172.47 mm^2. The minimum value of measurement was 111.94 mm^2 and the maximum was 1408.29 mm^2. Substantial variability was seen in the measurements of the annular area among involved individuals as the median was found to be 637.42 mm^2 and IQR (216.66 mm) ranged between 532.63 mm^2 and 749.11 mm^2.

4. Anterior leaflet length: The mean of 19.09 mm for the length of the mitral valve anterior leaflet was documented with a standard deviation of 4.35 mm and 2.0 mm of minimum value and 36.0 mm of maximum value for the anterior leaflet length. A wide range of variability was observed as the median was measured to be 19.0 mm with IQR (5.60 mm) ranged between 16.4 mm and 22.0 mm.
5. Anterior leaflet thickness: The mean thickness of the anterior leaflet of the mitral valve was found to be 2.70 mm among participants with a standard deviation of 1.30 mm, and measurement values extending from a minimum of 0.2 mm and a maximum of 20.0 mm. The median was documented to be 2.7 mm and IQR (1.10 mm) ranged from 2.0 mm to 3.1 mm, indicating variability across the study population.
6. The posterior leaflet length: The mean of posterior mitral valve leaflet length measurements was found to be 16.1 mm with a standard deviation of 3.62 mm, the measurement values extending from 5.8 mm to 30.0 mm. The variability of posterior leaflet length was moderate as the median was 16.0 mm and IQR (4.20 mm) spanned between 14.0 mm to 18.25 mm.
7. Posterior leaflet thickness: The posterior mitral valve leaflet had a mean thickness of 2.75 mm with a standard deviation of 1.97 mm, a minimum of 0.2 mm, and a maximum of 37.0 mm thickness. A wide variability was observed in the thickness of the posterior leaflet the median was found to be 2.8 mm and IQR (1.20 mm) extended from 2.0 mm to 3.2 mm.
8. Intercommissural distance: The intercommissural distance measurements ranged from 17.0 mm to 41.6 mm with a mean of about 31.14 mm with a standard deviation of 4.34 mm. The median was found to be 31.0 mm and IQR (5.00 mm) was between 29.0 mm and 34.0 mm. This represented moderate variability in the intercommissural distance measurement among the participants.
9. C-septal distance: The minimum measurement taken for the C-septal distance was 16.0 mm and the maximum was 39.0 mm with a mean of 26.49 mm with a standard deviation of 4.1 mm. A moderate variability was documented in the C-septal distance with a median of 26.0 mm and IQR (6.10 mm) between 23.5 mm and 29.5 mm.

10. Interpapillary distance: A mean of 30.18 mm was found for measured interpapillary distance among participants with a standard deviation of 5.11 mm. The lowest measurement was found to be 12.0 mm and the highest was 45.9 mm. A broader range of variability in the interpapillary distance was noted as the median was 30.0 mm and IQR (7.00 mm) was between 27.0 mm and 34.0 mm.

11. Systolic dimension of the left ventricle: The dimension of the left ventricle in the systolic phase had a mean of 28.5 mm among the participants with a standard deviation of 5.28 mm. The minimum dimension was 16 mm while the maximum dimension was 55.7 mm. During systole, variability was noted in the size of the left ventricle and the measured sizes had a median of 28.0 mm, and IQR (7.00 mm) spanning between 25.0 mm and 32.0 mm was found.
12. Diastolic dimension of the left ventricle: The dimension measured of the left ventricle in diastole had a mean of 42.15 mm with a standard deviation of 5.8 mm, with a lowest measured dimension of 9 mm and a highest of 61.8 mm. The result represented a significant variability in the size of the left ventricle during systole with a median of 42.0 mm and IQR (7.00 mm) between 39.0 mm and 46.0 mm.
13. Septal thickness: The mean thickness was 8.35 mm with a standard deviation of 5.8 mm in participants. The minimum thickness measured was 4 mm and the maximum was 11 mm. The median was 8.0 mm and IQR (2.20 mm) was between 7.0 mm and 9.2 mm, this indicated less variability among the participants in the septal wall thickness.
14. Posterior wall thickness of the left ventricle: The mean thickness of the posterior wall of the left ventricle was about 8.49 mm in the individuals included in the study with a standard deviation of 4.37 mm. The measurements ranged from 4.0 mm to 9.1 mm. Even posterior wall thickness showed variability. It had a median of about 8.0 mm and IQR (1.80 mm) between 7.2 mm and 9.0 mm.

It demonstrated a comprehensive analysis of measurements of the echocardiographic parameters. Although the data was not normally distributed, the mean and standard deviation of the measurements were noted along with the median and interquartile range to provide a detailed analysis of the data distribution. Overall, the results presented a wide range of values and variability across echocardiographic parameters, accentuating the diversity in the heart's mitral valve and its geometry along with the left ventricle anatomy in the studied population.

In the current study, all echocardiographic parameters were compared between genders. Table 4.5 demonstrates these comparisons in ranks and the sum of ranks as Mann-Whitney U test was applied. The study represented that the annular diameter (long-axis) in males had a mean rank of 201.49 (sum of ranks= 36671.50) which was higher than females who had a mean rank of 185.39 (sum of ranks=37633.50) but no significant difference were found in the annular diameter (long-axis) between males and females as the p-value was 0.15. Similarly, the annular diameter (4-chamber) and annular area in males had a mean rank of 197.51 (sum of ranks=35947.0) and 197.4 (sum of ranks=35926.0) respectively, which was higher as compared to females who had a mean rank of 188.96 (sum of ranks=38358.0) for annular diameter (4-chamber) and mean rank of 189.06 (sum of ranks=38379.0) for the annular area. The p-value for the annular diameter (4-chamber) was 0.451 and for the annular area was 0.463, showing no significant difference. Further, males had a mean rank of 200.22 (sum of ranks=36440.0) and females had a mean rank of 186.53 (sum of ranks=37865.0) for the anterior leaflet length of the mitral valve with a p-value of 0.227 while for anterior leaflet thickness, males had a mean rank of 196.18 (sum of ranks=35705.0) and females had 190.15 (sum of ranks=38600.0) with a p-value of 0.593, indicating no significance. For posterior leaflet of the mitral valve had a mean rank of 207.94 (sum of ranks=37845.0) in males and 179.61 (sum of ranks=36460.0) in females with a p-value of 0.012, indicating a significant difference between the genders while posterior leaflet thickness of mitral valve showed no significance having mean rank of 192.63 in males and 193.33 in females with sum of ranks of 35058.0 and 39247.0 respectively with a p-value of 0.950. Intercommissural distance of the mitral valve showed a mean rank of 194.44 (sum of ranks=35388.50) in males and 191.71 (sum of ranks=38915.50) in females with a p-value of 0.809 while C-septal distance showed a mean rank of 218.63 (sum of ranks=39791.0) in males and 170.02 (34514.00) in females with a p-value of 0.000, which was highly significant. The interpapillary distance indicated no significance as the p-value was 0.798 having a mean rank of 191.47 (sum of ranks=34847.50) in males and 194.37 (sum of ranks=39457.50) in females. The measurements of the left ventricle showed significant differences between the genders, as for the systolic dimension of the left ventricle the mean rank in males was 211.25 (sum of ranks=38447.0) and in females was 176.64 (sum of ranks=35858.0) with a p-value of 0.002 and diastolic dimension of the left ventricle showed mean rank of 214.34 (sum of ranks=39010.50) in males and 173.86 (sum of ranks=35294.5) in females with a p-value of 0.000. Septal thickness indicated a mean rank of 214.19 (sum of ranks=38983.0) in males and 174.00 (sum of ranks=35322.0) with a p-value of 0.000 and for posterior wall thickness of left ventricle, the mean rank of 209.37 (sum of ranks=37687.0) in males and 176.60 (sum of ranks=35849.0) in females with a p-value of 0.003. In total, males showed higher ranking data of these echocardiographic parameters which means males tend to have larger measurements as compared to females but only posterior leaflet length, c-septal distance, systolic and diastolic dimension of the left ventricle, septal wall thickness and posterior wall thickness of left ventricle showed statistically significant difference between males and females which sum ranks was higher in females because of difference in sample size.

In Table 4.6, echocardiographic parameters measurements are compared between different age groups. The annular diameter (long-axis) showed mean rank of 154.62, 197.55, 200.59, and 183.31in the age groups of 18-30 years, 31-45 years, 46-65 years, and >65 years respectively, which represented the largest diameter in the age group of 46-65 years and smallest in the age group of 18-30 years but no significant difference as the p-value noted to be 0.113. For annular diameter (4-chamber) the mean rank of 172.07 was noted in 18-30 years of age which was lowest compared to other age groups, 31-45 years had the mean rank of 201.69 which was the largest, 46-65 years had a mean rank of 196.92 and >65 had 174.86 of mean rank with a p-value of 0.314. The annular area of the mitral had the mean rank of 160.91(smallest area) in 18-30, 203.57 (largest area) in 31-45, 197.51 in 46-65, and 177.11 in >65 with a p-value of 0.142. The mean rank of 199.61 (largest length) in the 18-30 years, 198.48 in the 31-45 years, 191.12 in 46-65 years, and 183.09 (smallest length) in >65 years of age group was noted with a p-value of 0.840. The anterior mitral valve leaflet thickness presented a mean rank of 180.87 in 18-30 years (lowest thickness), 192.41 in 31-45 years, 194.07 in 46-65 years, and highest in the >65 years group with a mean rank of 199.55 but with no significance as the p-value was 0.885. The mean rank of 174.17 in 18-30 years which showed the shortest length among different age groups for posterior mitral valve leaflet, 31-45 years had a mean rank of 194.92, 46-65 years had 199.23 (largest), and >65 years had 179.19. Similar to the anterior leaflet thickness, posterior leaflet thickness showed the lowest mean rank in the 18-30 years of age group while highest in the >65 years with a mean rank of 202.12, 31-45 had a mean rank of 190.22 and 46-65 had 200.85 and the p-value was noted to be 0.069. The 18-30 years age group participants had a mean rank of 204.87 (largest) for the intercommissural distance, 31-45 years had 201.21, 46-65 years had 192.82 and the lowest distance was noted in the >65 years age group with a mean rank of 166.39 with a p-value of 0.280. For c-septal distance, 18-30 years had a mean rank of 188.95, 31-45 years had 197.48, 46-65 years had 200.18 (largest) and >65 years had 158.44 (smallest) with a p-value of 0.124. Similarly, interpapillary distance did not present any statistical difference among age groups (p-value=0.067), 18-30 years had a mean rank of 223.70 (largest), 31-45 years had 201.44, 46-65 years had 189.71 and >65 years had 163.36 (lowest). The systolic dimension of the left ventricle showed no significance unlike the diastolic dimension of the left ventricle having a p-value of 0.072 and 0.045 respectively. The mean rank for the systolic dimension was 166.04 in 18-30 years, 206.06 in 31-45 years, 197.93 in 46-65 years, and 166.00 in the>65 years of age group while statistically significant differences among age groups were noted for the diastolic dimension of the left ventricle with a p-value of 0.045. The 18-30 years group had a mean rank of 183.34, the 31-45 years group had the largest diastolic dimension with a mean rank of 208.74, 195.57 mean rank in the 46-65 years and the smallest dimension was represented by the age group of >65 years with a mean rank of 155.84. The septal thickness and posterior wall thickness also showed statistically significant results among age groups. The mean rank of 161.54 (lowest) in the 18-30 years group, 178.21 in the 31-45 years, 202.62 in the 46-65 years and 212.67 (highest) in the>65 years of age group for septal thickness with a p-value of 0.043y. Similarly, for the posterior wall thickness of the left ventricle the 18-30 years had the lowest mean rank of 159.30, 31-45 years had 176.92, 46-65 years had 202.13, and >65 years had the largest mean rank of 211.93 indicating thickest posterior wall of the left ventricle was found in the age group of >65 years with a p-value of 0.034. These findings suggested significant age-related variations in the measurements of the left ventricle but no significant results for mitral valve measurement were noted.

Table 4.7, demonstrates the echocardiographic parameter measurement variability across different ethnicities. The results revealed the mean rank of 170.43 in Sindhi, 193.23 in Punjabi, 169.16 in Balochi, 208.79 in Pashtun, 194.01in Urdu speaking and 217.47 in Hindku for annular diameter in the long axis indicating the smallest diameter in Balochi and largest diameter in Hindku but with a p-value of 0.463. The annular diameter (4-chamber) showed statistically significant variation among the ethnic groups with a p-value of 0.012, the result exhibited the mean rank of 184.34 in Sindhi, 205.57 in Punjabi, 239.50 in Balochi, 218.89 in Pashtun, 176.62 in Urdu speaking, and 244.53 in Hindku. The Hindku ethnic group significantly had a larger annular diameter measured in a 4-chamber view while Urdu speaking had the smallest. The mean rank of 173.33 was noted in Sindhi (lowest), 206.17 in Punjabi, 210.19 in Balochi, 222.75 in Pushtun (highest), 182.82 in Urdu speaking and 217.15 in Hindku with a p-value of 0.114 for the annular area. For anterior leaflet length, the mean ranks among ethnic groups were as follows, 186.58 in Sindhi, 190.59 in Punjabi, 161.28 in Balochi (lowest), 210.72 in Pashtun, 189.79 in Urdu speaking, and 230.59 in Hindku (highest) with a p-value of 0.423. The anterior leaflet of mitral valve thickness showed mean ranks of 221.74 in Sindhi (highest), 187.92 in Punjabi, 140.06 in Balochi (lowest), 173.14 for Pashtun, 198.37 in Urdu speaking and 176.88 in Hindku with a p-value of 0.088. The mean rank for posterior mitral valve leaflet length was 192.88 in Sindhi, 196.81 in Punjabi, 162.53 in Balochi(lowest), 212.91 in Pashtun (highest), 189.45 in Urdu speaking and 189.47 in Hindku with a p-value of 0.671 while the mean rank of posterior mitral valve leaflet thickness was noted to be 202.18 in Sindhi, 175.62 in Punjabi, 152.03 in Balochi (lowest thickness), 166.08 in Pashtun, 207.37 in Urdu speaking (highest thickness) and 176.41 in Hindku with a p-value of 0.059, indicating no significant difference in length and thickness of the posterior mitral valve leaflets among the ethnic groups. For intercommissural distance, the mean ranks among ethnicities were 206.00 in Sindhi, 212.20 in Punjabi (highest), 192.94 in Balochi, 209.55 in Pashtun, 179.91 for Urdu speaking (lowest), and 197.38 in Hindku with a p-value of 0.288. For the c-septal distance, the mean ranks were 189.39 in Sindhi, 182.90 in Punjabi, 174.59 in Balochi (lowest), 217.55 in Pashtun (highest), 191.57 in Urdu speaking, and 192.74 in Hindku with a p-value of 0.922. The mean rank for interpapillary distance was 189.39 in Sindhi, 194.04 in Punjabi, 185.88 in Balochi (lowest), 217.55 in Pashtun (highest), 186.42 in Urdu speaking, and 206.82 in Hindku with a p-value of 0.599. The mean rank was noted as 187.60 in Sindhi, 191.69 in Punjabi, 196.34 in Balochi, 223.57 in Pashtun, 184.77 in Urdu speaking (lowest), and 209.74 in Hindku with a p-value of 0.345 for systolic diameter. For the diastolic dimension of the left ventricle, the mean rank was determined to be 175.82 in Sindhi (lowest), 177.80 in Punjabi, 194.97 in Balochi, 217.74 in Pashtun (highest), 198 in Urdu speaking and 211.21 in Hindku and a p-value of 0.389 which represented no significance. The septal thickness had a mean rank of 165.21 in Sindhi, 226.93 in Punjabi, 174. 0 in Balochi, 202.03 in Pashtun, 188.09 in Urdu speaking, and 212.59 in Hindku with a p-value of 0.077. While other left ventricle parameters showed no significant differences among different ethnic groups, posterior wall thickness documented statistically significant variations among ethnicities with a p-value of 0.006. The study showed a mean rank of 164.17 in Sindhi, 238.62 in Punjabi, 218.13 in Balochi, 183.88 in Pashtun, 183.70 in Urdu speaking, and 221.65 in Hindku that identified the thickest posterior wall of the left ventricle in Punjabi while the least thick wall in Sindhi. Out of all parameters, only the annular diameter measured in 4-chamber and the posterior wall thickness of the left ventricle represented statistically significant variation among the studied ethnic groups.

The variation of echocardiographic parameters concerning the family history of cardiac problems showed some significant results as shown in the Table 4.8. The annular diameter in the long axis and the annular diameter in the 4-chamber view along with the annular area showed significant variations concerning family cardiac history with a p-value of 0.001, 0.013, and 0.005 respectively. Participants with a family cardiac history had a mean rank of 215.73 (sum of ranks=33006.00), 210.55 (sum of ranks=32168.00), and 212.55 (sum of ranks=32519.50) for annular diameter (long-axis), annular diameter (4-chamber), and annular area respectively while participants with no family history had a mean rank of 178.01 (sum of ranks=33006.00), 181.63 (sum of ranks=42137.00), and 180.11 (sum of ranks=41785.50) respectively. This result reflected the potential tendency of annular diameters and annular area to be larger among the participants having a family cardiac history as compared those having no family history. For anterior leaflet length, anterior leaflet thickness, posterior leaflet length, and posterior leaflet thickness showed no significant association with family cardiac history and the mean rank for these parameters was noted to be 201.25 (sum of ranks=30791.00), 192.38 (sum of ranks=29434.00), 205.62 (sum of ranks=31459.50), 192.38 (sum of ranks=29425.00) respectively having family history while 187.56 (sum of ranks=43514.00), 193.41 (sum of ranks=44871.00), 184.68 (sum of ranks=42845.50) and 193.45 (sum of ranks=44880.00) respectively with no cardiac history. The p-value noted for anterior leaflet length was 0.237, 0.929 for anterior leaflet thickness, 0.070 for posterior leaflet length, and 0.922 for posterior leaflet thickness. Similarly, intercommissural distance, c-septal distance, and interpapillary distance in the participants having family cardiac history had the mean rank of 200.33, 204.48, and 198.58 respectively while participants having no family history had a mean rank of 188.16, 185.43, and 189.32 respectively. The p-value noted for intercommissural distance was 0.293, the c-septal distance was 0.10 and for interpapillary distance was 0.424, showing no significant results. On the other hand, systolic and diastolic dimensions showed statistically significant results. The mean rank for the systolic dimension of the left ventricle was found to be 212.51 (sum of ranks=32514.50) and 180.13 (sum of ranks=41790.50) in participants with family cardiac history and with no history, respectively with a p-value of 0.05 while for the diastolic dimension, the mean rank was 217.25 (sum of ranks=33238.50) and 177.01 (sum of ranks=41066.50) with a p-value of 0.001 in individuals with family history and individuals with no history respectively. These findings suggested the potential association of left ventricular dimension with a family cardiac history, having larger dimensions in the participants with a family history of cardiac problems. The septal thickness and posterior wall thickness had no significant association with a family cardiac history, as they had a mean rank of 195.93 (sum of ranks=29977.00) and 194.86 (sum of ranks=29423.50) respectively in individuals with family history and 191.07 (sum of ranks=44328.00) for septal thickness and 190.14 (sum of ranks=44112.50) for posterior wall thickness with no family history with a p-value of 0.671 and 0.680 respectively.

Table 4.9, shows the data of measurements of echocardiographic parameters in relation to smoking status among the study population. For annular diameter both in the long axis and 4-chamber, the mean rank among the smokers was found to be 208.99 (sum of ranks=17346.50) and 205.20 (sum of ranks=17031.50) and 188.60 (sum of ranks=56958.50) and 189.65 (sum of ranks=57273.50) in non-smokers respectively with a p-value of 0.139 for annular diameter (long-axis) and 0.259 for annular diameter (4-chamber). The mean rank for the annular area was 205.49 (sum of ranks=17055.50) in smokers and 189.57 (sum of ranks= 57249.50) in non-smokers with a p-value of 0.248. The mean rank for anterior leaflet length and thickness was found to be 189.20 (sum of ranks=15704.00) and 190.43 (sum of ranks=15806.00) in smokers and in non-smokers, it was found to be 194.04 (sum of ranks=58601.00) and 193.71 (sum of ranks=58499.00) with a p-value of 0.725 and 0.811 respectively. The mean rank for posterior leaflet length and thickness was documented to be 203.10 (sum of ranks=16857.50) and 186.23 (sum of ranks=15457.50) in smokers and 190.22 (sum of ranks=57447.50) and 194.86 (sum of ranks=58847.50) in non-smokers with a p-value of 0.350 for length and 0.530 for thickness. For intercommissural distance the mean rank was 203.52 (sum of ranks=16892.00) in smokers and 190.11 (sum of ranks=57413.00) in non-smokers with a p-value of 0.330. The c-septal in smokers had a mean rank of 215.28 (sum of ranks=17868.00) and in non-smokers, it was 186.88 (sum of ranks=56437.00) with a p-value of 0.039 that was statistically significant. For interpapillary distance, the mean rank was 191.69 (sum of ranks=15910.00) in smokers while in non-smokers was 193.36 (sum of ranks=58395.00) with a p-value of 0.903. The systolic and diastolic dimensions showed significant results with a p-value of 0.007 and 0.037 respectively, having mean rank of 222.07 (sum of mean ranks=18432.0) in smokers and 185.01 (sum of ranks=55873.0) in non-smokers for systolic dimensions and mean rank of 215.57 (sum of ranks=17892.50) in smokers and 186.80 (56412.50) in non-smokers. The findings indicate a significantly larger dimension in smokers as compared to non-smokers. The septal thickness and posterior wall thickness showed mean rank of 205.66 and 211.57 in smokers and 189.52 and 186.67 in non-smokers with a p-value of 0.235 and 0.67 respectively. On the whole, the smokers had larger values for the measured parameters as compared to non-smokers but only c-septal distance, systolic dimension, and diastolic dimension of the left ventricle showed a significant increase in smokers.

Further, the variations of the echocardiographic parameters were assessed with the co-morbidities of the participants. As shown in the Table 4.10, no significant results were found for co-morbidities although a higher mean rank of 287.50 was found in cancer patients for annular diameter (long-axis), the higher mean rank of 323.75 in asthma patients for annular diameter (4-chamber), cancer patients for the annular area (mean rank=284.67), coronary artery bypass grafting (CABG) for anterior leaflet length (mean rank=348.0) and also anterior leaflet thickness (mean rank=283.25), atrial septal defect for posterior leaflet length (mean rank=339.50), CABG for posterior leaflet thickness (mean rank=312.75), atrial septal defect for intercommissural distance (mean rank=327.50), asthma for c-septal distance (mean rank=213.75), atrial septal defect for interpapillary distance (mean rank=296.0), diabetes mellitus for systolic dimension of the left ventricle (mean rank=271.42), asthma for diastolic dimension (mean rank=297.00), ischemic heart disease for septal thickness (mean rank=258.70), and higher mean rank of 266.00 for posterior wall thickness was found in atrial septal defect patients.

The body surface area (BSA) was correlated with all the echocardiographic parameters by applying the non-parametric Spearman's correlation analysis. As shown in the Table 4.11, BSA correlated positively with most of the parameters, which included, annular diameter in the long axis (correlation coefficient=0.401), annular diameter in 4-chamber (correlation coefficient=0.418), annular area (correlation coefficient=0.481), anterior leaflet length (correlation coefficient=0.199), posterior leaflet length (correlation coefficient=0.246), intercommissural distance (correlation coefficient=0.273), c-septal distance (correlation coefficient=0.354), interpapillary distance (correlation coefficient=0.370), systolic dimension (correlation coefficient=0.336) and the diastolic dimension (correlation coefficient=0.443) of the left ventricle with a p-value of 0.000 suggesting larger BSA is associated with larger mitral valve and left ventricle parameters. The thickness parameters, anterior leaflet thickness, posterior leaflet thickness, septal thickness, and posterior wall thickness did not show any positive correlation with the BSA, indicating thickness do not vary with variation in the BSA of the individuals included in the study

Table 4.12, shows the correlation between the echocardiographic measurements of the mitral valve and left ventricle by using Spearman's rank correlation coefficients. The correlation between the annular diameter (long axis) and the systolic dimension of the left ventricle presented a coefficient of 0.400 with a p-value of 0.00. Similarly, the annular diameter (4-chamber) and annular area showed a coefficient of 0.262 and 0.377

respectively with a p-value of 0.000, suggesting that as the annular diameters and annular area increases, systolic dimension also tends to increase, showing a positive correlation between the parameters. The anterior leaflet length and thickness did not show any significant correlation with the systolic dimension having a correlation coefficient of 0.032 and 0.007 respectively and a p-value greater than 0.05. On the other hand, posterior mitral valve leaflet length showed a weak positive correlation with a coefficient of 0.205 and a p-value of 0.000 but posterior leaflet thickness did not correlate with the systolic dimension measurement with a coefficient of 0.032 and p-value of 0.525. Intercommissural distance, c-septal distance, and interpapillary distance were positively correlated with systolic dimension having a coefficient of 0.221, 0.314, and 0.264 respectively with p-value 0.000. The findings suggested that the positive correlation between annular diameters, annular area, posterior leaflet length, c-septal distance, intercommissural distance, and interpapillary with the systolic dimension of the left ventricle indicated the increase in one of these parameters tends to increase the size of the left ventricle in systole. Then the mitral valve parameters were correlated with the diastolic dimension of the left ventricle, in which the annular diameter both in the log-axis and 4-chamber along with annular showed a positive correlation with a coefficient value of 0.440, 0.259, and 0.424 respectively with a p-value of 0.000. The anterior and posterior leaflet lengths both showed a positive correlation with a coefficient of 0.152 (p-value=0.003) and 0.204 (p-value=0.000) respectively while the anterior leaflet thickness (correlation coefficient=0.029, p-value=0.574) and posterior leaflet thickness (correlation coefficient=0.029, p-value=0.574) did not show any positive correlation. Similar to the systolic dimension, the diastolic dimension also had a positive correlation with intercommissural distance (correlation coefficient=0.239), c-septal distance (correlation coefficient=0.280), and interpapillary distance (correlation coefficient=0.256) with a p-value of 0.000. For septal thickness, only the annular diameter (long-axis), annular area, posterior leaflet length, and c-septal distance showed significant results having a correlation coefficient of 0.276, 0.204, 0.109, and 0.188 with a p-value of 0.000 for annular diameter (long-axis), annular area and c-septal distance and a p-value of 0.032 for posterior leaflet length. Lastly, posterior wall thickness was correlated with the mitral valve parameters and showed a positive correlation with annular diameter (long-axis), annular area, and c-septal distance with a p-value of 0.00

and correlation coefficient of 0.269, 0.219, and 0.135 respectively. These positive correlations suggested an increase in the measurement of the mitral parameters tends to show an increase in measurements of left ventricle parameters on the echocardiography.

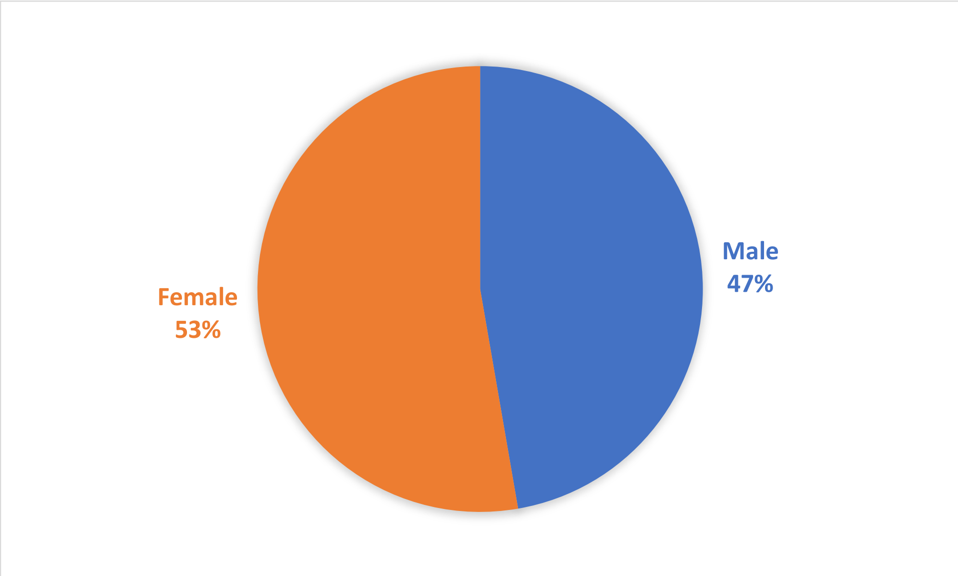

Figure 4.1: Gender distribution of participants within the study population

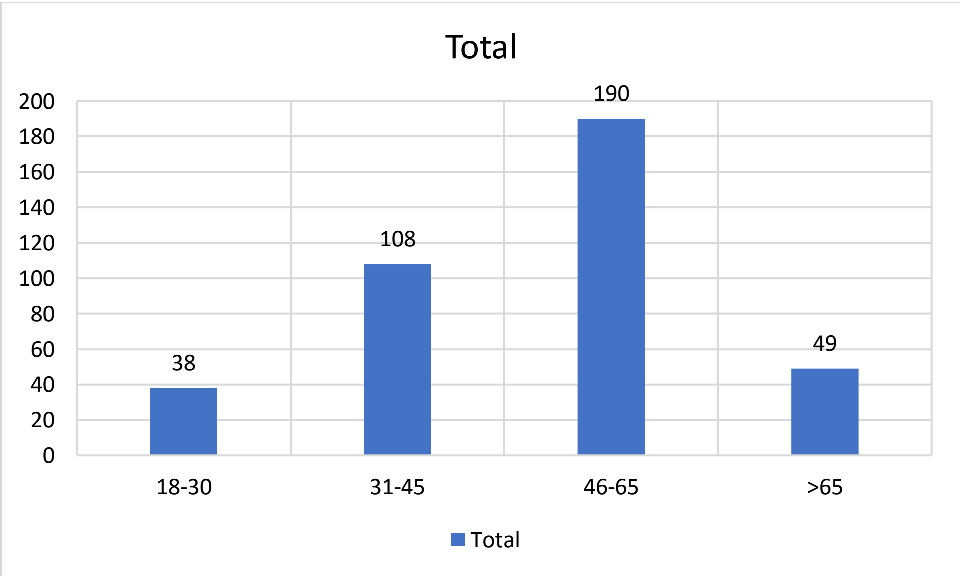

Figure 4.2: Distribution of study participants into age group (in years)

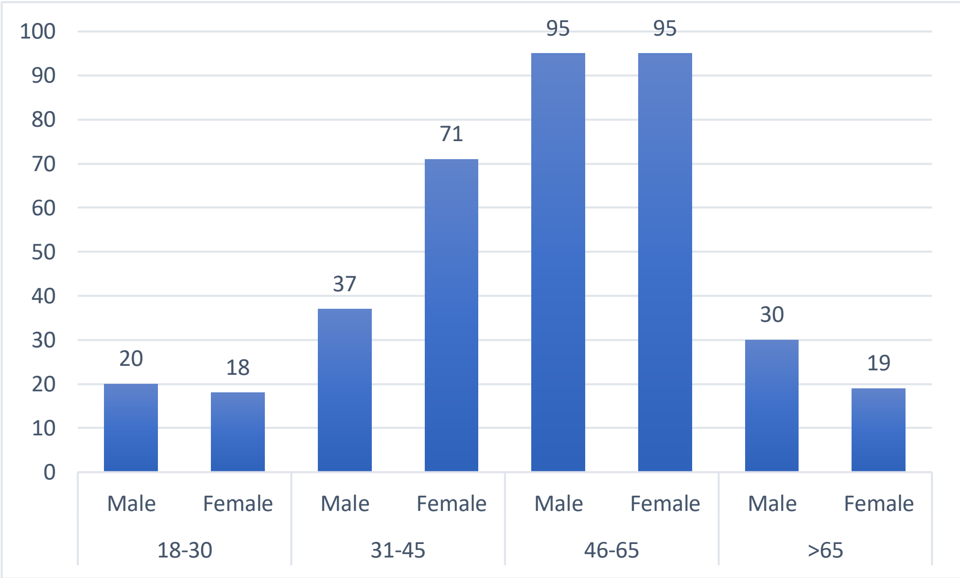

Figure 4.3: Gender distribution of participants within each age group (in years)

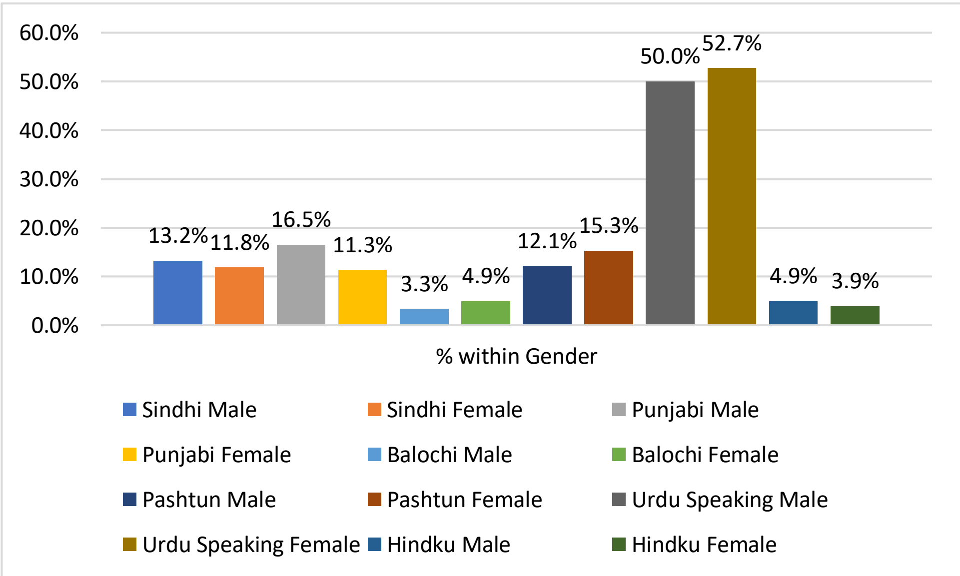

Figure 4.4: Distribution of study participants in Ethnicities

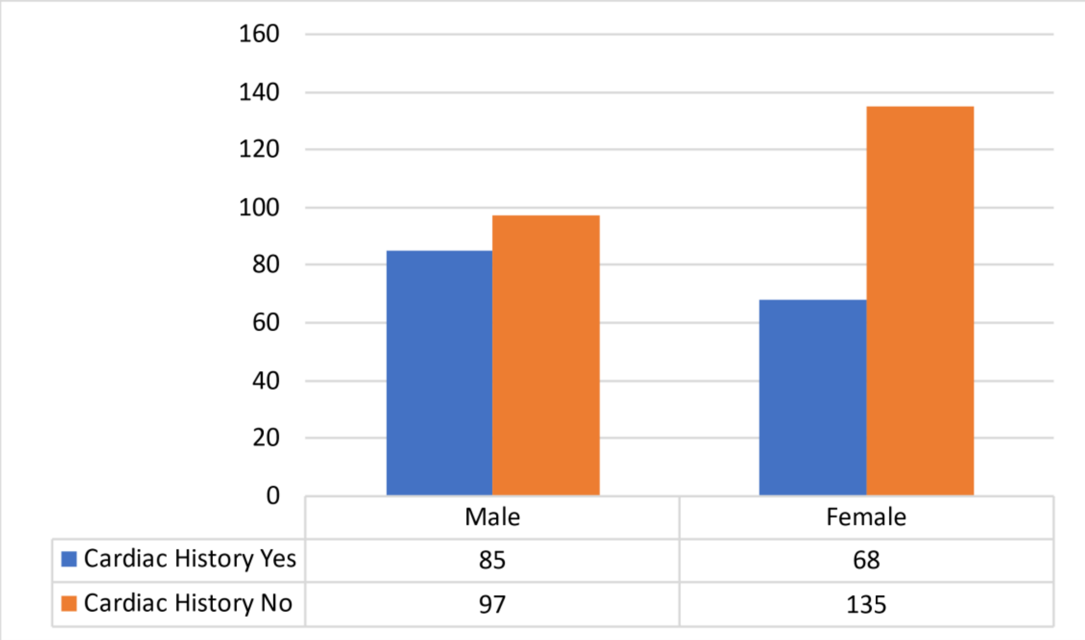

Figure 4.5: Distribution of study participants based on Family Cardiac history

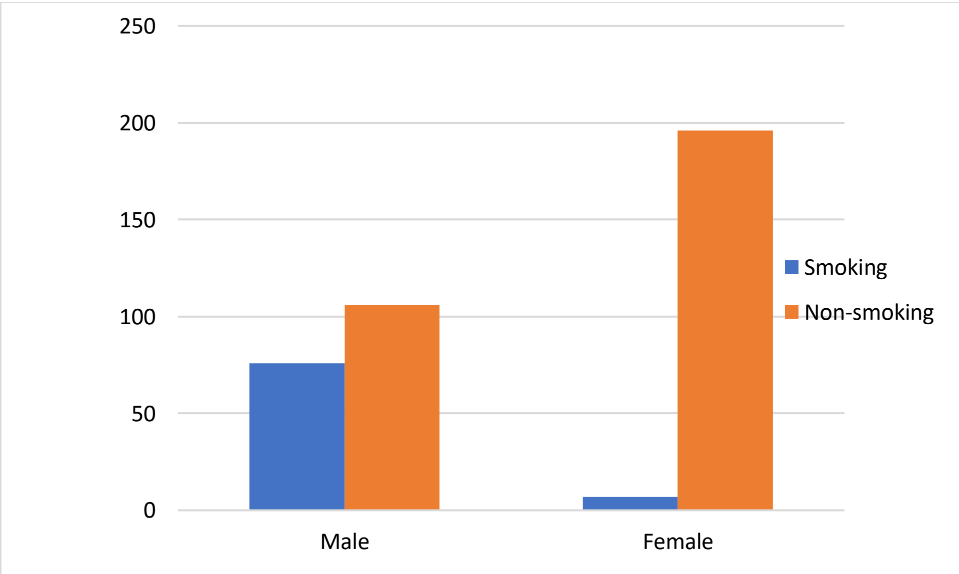

Figure 4.6: Gender distribution of participants based on Smoking

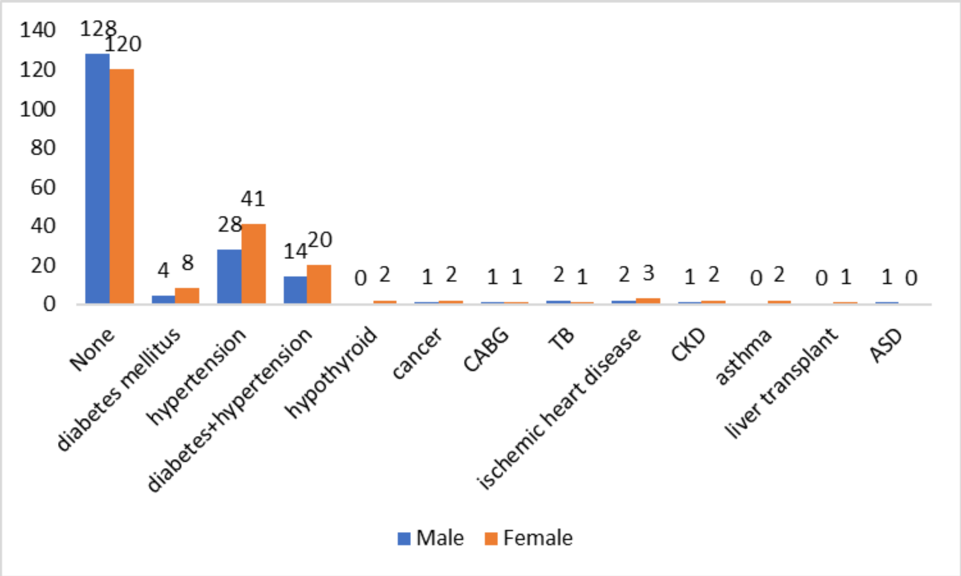

Figure 4.7: Distribution of study participants based on Co-morbidities

Table 4.1 Tests of Normality

Parameters	Kolmogorov-Smirnov[a]			Shapiro-Wilk		
	Statistic	df	Sig.	Statistic	df	Sig.
Body surface area	.068	383	.000	.987	383	.001
Annular diameter long axis	.055	383	.007	.984	383	.000
Annular diameter four chamber	.072	383	.000	.991	383	.016
Annular area	.068	383	.000	.971	383	.000
Anterior leaflet length	.054	383	.009	.992	383	.041
Anterior leaflet thickness	.198	383	.000	.629	383	.000
Posterior leaflet length	.055	383	.007	.992	383	.036
Posterior leaflet thickness	.226	383	.000	.352	383	.000
Intercommissural distance	.076	383	.000	.988	383	.004
C-septal distance	.076	383	.000	.988	383	.003
Interpapillary distance	.078	383	.000	.987	383	.002
Systolic dimension of left ventricle	.102	383	.000	.949	383	.000
Diastolic dimension of left ventricle	.055	383	.008	.974	383	.000
Septal thickness	.158	383	.000	.936	383	.000
Posterior wall thickness of left ventricle	.353	383	.000	.167	383	.000

Tests applied: Kolmogorov-Smirnov and Shapiro-Wilk Test

Table 4.2: Measurement of echocardiographic parameters in the study population (mm)

Parameters	N	Mean	Std. Deviation	Minimum	Maximum	Percentiles			IQR
						25th	50th (Median)	75th	
Annular diameter long axis	385	27.7091	4.38672	15.00	49.00	24.5000	28.0000	30.0000	5.50
Annular diameter four chamber	385	30.0278	4.50162	17.00	46.00	27.0000	30.0000	33.0000	6.00
Annular area	385	655.3460	172.47125	111.94	1408.29	532.6300	637.4200	749.1100	216.66
Anterior leaflet length	385	19.0935	4.35330	2.00	36.00	16.4000	19.0000	22.0000	5.60
Anterior leaflet thickness	385	2.7075	1.30545	.20	20.00	2.0000	2.7000	3.1000	1.10
Posterior leaflet length	385	16.1005	3.62276	5.80	30.00	14.0000	16.0000	18.2500	4.20
Posterior leaflet thickness	385	2.7576	1.97597	.20	37.00	2.0000	2.8000	3.2000	1.20
Intercommissural distance	385	31.1481	4.34401	17.00	41.60	29.0000	31.0000	34.0000	5.00
C-septal distance	385	26.4913	4.10185	16.00	39.00	23.5000	26.0000	29.5000	6.10
Interpapillary distance	385	30.1842	5.11363	12.00	45.90	27.0000	30.0000	34.0000	7.00
Systolic dimension of left ventricle	385	28.5732	5.28394	16.00	55.70	25.0000	28.0000	32.0000	7.00
Diastolic dimension of left ventricle	385	42.1571	5.80827	9.00	61.80	39.0000	42.0000	46.0000	7.00
Septal thickness	385	8.3551	1.22639	4.00	11.00	7.0000	8.0000	9.2000	2.20
Posterior wall thickness of left ventricle	383	8.4987	4.37876	4.00	91.00	7.2000	8.0000	9.0000	1.80

Descriptive statistics in Median and Interquartile Range (IQR)

Table 4.3: Measurement of Body Surface Area in the Study Population (m^2)

	N	Mean	Std. Deviation	Minimum	Maximum	Percentiles			IQR
						25th	50th (Median)	75th	
Body surface area	385	1.7537	.20320	1.17	2.52	1.6450	1.7500	1.8700	0.23

Statistical results shown in Median and Interquartile Range (IQR)

Table 4.4: Measurement of Body Surface Area m^2 (Based on Gender)

	Gender	N	Mean Rank	Sum of Ranks	p-value
Body Surface Area	Male	182	221.29	40275.50	0.000**
	Female	203	167.63	34029.50	

Test applied: Mann-Whitney U Test; p-value ≤ 0.05: significant (*); p-value ≤ 0.01: highly significant (**)

Table 4.5: Measurement of echocardiographic parameters mm (Based on Gender)

Parameters	Gender	N	Mean Rank	Sum of Ranks	p-value
Annular diameter long axis	male	182	201.49	36671.50	0.156
	female	203	185.39	37633.50	
Annular diameter four chamber	male	182	197.51	35947.00	0.451
	female	203	188.96	38358.00	
Annular area	male	182	197.40	35926.00	0.463
	female	203	189.06	38379.00	
Anterior leaflet length	male	182	200.22	36440.00	0.227
	female	203	186.53	37865.00	
Anterior leaflet thickness	male	182	196.18	35705.00	0.593
	female	203	190.15	38600.00	
Posterior leaflet length	male	182	207.94	37845.00	0.012*
	female	203	179.61	36460.00	
Posterior leaflet thickness	male	182	192.63	35058.00	0.950
	female	203	193.33	39247.00	
Intercommissural distance	male	182	194.44	35388.50	0.809
	female	203	191.71	38916.50	
Cseptal distance	male	182	218.63	39791.00	0.000**
	female	203	170.02	34514.00	
Interpapillary distance	male	182	191.47	34847.50	0.798
	female	203	194.37	39457.50	
Systolic dimension of left ventricle	male	182	211.25	38447.00	0.002**
	female	203	176.64	35858.00	
Diastolic dimension of left ventricle	male	182	214.34	39010.50	0.000**
	female	203	173.86	35294.50	
Septal thickness	male	182	214.19	38983.00	0.000**
	female	203	174.00	35322.00	
Posterior wall thickness of left ventricle	male	180	209.37	37687.00	0.003**
	female	203	176.60	35849.00	

Test applied: Mann-Whitney Test; p-value ≤ 0.05: significant (*); p-value ≤ 0.01: highly significant (**).

Table 4.6: Measurement of echocardiographic parameters (Based on Age in years)

Parameters	Age	N	Mean Rank	p-value
Annular diameter long axis	18-30	38	154.62	0.113
	31-45	108	197.55	
	46-65	190	200.59	
	>65	49	183.31	
Annular diameter four chamber	18-30	38	172.07	0.314
	31-45	108	201.69	
	46-65	190	196.92	
	>65	49	174.86	
Annular area	18-30	38	160.91	0.142
	31-45	108	203.57	
	46-65	190	197.51	
	>65	49	177.11	
Anterior leaflet length	18-30	38	199.61	0.840
	31-45	108	198.48	
	46-65	190	191.12	
	>65	49	183.09	
Anterior leaflet thickness	18-30	38	180.87	0.885
	31-45	108	192.41	
	46-65	190	194.07	
	>65	49	199.55	
Posterior leaflet length	18-30	38	174.17	0.479
	31-45	108	194.92	
	46-65	190	199.23	
	>65	49	179.19	
Posterior leaflet thickness	18-30	38	149.91	0.069
	31-45	108	190.22	
	46-65	190	200.85	
	>65	49	202.12	
Intercommissural distance	18-30	38	204.87	0.280
	31-45	108	201.21	
	46-65	190	192.82	
	>65	49	166.39	
Cseptal distance	18-30	38	188.95	0.124
	31-45	108	197.48	

	46-65	190	200.18	
	>65	49	158.44	
Interpapillary distance	18-30	38	223.70	0.067
	31-45	108	201.44	
	46-65	190	189.71	
	>65	49	163.36	
Systolic dimension of left ventricle	18-30	38	166.04	0.072
	31-45	108	206.06	
	46-65	190	197.93	
	>65	49	166.00	
Diastolic dimension of Left ventricle	18-30	38	183.34	0.045*
	31-45	108	208.74	
	46-65	190	195.57	
	>65	49	155.84	
Septal thickness	18-30	38	161.54	0.043*
	31-45	108	178.21	
	46-65	190	202.62	
	>65	49	212.67	
Posterior wall thickness of left ventricle	18-30	38	159.30	0.035*
	31-45	108	176.92	
	46-65	189	202.13	
	>65	48	211.93	

Test applied: Kruskal-Wallis Test; p-value ≤ 0.05: significant (*); p-value ≤ 0.01: highly significant (**).

Table 4.7: Measurement of echocardiographic parameters (Based on Ethnicity)

Parameters	Ethnicity	N	Mean Rank	p-value
Annular diameter long axis	Sindhi	48	170.43	0.463
	Punjabi	53	193.23	
	Balochi	16	169.16	
	Pashtun	53	208.79	
	Urdu speaking	198	194.01	
	Hindku	17	217.47	
Annular diameter four chamber	Sindhi	48	184.34	0.012*
	Punjabi	53	205.57	
	Balochi	16	239.50	
	Pashtun	53	218.89	
	Urdu speaking	198	176.62	
	Hindku	17	244.53	
Annular area	Sindhi	48	173.33	0.114
	Punjabi	53	206.17	
	Balochi	16	210.19	
	Pashtun	53	222.75	
	Urdu speaking	198	182.82	
	Hindku	17	217.15	
Anterior leaflet length	Sindhi	48	186.58	0.423
	Punjabi	53	190.59	
	Balochi	16	161.28	
	Pashtun	53	210.72	
	Urdu speaking	198	189.79	
	Hindku	17	230.59	
Anterior leaflet thickness	Sindhi	48	221.74	0.088
	Punjabi	53	187.92	
	Balochi	16	140.06	
	Pashtun	53	173.14	
	Urdu speaking	198	198.37	
	Hindku	17	176.88	
Posterior leaflet length	Sindhi	48	192.88	0.671
	Punjabi	53	196.81	
	Balochi	16	162.53	
	Pashtun	53	212.91	

	Urdu speaking	198	189.45	
	Hindku	17	189.47	
Posterior leaflet thickness	Sindhi	48	202.18	0.059
	Punjabi	53	175.62	
	Balochi	16	152.03	
	Pashtun	53	166.08	
	Urdu speaking	198	207.37	
	Hindku	17	176.41	
Intercommissural distance	Sindhi	48	206.00	0.288
	Punjabi	53	212.20	
	Balochi	16	192.94	
	Pashtun	53	209.55	
	Urdu speaking	198	179.91	
	Hindku	17	197.38	
Cseptal distance	Sindhi	48	189.39	0.922
	Punjabi	53	182.90	
	Balochi	16	174.59	
	Pashtun	53	191.57	
	Urdu speaking	198	198.47	
	Hindku	17	192.74	
Interpapillary distance	Sindhi	48	189.39	0.599
	Punjabi	53	194.04	
	Balochi	16	185.88	
	Pashtun	53	217.55	
	Urdu speaking	198	186.42	
	Hindku	17	206.82	
Systolic dimension of left ventricle	Sindhi	48	187.60	0.345
	Punjabi	53	191.69	
	Balochi	16	196.34	
	Pashtun	53	223.57	
	Urdu speaking	198	184.77	
	Hindku	17	209.74	
Diastolic dimension of left ventricle	Sindhi	48	175.82	0.389
	Punjabi	53	177.80	
	Balochi	16	194.97	
	Pashtun	53	217.74	

	Urdu speaking	198	192.89	
	Hindku	17	211.21	
Septal thickness	Sindhi	48	165.21	0.77
	Punjabi	53	226.93	
	Balochi	16	174.00	
	Pashtun	53	202.03	
	Urdu speaking	198	188.09	
	Hindku	17	212.59	
Posterior wall thickness of left ventricle	Sindhi	48	164.17	0.006**
	Punjabi	53	238.62	
	Balochi	16	218.13	
	Pashtun	52	183.88	
	Urdu speaking	197	183.70	
	Hindku	17	221.65	

Test applied: Kruskal-Wallis Test; p-value ≤ 0.05: significant (*); p-value ≤ 0.01: highly significant (**)

Table 4.8: Measurement of echocardiographic parameters (Based on Family Cardiac History)

Parameters	Family cardiac history	N	Mean Rank	Sum of Ranks	p-value
Annular diameter long axis	yes	153	215.73	33006.00	0.001**
	no	232	178.01	41299.00	
Annular diameter four chamber	yes	153	210.25	32168.00	0.013*
	no	232	181.63	42137.00	
Annular area	yes	153	212.55	32519.50	0.005**
	no	232	180.11	41785.50	
Anterior leaflet length	yes	153	201.25	30791.00	0.237
	no	232	187.56	43514.00	
Anterior leaflet thickness	yes	153	192.38	29434.00	0.929
	no	232	193.41	44871.00	
Posterior leaflet length	yes	153	205.62	31459.50	0.070
	no	232	184.68	42845.50	
Posterior leaflet thickness	yes	153	192.32	29425.00	0.922
	no	232	193.45	44880.00	
Intercommissural distance	yes	153	200.33	30651.00	0.293
	no	232	188.16	43654.00	
C-septal distance	yes	153	204.48	31285.00	0.100
	no	232	185.43	43020.00	
Interpapillary distance	yes	153	198.58	30383.00	0.424
	no	232	189.32	43922.00	
Systolic dimension of left ventricle	yes	153	212.51	32514.50	0.005**
	no	232	180.13	41790.50	
Diastolic dimension of left ventricle	yes	153	217.25	33238.50	0.001**
	no	232	177.01	41066.50	
Septal thickness	yes	153	195.93	29977.00	0.671
	no	232	191.07	44328.00	
Posterior wall thickness of left ventricle	yes	151	194.86	29423.50	0.680
	no	232	190.14	44112.50	

Test applied: Mann-Whitney Test; p-value ≤ 0.05: significant (*); p-value ≤ 0.01: highly significant (**)

Table 4.9: Measurement of echocardiographic parameters (Based on Smoking)

Parameters		N	Mean	Sum of Ranks	p-value
Annular diameter (long axis)	Yes	38	208.99	18268.00	0.139
	No	302	188.60	56037.00	
Annular diameter (four chamber)	Yes	38	205.20	17346.50	0.259
	No	302	189.67	56958.50	
Annular area	Yes	38	205.49	17055.50	0.248
	No	302	189.57	57249.50	
Anterior leaflet length	Yes	38	189.20	15704.00	0.725
	No	302	194.04	58601.00	
Anterior leaflet thickness	Yes	38	190.43	15806.00	0.811
	No	302	193.71	58499.00	
Posterior leaflet length	Yes	38	203.10	16857.50	0.350
	No	302	109.22	57447.50	
Posterior leaflet thickness	Yes	38	186.23	15457.50	0.530
	No	302	194.86	58847.50	
Intercommissural distance	Yes	38	203.52	16892.00	0.330
	No	302	190.11	57413.00	
Cseptal distance	Yes	38	215.28	17868.00	0.039*
	No	302	186.88	56437.00	
Interpapillary distance	Yes	38	191.69	15910.00	0.903
	No	302	193.36	5839500	
Systolic dimension of left ventricle	Yes	38	222.07	18432.00	0.007**
	No	302	185.01	55873.00	
Diastolic dimension of left ventricle	Yes	38	215.57	17892.50	0.037*
	No	302	186.80	56412.50	
Septal thickness	Yes	38	205.66	17070.00	0.235
	No	302	189.52	57235.00	
Posterior wall thickness of left ventricle	Yes	38	211.57	17349.00	0.067
	No	302	186.67	56187.00	

Test applied: Mann-Whitney Test; p-value ≤ 0.05: significant (*); p-value ≤ 0.01: highly significant (**)

Table 4.10: Measurement of echocardiographic parameters (Based on Co-morbidities)

Parameters		N	Mean	p-value
Annular diameter (ong axis	None	248	185.79	0.197
	diabetes mellitus	12	247.58	
	hypertension	69	192.03	
	diabetes+hypertension	34	228.16	
	hypothyroid	2	168.0	
	cancer	3	287.50	
	CABG	2	128.25	
	TB	3	166.0	
	ischemic heart disease	5	264.0	
	CKD	3	157.333	
	asthma	2	195.50	
	liver transplant	1	35.50	
	ASD	1	80.0	
Annular diameter (four chamber)	None	248	183.68	0.398
	diabetes mellitus	12	201.83	
	hypertension	69	204.90	
	diabetes+hypertension	34	212.96	
	hypothyroid	2	243.0	
	cancer	3	241.17	
	CABG	2	217.0	
	TB	3	195.0	
	ischemic heart disease	5	280.90	
	CKD	3	125.0	
	asthma	2	323.75	
	liver transplant	1	204.0	
	ASD	1	92.0	
Annular area	None	248	183.09	0.325
	diabetes mellitus	12	233.38	
	hypertension	69	202.95	
	diabetes+hypertension	34	225.72	
	hypothyroid	2	212.50	
	cancer	3	284.67	
	CABG	2	175.5	
	TB	3	170.83	
	ischemic heart disease	5	220.40	
	CKD	3	152.67	
	asthma	2	284.25	

	liver transplant	1	77.50	
	ASD	1	71.0	
Anterior leaflet length	None	248	194.13	0.368
	diabetes mellitus	12	199.17	
	hypertension	69	185.36	
	diabetes+hypertension	34	181.94	
	hypothyroid	2	168.50	
	cancer	3	252.50	
	CABG	2	348.0	
	TB	3	114.67	
	ischemic heart disease	5	241.40	
	CKD	3	144.83	
	asthma	2	297.50	
	liver transplant	1	85.50	
	ASD	1	339.50	
Anterior leaflet thickness	None	248	195.43	0.703
	diabetes mellitus	12	235.08	
	hypertension	69	173.38	
	diabetes+hypertension	34	198.0	
	hypothyroid	2	215.0	
	cancer	3	258.50	
	CABG	2	283.25	
	TB	3	154.50	
	ischemic heart disease	5	137.30	
	CKD	3	239.17	
	asthma	2	179.50	
	liver transplant	1	138.50	
	ASD	1	186.50	
Posterior leaflet length	None	248	188.05	0.494
	diabetes mellitus	12	233.79	
	hypertension	69	207.33	
	diabetes+hypertension	34	175.53	
	hypothyroid	2	200.50	
	cancer	3	236.17	
	CABG	2	308.0	
	TB	3	201.50	
	ischemic heart disease	5	177.40	
	CKD	3	125.33	
	asthma	2	275.75	
	liver transplant	1	104.50	
	ASD	1	339.50	
Posterior leaflet thickness	None	248	196.41	0.783

	diabetes mellitus	12	198.50	
	hypertension	69	179.04	
	diabetes+hypertension	34	197.51	
	hypothyroid	2	187.25	
	cancer	3	227.67	
	CABG	2	312.75	
	TB	3	120.50	
	ischemic heart disease	5	135.20	
	CKD	3	219.83	
	asthma	2	170.75	
	liver transplant	1	131.0	
	ASD	1	291.0	
Intercommissural distance	None	248	194.84	0.581
	diabetes mellitus	12	193.92	
	hypertension	69	204.06	
	diabetes+hypertension	34	162.46	
	hypothyroid	2	303.0	
	cancer	3	218.67	
	CABG	2	182.75	
	TB	3	133.83	
	ischemic heart disease	5	187.00	
	CKD	3	139.67	
	asthma	2	144.50	
	liver transplant	1	55.0	
	ASD	1	327.50	
Cseptal distance	None	248	205.81	0.063
	diabetes mellitus	12	209.25	
	hypertension	69	159.14	
	diabetes+hypertension	34	195.21	
	hypothyroid	2	131.25	
	cancer	3	199.17	
	CABG	2	121.75	
	TB	3	84.17	
	ischemic heart disease	5	187.00	
	CKD	3	51.83	
	asthma	2	212.75	
	liver transplant	1	179.0	
	ASD	1	82.0	
Interpapillary distance	None	248	191.82	0.184
	diabetes mellitus	12	210.42	
	hypertension	69	218.43	
	diabetes+hypertension	34	152.26	

	hypothyroid	2	239.0	
	cancer	3	145.83	
	CABG	2	188.50	
	TB	3	100.67	
	ischemic heart disease	5	256.0	
	CKD	3	142.50	
	asthma	2	146.50	
	liver transplant	1	67.50	
	ASD	1	296.0	
Systolic dimension of left ventricle	None	248	193.87	0.218
	diabetes mellitus	12	271.42	
	hypertension	69	188.05	
	diabetes+hypertension	34	195.93	
	hypothyroid	2	156.50	
	cancer	3	229.83	
	CABG	2	79.50	
	TB	3	120.33	
	ischemic heart disease	5	188.50	
	CKD	3	14l.0	
	asthma	2	196.50	
	liver transplant	1	11.50	
	ASD	1	30.00	
Diastolic dimension of left ventricle	None	248	198.14	0.489
	diabetes mellitus	12	198.25	
	hypertension	69	191.14	
	diabetes+hypertension	34	173.38	
	hypothyroid	2	137.50	
	cancer	3	262.50	
	CABG	2	208.0	
	TB	3	76.33	
	ischemic heart disease	5	164.90	
	CKD	3	137.83	
	asthma	2	297.0	
	liver transplant	1	81.50	
	ASD	1	81.50	
Septal thickness	None	248	187.78	0.734
	diabetes mellitus	12	202.75	
	hypertension	69	197.73	
	diabetes+hypertension	34	225.04	
	hypothyroid	2	158.0	
	cancer	3	125.67	
	CABG	2	155.25	

	TB	3	125.67	
	ischemic heart disease	5	258.70	
	CKD	3	221.17	
	asthma	2	178.0	
	liver transplant	1	155.50	
	ASD	1	155.50	
Posterior wall thickness of left ventricle	None	248	186.26	0.210
	diabetes mellitus	12	188.54	
	hypertension	69	202.96	
	diabetes+hypertension	34	228.69	
	hypothyroid	2	82.75	
	cancer	3	129.67	
	CABG	2	60.50	
	TB	3	160.83	
	ischemic heart disease	5	256.830	
	CKD	3	213.17	
	asthma	2	86.50	
	liver transplant	1	156.0	
	ASD	1	266.0	

Test applied: Kruskal-Wallis Test; p-value ≤ 0.05: significant (*); p-value ≤ 0.01: highly significant (**).

Table 4.11: Correlation between BSA with echocardiographic parameters

Parameter	Spearman correlations coefficient (p)	Significance (p-value)
Annular diameter (long axis)	0.401	0.000**
Annular diameter (four chamber)	0.418	0.000**
Annular area	0.481	0.000**
Anterior leaflet length	0.199	0.000**
Anterior leaflet thickness	0.012	0.814
Posterior leaflet length	0.246	0.000**
Posterior leaflet thickness	0.017	0.733
Intercommissural distance	0.273	0.000**
C-septal distance	0.354	0.000**
Interpapillary distance	0.370	0.000**
Systolic dimension of left ventricle	0.336	0.000**
Diastolic dimension of left ventricle	0.443	0.000**
Septal thickness	0.092	0.068
Posterior wall thickness of left ventricle	0.069	0.166

Test applied: Spearman correlations coefficient (p) Test; p-value ≤ 0.05: significant (*); p-value ≤ 0.01: highly significant (**).

Table 4.12: Correlation between Mitral Valve parameters with Left Ventricular Dimensions

Parameters		Systolic dimension of left ventricle	Diastolic dimension of left ventricle	Septal thickness	Posterior wall thickness of left ventricle
Annular Diameter (long Axis)	Correlations Coefficient	0.400	0.440	0.276	0.269
	Sig (2-tailed)	0.000**	.0000**	0.000	0.000**
Annular diameter (4-chamber)	Correlations Coefficient	0.262	0.259	0.052	0.084
	Sig (2-tailed)	0.000**	0.000**	0.310	0.099
Annular area	Correlations Coefficient	0.377	0.424	0.204	0.219
	Sig (2-tailed)	0.000**	0.000**	0.000	0.000**
Anterior leaflet length	Correlations Coefficient	0.032	0.152	-0.090	-0.085
	Sig (2-tailed)	0.526	0.003**	0.077	0.095
Anterior leaflet thickness	Correlations Coefficient	0.007	0.029	-0.039	0-.078
	Sig (2-tailed)	0.892	0.574	0.447	0.127
Posterior leaflet length	Correlations Coefficient	0.205	0.204	0.109	0.094
	Sig (2-tailed)	0.000**	0.000**	0.032	0.066
Posterior leaflet thickness	Correlations Coefficient	-.032	0.014	-0.010	-0.003
	Sig (2-tailed)	.525	0.785	0.844	0.961
Intercommissural distance	Correlations Coefficient	.221	0.239	-0.078	-0.022
	Sig (2-tailed)	.000**	0.000**	0.127	0.669
C-septal distance	Correlations Coefficient	.314	0.280	0.188	0.135
	Sig (2-tailed)	.000**	0.000**	0.000	0.008**
Interpapillary distance	Correlations Coefficient	.264	0.256	-0.045	0.081
	Sig (2-tailed)	.000**	0.000**	0.381	.0112

Test applied: Spearman correlations coefficient (p) Test; p-value ≤ 0.05: significant (*); p-value ≤ 0.01: highly significant (**).

CHAPTER 5

DISCUSSION

5.1 Sequence of discussion experiment/ hypothesis wise

The current study intended to explicate the mitral valve structure and its geometry among the representative proportion of the Pakistani population. Despite having an intricate structure and critical functioning, the anatomical variations in the structure of the mitral valve and its geometry have not been thoroughly studied and reported as there is limited literature on the heterogenous Pakistani population with diverse ethnic and cultural backgrounds.

The primary focus of this study was to determine the normal reference values for the echocardiographic parameters of the mitral valve and its geometry using 2-dimensional transthoracic echocardiography and investigated the correlation of morphological variations of the mitral valve as well as the left ventricle of the heart with demographic factors that included age, gender, and ethnicity along with physiological variable, that is body surface area within the population of Pakistan. This study assessed the influence of the variations of the mitral valve parameters with left ventricle parameters through echocardiography. These parameters included the annular diameter in both the long-axis and 4-chamber view, the annular area was calculated by the formula stated in the study (Sadeghpour et al., 2008), also the lengths and thickness of the anterior and posterior mitral valve leaflets, intercommissural distance, c-septal distance, and interpapillary distance. The parameters of the left ventricle comprised of systolic and diastolic dimensions, septal wall, and posterior wall of the left ventricle were incorporated in the current study. All parameters except the systolic dimension, were measured in the end-diastolic phase when the mitral valve is relaxed and most open providing the most constant reference point, also this phase allows maximum filling of the ventricular chambers of the heart that facilitates the most reliable measurement of the cardiac dimensions. Most of the measurements were obtained from a parasternal long-axis view, which included annular diameter (long-axis), length and thickness of the mitral valve leaflets, c-septal distance, systolic and diastolic dimensions, septal wall and posterior wall thickness. The intercommissural distance and papillary distance were measured in the parasternal short-axis view and only the annular diameter was measured in the 4-chamber view of the echocardiography.

In the current study, in the parasternal long-axis, the annular diameter was measured with a mean of 27.7 mm with a standard deviation (SD) of 4.38 mm and a mean of 30.02 mm with an SD of 4.501 in a 4-chamber view, indicating moderate variability among the studied population. The mean annular area was calculated to be 655.346 mm^2 with an SD of 172.47 mm^2. Although the results showed considerable variability in the size of the annulus across the study population and men had higher mean rank than female for annular diameters and area but no significance was found between the genders. The diameter and annular area of the mitral valve strongly correlated with the BSA of the entire study participants. The study by Jolley et al. (2017) also stated the positive correlation between the BSA of the participants with area of the mitral valve measured using 3D- Transthoracic echocardiography. Similarly, Rajila Rajendran et al. (2011) conducted a study on 406 subjects using the 2D-echocardiography and reported an increase in the diameter of the mitral valve with the increasing BSA of the participants. It was noted that with every 0.1m^2 increase in the BSA increased the diameter by 0.2-0.6 mm. The authors also documented the positive correlation between the mitral annulus diameter and left ventricle size, underlining the uniform trend of increased mitral valve diameter associated with increasing dimensions of the left ventricle. This finding was also consistent with the results of the current study and spotlighting the importance evaluating the dimensions of the left ventricle when analyzing the mitral valve dimensions as it can influence size of the left ventricle. Blanke et al. (2015) reported the similar findings by using ECG-gated cardiac Computed Tomography Scan, that also highlighted a significant association of the mitral area with BSA, gender and size of left ventricle. Individuals having large body surface area tend to have larger area along with men having larger area too. It was also observed that the variation in mitral valve area had a positive correlation with left ventricular end-diastolic volume that indicated increase in mitral valve area will increase the size of the left chamber or vice versa. Another study conducted by Ring et al. (2018) assessed normal values for mitral valve parameters in 103 patients using 3D transesophageal echocardiography (TEE). The researchers documented variation in mitral valve area with respect to gender, as men having larger mitral valve diameter and area but showed no significance when the measurements were adjusted for body surface area. Also left ventricular mass did not report to influence the mitral valve parameter. Even Naoum et al. (2016) examined mitral annular diameters by Cardiac Computed Tomography that showed extensive variation with men having larger diameters.

Moreover, the current study also reported no significance between annular diameter and area of the mitral valve and different age groups, that included young adults (18-30 years), middle-aged adults (31-45 years), older adults (46-65 years) and elderly (>65 years). Similarly, Nemes et al. (2020) conducted study on 204 subjects with a mean age of 33.88 ± 12.97 years divided into various age groups and mitral annular diameter and annular area were assessed using three-dimensional speckle-tracking echocardiography. The annular diameter and area measured at end-diastolic phase had no significance with the gender and age of the participants, although the study highlighted the significant difference of annular diameter and area measured at end-systolic phase for both age and gender. In contrast, Dwivedi et al. (2014) conducted research in the South Birmingham on 554 subjects with no valve pathology, out of which 211 were smokers who were over 60 years of age and had co-morbidities like hypertension and diabetes. The study found that the annular diameter was larger in men compared to women and were generally larger at end-diastole than at end-systole. Although this finding was contradictory to the current study, similar finding was highlighted that stated no significance was noted between size of the annular diameter and cardiovascular risk factors like diabetes and hypertension. On the other hand, Nemes et al. (2015) conducted a study to examine the variation in the size of the annulus of the mitral valve in association with Type 1 diabetes mellitus in 18 young patients who were compared with 20 healthy controls with similar gender and age. The imaging modalities that were used were 2D Doppler echocardiography and 3D- speckle tracking echocardiography. The investigators reported a significant enlargement of mitral valve annulus along with mitral annular diameter index and mitral annular area index in patients with type 1 diabetes as compared to the controls. These findings suggested early changes in the size of the mitral annulus due to type 1 diabetes even in the young patients and this may affect the structure and functioning of the mitral valve before other symptoms manifest. This study contradicted with the current study as the study showed no significant association of the mitral valve parameters with co-morbidities like hypertension and diabetes mellitus.

The current study demonstrated the significant difference in annular diameter and area of the mitral valve related to the family history of various cardiac problems. This finding corresponds with the study conducted by Yu et al. (2022) at UK Biobank that identified specific genes like Titin Bcl2-associated athanogene 3 (TTN BAG3) and newer genes like Erb-B2 Receptor Tyrosine Kinase 4 (ERBB4) and Hepatoma-derived growth factor-like protein 1 (HDGFL1) that influenced the size of the mitral valve. The association of the annular diameter of the mitral valve with family cardiac history underscores the genetic components that justify the variation in the annular diameter measurement. This finding strengthens the relevance to reflect on the genetic and family factor to comprehend mitral valve structure as it can be an important determinant for evaluating cardiovascular risks.

With respect to the cadaveric studies, BS and Varsha (2019) measured the annular diameter and area of the mitral valve on 50 autopsied adult cadaveric human hearts of both males and females aged between 20 to 70 years conducted at the Department of Anatomy, Vydehi Institute of Medical Sciences and Research Centre, Bangalore, India. It was exhibited in the study that except for the diameter of the mitral annulus which was larger in females, all other parameters including mitral area were greater in males than females, however, the differences were not statistically significant. Krawczyk-Ożóg et al. (2017) also conducted a study on 200 autopsied human hearts in Poland. The mitral annulus area was found to be 485.4 ± 171.4 mm² which was smaller than the individuals included in the current study suggesting variation of the mitral area among different population. Significant differences were observed between both genders, with decreased values in women contradicting with the current study. The individual belonging to the Caucasian ethnicity also showed positive association of the mitral valve dimension with the gender and age as investigated by Ricci et al. (2021) by using cardiovascular magnetic resonance. The annular diameters and annular area were larger in men than women and these dimensions increased with the increasing age. The findings in the current study only had a significant difference in the annular diameter (4-chamber view) across the various major ethnicities in the Pakistani population.

The current study documented the measurements of length of anterior mitral leaflet to be greater than posterior leaflet and the thickness of the posterior leaflet was slightly greater than the anterior mitral valve leaflet in the entire study population. This finding had a similarity with the study conducted in India by Savalgi et al. (2022) in 50 embalmed human hearts aged between 20 to 60 years which documented that the mean length of the anterior mitral leaflet was larger than the mean length of the posterior mitral leaflet while the thickness of the posterior leaflet was greater as compared to anterior leaflet of the mitral valve. This study also suggested, men having larger mitral valve diameter in comparison to women and slight increase in the width of the posterior leaflet in female which was contradictory as the significant difference was only found in posterior leaflet length between genders. Charanya, Rajathi, and Vishali (2017) also reported similar findings of anterior mitral valve leaflet being longer than the posterior leaflet in all the studied specimens. Torres et al. (2014) also found anterior leaflet length with a mean of 13.4 mm which was greater than posterior leaflet length with a mean of 7.8 mm in the representative population of Argentina measured by 3D – Transesophageal echocardiography. While, Sriambika, Nim, and Bage (2018) reported that the anterior mitral valve leaflet was found to be thicker that the posterior leaflet by measuring the leaflet obtained from dissected cadaver. Mishra et al. (2014) also investigated in the cadaveric that the higher maximum height of 3.74 cm for the anterior leaflet which was greater than the maximum height of the posterior leaflet which was 2.55 cm and posterior leaflet also exhibited greater maximum length as compared to anterior leaflet length which did not align with findings of the current study. Gumpangseth et al. (2020) conducted research on 60 fresh embalmed hearts between 20 to 90 years of ages in Thailand that showcased the applicability of heart valves' morphometric parameters as an age indicator. The study suggested a statistically significant moderate positive correlation between age and length of leaflets of the mitral valve that tends to increase with the increasing age unlike the current study that showed no significant relation between them.

In contrast, Mihăilă et al. (2014) examined the measurements taken by 3-dimensional TEE and 3-dimensional TTE that showed that men had higher measurements involving anterior mitral leaflet length along with the area, and diameters of the mitral annulus (MA) in comparison with women but these measurements were significantly correlated with body surface area similar to the current study. Similar to the current study, Xu et al. (2021) found a significant association of the size of a mitral leaflet following the BSA of the participants and left ventricle size but in contrast, the researchers also found an association with gender. The measurement taken by Cardiac Computed Tomography (CCT) showed similar findings with significant variation between genders with men having larger mitral valve dimensions than women were observed by Kapadia (n.d). The dimensions comprised anterior and posterior length and thickness respectively and also the annular area which was also reported to have a strong correlation with the BSA of the participants but not with the age. But Henry et al. (2022) reported significant variation across both genders, male and female, as well as various age groups by employing data from the World Alliance of Societies of Echocardiography study. The study consisted of 618 normal participants, 301 men, and 311 women, and they were divided into different age groups: 18-40 years, 41-65 years, and >65 years to identify differences correlated with gender and age by analyzing three-dimensional (3D) transthoracic echocardiography scans of the participants. Gender-related differences showed larger mitral valve annular diameter and area in males and even valve leaflet area and length were larger in males.

Various parameters showed statistically significant differences across age groups, anterolateral-posteromedial diameter was slightly larger in the middle-aged group as compared to young and older age groups. The anterior leaflet area of the mitral valve was larger in the younger and middle-aged group while the posterior leaflet area was slightly larger in the oldest group. The anterior leaflet was found to be longer in the youngest and middle age groups while the length of the posterior leaflet was slightly longer in middle age group only. The results highlighted the variations of the mitral annular and leaflet measurements among gender and variations with age, with certain parameters being significantly different across these categories which were not similar to the findings of the current study. Even Henry et al. (2022) in a sample size of 748 normal individuals other than determining age and gender-related mitral valve measurements also compared these measurements across various major races in the world that showcased smaller dimensions in the Asian population to which the Pakistani population belong in comparison of White and Black population.

In contrast, Salahuddin et al. (2012) presented a unique case of mitral valve leaflet exposure to chronic smoking in a male aged 52 years known as the “smoking mitral valve”. Echocardiography revealed an increase thickness of the mitral valve draws attention to the prospective influence of smoking on cardiac health especially modification in the structure of the mitral leaflets. Although the current study did not determine any significant association between smoking and mitral valve leaflet dimensions which my due to the rare case or different study population, this case emphasizes necessity to acknowledge these morphological changes that may lead to rare presentation of diseases of the heart valve.

The c-septal distance in the current study established significant differences with gender, smoking status of the participants and also showed positive correlation with the left ventricular parameters, including systolic and diastolic parameters, septal thickness and posterior wall thickness. It was measured to 26.49 ± 4.10 mm showing variability among the participants. Although being one of the vital variables no previous studies showed variations related to c-septal distance. The findings from the current study accentuated the need for gender-specific ranges for c-septal distance and also the integration of smoking status into echocardiographic assessments.

The intercommissural distance (IC) is a crucial criterion of the mitral valve geometry for quantification of the therapeutic evaluation for surgical strategy. In the current study, the IC distance measurement ranged from 17.0 mm to 41.60 mm with a mean of 31.15 mm and an SD of 4.34 mm measured using 2D- Transthoracic echocardiography. This variation highlights the meticulous review of each individual's attributes when analyzing these measurements in the population. The study aligned with findings of the Abdelghani et al. (2017) who documented an IC distance of 39.3 ± 4.6 mm in the participants by using cardiac computed tomography angiography scans. While Mojtaj et al. (2018) measured an IC distance of 2.7 cm (ranging from 1.79 to 3.82 cm) on cadaveric heart specimens which was lower than the IC distance measured in the current study. This divergence between the results of the two studies may be due to the contrasting modalities used or the difference in the study population. In a previous study by Fyrenius, Engvall, and Janerot-Sjöberg (2001) it was accentuated that the IC distance is highest in the end-systole period. This observation is coherent with the positive correlation of IC distance with dimensions of the left ventricles. Measurements taken at the end-systolic phase yielded reliable outcomes in normal-weighted individuals. This implies that the IC distance is prone to bodily changes throughout the cardiac cycle similar to the current study that showed significance of IC distance with BSA of the individual and due to these variations, it should always be considered when assessing the mitral valve geometry.

In the current study data, the interpapillary muscle distance was noted to be 30.18 ± 5.11 mm that showed greater discrepancy with the interpapillary distance measured by the Sonne et al. (2009) which lesser distance of 17.7 ± 4.8 mm. This variability may be due to the different diagnostic tools used as the latter was measured by real-time 3D- Transthoracic echocardiography. Similar to the current study, interpapillary distance as well as the annular was not associated with the age but strongly linked with the BSA, making a major determinant of the mitral valve dimension and also the measurement of the annular area aligned with the current study. The interpapillary distance had a positive association with the left ventricular size. As there is an increase in the left ventricular dimension, interpapillary distance tends to increase. This interrelation attributed to the fact that increased volumes and dimension of the left ventricle which corresponds with larger interpapillary distance which is the structural modification to confirm to elevated cardiac size and function. Similar to it, Kalyanasundaram et al. (2010) observed lessening in the interpapillary distance is consistent with a reduction in the dimension of the left ventricle. This harmonized decrease signifies that the mitral valve and left ventricle accommodate dynamically during the cardiac cycle to sustain optimal valve closure. This study revealed 39% reduction in the interpapillary distance during systole that indicates adaptation of valve to ventricular contraction in systole.

The current study showed significant variation of left ventricular dimensions with gender, age, and family cardiac history. The average systolic dimension of the current study was noted as 28.57 ± 5.28 mm and the average diastolic dimension of the left ventricle was 42.16 ± 5.81 mm. These readings demonstrate a substantial decrease in the left ventricular dimension in the systolic phase which is anticipated as during this phase contraction of the heart occurs and blood is ejected into the systemic circulation. The current study showed significant variation of left ventricular dimensions with gender, age, and family cardiac history. It was found that males significantly exhibited larger dimensions of the left ventricle than females and also showed age-related changes along with the family history of cardiac disease and smoking status of the participants that had significant influence on the dimensions of the left ventricle. Also, septal wall thickness and posterior wall thickness of the left ventricle were also measured with posterior wall thickness wider ranged variability across the study population. Both septal and posterior wall thickness were influenced significantly by age and gender but not by BSA, unlike ventricular dimensions. Even posterior wall thickness showed variation among different ethnicities.

Asch et al. (2019) documented the variability in the measurements of the left ventricle based on gender, age, and race. It was reported men having larger left ventricular dimensions which is likely due to the increased body surface area in men and also observed age-related in which younger individual exhibited different measurement of dimensions than the older adults that aligned with current study. The researchers also provided data on the variability of these measurements indicating larger left ventricle dimensions and volumes in the Australian population and smaller in Indians suggesting alignment with variation in the posterior wall thickness within the ethnic group across Pakistan. Such difference highlights the need for specific reference values tailored to the differences in different populations to better clinical practice. Similarly, Majonga et al. (2018) from various studies analyzed and compared the sizes of the left atrium and left ventricle adjusted for body surface area. Significant variations in LV dimensions existed across different ethnic populations, as evidenced by studies from India, Italy, Zimbabwe, the USA, Germany, and the UK that showed Zimbabwean children had a thicker interventricular septum compared to German children. The study emphasized the necessity of standardized echocardiographic methods and BSA normalization techniques considering demographic differences to establish accurate reference values for the size of heart chambers. Ugwuanyi (2020) while reporting the normative value for the left ventricular dimension in the Nigerian Population observed the significant variation in interventricular septal thickness between genders that corresponds to the current study.

5.2 IMPLICATIONS OF THE STUDY:

5.2.1 Theoretical implication:

This study enhances the knowledge of mitral valve anatomy by underlining the influence of physiological and demographic factors on its geometry. It suggested the necessity to adjust the standard reference values to specific populations as it highlights the importance of including ethnic and genetic aspects in echocardiographic assessments. The study findings endorse the establishment of standard ranges that should be regional-specific for the population of Pakistan and the inclusion of family history and smoking status into cardiovascular assessments. Moreover, the recorded variations in various studies accentuate the necessity for a systematic approach in cardiac imaging measurements and standardization of body surface area to augment clinical precision and diagnostic accuracy.

5.2.2 Practical implications:

The current study brings attention to the requirement of tailoring the echocardiographic reference values specified to the demographic factors like age, gender, and family cardiac history and physiological factors like body surface area that showed a strong correlation with most of the mitral valve and left ventricle parameters. Our population being different from the Western population both physiologically, culturally, and genetically, should endorse for customized baseline values for the evaluation of the measurement and functioning of the heart instead of referring to the values standardized for the Western population. The study indicated significant findings for family cardiac history which can help in the early assessment and diagnosis of cardiac disease through echocardiography and even provide a basis for preventive measures customized for different regional populations within Pakistan. By all these factors, we will able achieve greater accuracy and precision in diagnosis of heart valvular diseases as Rheumatic heart disease more prevalent in our population. This will also help in tailoring the treatments and surgical strategies by cardiac specialists for better outcomes in the cardiac patients.

5.2.3 Policy implications: N/A

5.3 LIMITATIONS AND STRENGTHS OF THE STUDY:

(A) Limitations:

- Single-centered study, therefore results cannot be generalized
- Results cannot be compared with different modalities (CT scans and MRI)

(B) Strengths:

- The study concentrates exclusively on mitral valve variance in the Pakistani population and aims to identifies the research gap in Pakistani literature
- It will add to the existing scientific knowledge and contribute to the extensive understanding of mitral valve anatomy that will provide insights into the broader implications for cardiac and clinical practice
- It will encompass participants from different age groups, genders, body surface areas, and ethnic backgrounds, which will aim to target a diverse and representative sample of the Pakistani population
- It will help to identify explicit mitral valve characteristics concerning age, gender, body surface area, and ethnicity that will possibly direct cardiologists to treat patients with valve diseases by selecting appropriate interventions
- By identifying unique mitral valve traits in connection to factors like age, gender, body surface area, and ethnicity, it will be possible for cardiologists to choose the best treatments for individuals with mitral valve problems
- It will also have an associate of a researcher with experts in advanced imaging cardiology to ensure a comprehensive and rigorous analysis of mitral valve variation and will enhance the study’s validity and reliability

5.4 RECOMMENDATIONS:

- It is recommended to establish baseline values for the dimensions of mitral valve as well as left ventricle, customized in accordance to the findings of the current study specific to the population of Pakistan both for males and female that exhibit different physiological factors.
- The established values for various cardiac parameters should be normalized and should be used in the daily clinical practice for appropriate diagnosis.
- This study should also be conducted in various cardiac centers in different provinces across Pakistan for better understanding of the influence of cultural and ethnic backgrounds on the morphology and functioning of the heart.
- Cohort studies should be conducted to evaluate the progression of variability in different heart structures over time with age and that can demonstrate different measurements at different stages of life for the people of Pakistan that can help in tailoring the cardiac interventions for better outcomes in people belonging to different ages.
- This study provided baseline to study in detail, the influence of different co-morbidities prevalent in the Pakistani population on the structure of the heart for early diagnosis of cardiac problems relevant to the co-morbidity.
- This study also makes way to further investigate cardiac parameters by different modalities like 3-dimensional Transthoracic or Transesophageal echocardiography, Cardiac computed tomography, cardiac MRI to certify the reliability and accuracy of these measurements.
- Moreover, this research also leads to study the mitral valve and it subvalvular apparatus genetically to get the better understanding of impact of family cardiac history in our population.

5.5 CONCLUSION:

In conclusion, this study highlights significant variations in echocardiographic measurements influenced by gender, age, ethnicity, family history of cardiac diseases, smoking status, and body surface area (BSA). Males exhibited longer posterior mitral valve leaflets and larger C-septal distances, alongside greater left ventricular dimensions and wall thicknesses compared to females. Age-related changes revealed that the diastolic dimension of the left ventricle peaked in individuals aged 46-65 years before decreasing in those over 65, while both septal and posterior wall thickness increased with age. Ethnic differences were notable, with the Hindku and Balochi groups showing the largest annular diameters and Punjabi individuals having the thickest posterior walls. A family history of cardiac diseases correlated with larger mitral valve dimensions and left ventricular geometry, emphasizing the hereditary influence on cardiac structure. Additionally, smokers demonstrated larger C-septal distances and left ventricular dimensions compared to non-smokers. The study found significant positive correlations between most mitral valve parameters and left ventricular dimensions with BSA, indicating that body size plays a critical role in cardiac anatomy. Overall, these findings suggest that variations in mitral valve geometry are closely linked to changes in left ventricular dimensions and wall thicknesses, underlining the importance of considering these factors in cardiovascular assessments and management.

REFERENCES

Abdelghani, M., Spitzer, E., Soliman, O. I., Beitzke, D., Laggner, R., Cavalcante, R., ... Serruys, P. W. (2017). A simplified and reproducible method to size the mitral annulus: implications for transcatheter mitral valve replacement. *European Heart Journal–Cardiovascular Imaging*, *18*(6), 697-706. DOI: 10.1093/ehjci/jew132

Ahmed, B., Hussain, W., Hussain, J., Basit, A., Haider, J., Muhammad, A. S., & Raheem, A. (2022). Thirty-year trend of non-rheumatic valvular heart disease: a comparison of pakistan with south asia and global scenario. Pakistan Heart Journal, 55(4), 357–263 DOI: 10.47144/phj.v55i4.2452

Anderson, R. H., & Wells, F. C. (2021). How Should We Describe the Mitral Valve and Its Component Parts?. *Mitral Valve Disease: Basic Sciences and Current Approaches to Management*, 29-38. DOI: 10.1007/978-3-030-67947-7_3

Anderson, R. H., Razavi, R., & Taylor, A. M. (2004). Cardiac anatomy revisited. *Journal of anatomy*, *205*(3), 159–177. DOI: 10.1111/j.0021-8782.2004.00330.x

Anderson, R. H., Spicer, D. E., Hlavacek, A. M., Cook, A. C., & Backer, C. L. (2013). *Wilcox's surgical anatomy of the heart*. Cambridge University Press.

Arinc, H., Gunduz, H., Tamer, A., Ozhan, H., Akdemir, R., Ozkokeli, M., & Uyan, C. (2004). Aberrant right ventricular branch of right coronary artery with mitral valve prolapse. *Experimental & Clinical Cardiology*, *9*(4), 251.

Asch, F. M., Miyoshi, T., Addetia, K., Citro, R., Daimon, M., Desale, S., ... Kirkpatrick, J. (2019). Similarities and differences in left ventricular size and function among races and nationalities: results of the World Alliance Societies of Echocardiography Normal Values Study. *Journal of the American Society of Echocardiography*, *32*(11), 1396-1406. DOI: 10.1016/j.echo.2019.08.012

Asgar, A. W. (2016). Sizing the mitral annulus: is CT the future?. *JACC: Cardiovascular Imaging*, *9*(3), 281-282. DOI: 10.1016/j.jcmg.2015.10.019

Bahiraie, P., Soleimani, H., Heydari, N., Najafi, K., Karlas, A., Avgerinos, D. V., ... Kampaktsis, P. N. (2024). Mitral Valve Repair of the Anterior Leaflet: Are we there yet?. *Hellenic Journal of Cardiology*. DOI: 10.1016/j.hjc.2024.02.001

Bakose, R. Y., Al-Obaidi, A. D., Al-Obaidi, M. N., Al-Abbasi, H., AL-Bayati, M. O., Hashim, A. T., ... Al-Dabagh, J. D. (2023). Anatomy of the Heart. In *Heart Transplantation* (pp. 1-17). Cham: Springer International Publishing. DOI: 10.1007/978-3-031-17311-0_1

Blanke, P., Berger, A., Bilbey, N., Gao, M., Lauzier, P. T., Cheung, A., ... Leipsic, J. (2015). Influence of left ventricular geometry and body-surface area on mitral annulus dimensions: assessment by computed tomography. *Journal of the American College of Cardiology*, *65*(10S), A1262-A1262.

Blanke, P., Dvir, D., Cheung, A., Levine, R. A., Thompson, C., Webb, J. G., & Leipsic, J. (2015). Mitral annular evaluation with CT in the context of transcatheter mitral valve replacement. *JACC: Cardiovascular Imaging*, *8*(5), 612-615. DOI: 10.1016/j.jcmg.2014.07.028

Blanke, P., Dvir, D., Cheung, A., Ye, J., Levine, R. A., Precious, B., ... Leipsic, J. (2014). A simplified D-shaped model of the mitral annulus to facilitate CT-based sizing before transcatheter mitral valve implantation. *Journal of cardiovascular computed tomography*, *8*(6), 459-467. DOI: 10.1016/j.jcct.2014.09.009

BS, G., & Varsha, M. (2019). The Anatomical Study Of Mitral Valve Annulus In The Human Cadaveric Hearts For Bioprosthesis. International Journal of Anatomy and Research

Çandır, B. N., Ergin, Ç., Yılar, K., Coşkun, O., Kara, E., Kale, A., ... Gayretli, Ö. (2024). Morphometric evaluation of the left atrioventricular valve complex and its clinical relations. *Folia Morphologica*.

Capoulade, R., Piriou, N., Serfaty, J. M., & Le Tourneau, T. (2017). Multimodality imaging assessment of mitral valve anatomy in planning for mitral valve repair in secondary mitral regurgitation. *Journal of thoracic disease*, *9*(Suppl 7), S640. DOI: 10.21037/jtd.2017.06.99

Carpentier, A., Adams, D. H., & Filsoufi, F. (2010). Carpentier's reconstructive valve surgery. Elsevier Health Sciences.

Charanya, N., Rajathi, G., & Vishali, N. (2017). Morphological and morphometrical analysis of mitral valve annulus of heart in human adult cadavers. *Int J Anat Res*, *5*(3.3), 44054409. DOI: 10.16965/ijar.2017.350

Dal-Bianco, J. P., & Levine, R. A. (2013). Anatomy of the mitral valve apparatus: role of 2D and 3D echocardiography. *Cardiology clinics*, *31*(2), 151-164. DOI: 10.1016/j.ccl.2013.03.001

Dal-Bianco, J. P., Aikawa, E., Bischoff, J., Guerrero, J. L., Hjortnaes, J., Beaudoin, J., ... Leducq Transatlantic Mitral Network. (2016). Myocardial infarction alters adaptation of the tethered mitral valve. *Journal of the American College of Cardiology*, *67*(3), 275-287. DOI: 10.1016/j.jacc.2015.10.092

de Groot-de Laat, L. E., Ren, B., McGhie, J., Oei, F. B., Strachinaru, M., Kirschbaum, S. W., ... Geleijnse, M. L. (2016). The role of experience in echocardiographic identification of location and extent of mitral valve prolapse with 2D and 3D echocardiography. *The international journal of cardiovascular imaging*, *32*, 1171-1177. DOI: 10.1007/s10554-016-0895-z

de Hemptinne, Q., De Cannière, D., Vandenbossche, J. L., & Unger, P. (2015). Cardiac calcified amorphous tumor: a systematic review of the literature. *IJC Heart & Vasculature*, *7*, 1-5. DOI: 10.1016/j.ijcha.2015.01.012

Delwarde, C., Capoulade, R., Mérot, J., Le Scouarnec, S., Bouatia-Naji, N., Yu, M., ... Le Tourneau, T. (2023). Genetics and pathophysiology of mitral valve prolapse. *Frontiers in Cardiovascular Medicine*, *10*, 160. DOI: 10.3389/fcvm.2023.1077788

Deopujari, R., Sinha, U., & Athavale, S. A. (2013). Anatomy of left atrioventricular valve (mitral valve) leaflets in adult Indian cadavers. *International Journal of Morphology*, *31*(4). DOI: 10.4067/S0717-95022013000400021

Donal, E., & Panis, V. (2021). Interaction between mitral valve apparatus and left ventricle. Functional mitral regurgitation: A brief state-of-the-art overview. *Advances in Clinical and Experimental Medicine*, *30*(10), 991-997. DOI: 10.17219/acem/143324

Dwivedi, G., Mahadevan, G., Jimenez, D., Frenneaux, M., & Steeds, R. P. (2014). Reference values for mitral and tricuspid annular dimensions using two-dimensional echocardiography. Echo research and practice, 1(2), 43. DOI: 10.1530/ERP-14-0050

Espino, D. M., Shepherd, D. E., & Buchan, K. G. (2007). Effect of mitral valve geometry on valve competence. *Heart and Vessels*, *22*, 109-115. DOI: 10.1007/s00380-006-0937-x

Faletra, F. F., Nucifora, G., & Ho, S. Y. (2013). Echocardiographic anatomy of the mitral valve. *Echocardiography in Mitral Valve Disease*, 1-22. DOI: 10.1007/978-88-470-5435-6_1

Faletra, F. F., Leo, L. A., Paiocchi, V. L., Caretta, A., Viani, G. M., Schlossbauer, S. A., ... Ho, S. Y. (2019). Anatomy of mitral annulus insights from non-invasive imaging techniques. *European Heart Journal-Cardiovascular Imaging*, *20*(8), 843-857. DOI: 10.1093/ehjci/jez153

Faletra, F. F., Leo, L. A., Paiocchi, V., Schlossbauer, S., Narula, J., & Ho, S. Y. (2021). Multimodality imaging anatomy of interatrial septum and mitral annulus. *Heart*, *107*(4), 277-281. DOI: 10.1136/heartjnl-2020-318127

Fu, G., Zhou, Z., Huang, S., Chen, G., Liang, M., Huang, L., & Wu, Z. (2021). Mitral valve surgery in patients with rheumatic heart disease: Repair vs.

replacement. *Frontiers in cardiovascular medicine*, *8*, 685746 doi: 10.3389/fcvm.2021.685746

Fyrenius, A., Engvall, J., & Janerot-Sjöberg, B. (2001). Major and minor axes of the normal mitral annulus. *The Journal of heart valve disease*, *10*(2), 146-152.

Gao, H., Qi, N., Feng, L., Ma, X., Danton, M., Berry, C., & Luo, X. (2017). Modelling mitral valvular dynamics–current trend and future directions. *International Journal for Numerical Methods in Biomedical Engineering*, *33*(10), e2858. doi: 10.1002/cnm.2858

Gasior, T., Gavazzoni, M., Taramasso, M., Zuber, M., & Maisano, F. (2019). Direct percutaneous mitral annuloplasty in patients with functional mitral regurgitation: when and how. *Frontiers in cardiovascular medicine*, *6*, 152. doi: 10.3389/fcvm.2019.00152

Gentry III, J. L., Summers, M. R., Harb, S., Jaber, W., Pettersson, G., & Griffin, B. (2018). Iatrogenic left circumflex coronary artery fistula after mitral valve replacement. *CASE*, *2*(5), 218-221. doi: 10.1016/j.case.2018.04.004

Gomadam, P. S., Stacey, R. B., Johnsen, A. E., Kitzman, D. W., Kon, N. D., & Upadhya, B. (2014). Papillary fibroelastoma of the mitral valve chordae with systemic embolization. *Journal of Cardiology Cases*, *10*(4), 125-128. doi: 10.1016/j.jccase.2014.06.004

Gonzalez-Gomez, A., Fernandez-Santos, S., Fernandez-Golfin, C., & Zamorano, J. L. (2015). Mitral valve anatomy: pre-procedural screening and imaging techniques. *EuroIntervention*, *11*(Suppl W), W32-W36. DOI: 10.4244/EIJV11SWA8

Goodwin, R. L., & Biechler, S. V. (2019). Clinical anatomy and embryology of heart valves. In *Principles of heart valve engineering* (pp. 1-12). Academic Press.

Gumpangseth, T., Komutrattananont, P., Palee, P., Prasitwattanaseree, S., & Mahakkanukrauh, P. (2020). Image Analysis of Morphometric Evaluation from the Heart Valves for Age Estimation in Thai Population. *International Journal of Morphology*, *38*(3). DOI:10.4067/S0717-95022020000300726

Gunnal, S. A., Wabale, R. N., & Farooqui, M. S. (2015). Morphological study of chordae tendinae in human cadaveric hearts. Heart Views, 16(1), 1-12. doi: 10.4103/1995-705X.152994

Gupta, C., Shetti, V. R., & Manju, B. V. M. (2017). Dimensions of the human adult mitral valve in the embalmed cadaver. *Journal of Morphological Sciences*, *30*(1), 0-0.

Habib, G., Lancellotti, P., Antunes, M. J., Bongiorni, M. G., Casalta, J. P., Del Zotti, F., Dulgheru, R., El Khoury, G., Erba, P. A., Iung, B., Miro, J. M., Mulder, B. J., Plonska-Gosciniak, E., Price, S., Roos-Hesselink, J., Snygg-Martin, U., Thuny, F., Tornos Mas, P., Vilacosta, I., Zamorano, J. L., … ESC Scientific Document Group (2015). 2015 ESC Guidelines for the management of infective endocarditis: The Task Force for the Management of Infective Endocarditis of the European Society of Cardiology (ESC). Endorsed by: European Association for Cardio-Thoracic Surgery (EACTS), the European Association of Nuclear Medicine (EANM). European heart journal, 36(44), 3075–3128. DOI: 10.1093/eurheartj/ehv319

Hammer, K. (2009). High resolution 3D-imaging of the physiology and morphology of isolated adult cardiac myocytes from rat and mice.

Harb, S. C., & Griffin, B. P. (2017). Mitral valve disease: a comprehensive review. *Current cardiology reports*, *19*, 1-8. DOI: 10.1007/s11886-017-0883-5

Harky, A., Botezatu, B., Kakar, S., Ren, M., Shirke, M. M., & Pullan, M. (2021). Mitral valve diseases: pathophysiology and interventions. *Progress in Cardiovascular Diseases*, *67*, 98-104. DOI: 10.1016/j.pcad.2021.03.008

Henry, M. P., Cotella, J., Mor-Avi, V., Addetia, K., Miyoshi, T., Schreckenberg, M., ... Asch, F. M. (2022). Three-Dimensional transthoracic static and dynamic normative values of the mitral valve apparatus: results from the multicenter world alliance societies of echocardiography study. Journal of the American Society of Echocardiography, 35(7), 738-751. DOI: 10.1016/j.echo.2022.02.010

Henry, M., Cotella, J. I., Mor-Avi, V., & Investigators, W. A. S. E. (2022). Normative values of the mitral valve apparatus: a 3D multicenter WASE study exploring age and sex differences. *European Heart Journal-Cardiovascular Imaging*, *23*(Supplement_1), jeab289-191. DOI: 10.1093/ehjci/jeab289.191

Ho, S. Y. (2009). Anatomy and myoarchitecture of the left ventricular wall in normal and in disease. *European Journal of Echocardiography*, *10*(8), iii3-iii7. DOI: 10.1093/ejechocard/jep159

Ho, S. Y. (2020). Cardiac anatomy: The essentials. *Cardiology Plus*, *5*(3), 148-154. DOI:10.4103/cp.cp_19_20

Huang, A. L., Dal-Bianco, J. P., Levine, R. A., & Hung, J. W. (2023). Secondary Mitral Regurgitation: Cardiac Remodeling, Diagnosis, and Management. *Structural Heart*, *7*(3), 100129. DOI: 10.1016/j.shj.2022.100129

Iaizzo, P. A., Bateman, M. G., Quill, J. L., Rolfes, C. D., Howard, S. A., Eggum, J. H., ... Hill, A. J. (2012). The Atlas of Human Cardiac Anatomy: A free-access educational website.

Issa, Z. F., Miller, J. M., & Zipes, D. P. (2019). Typical atrioventricular bypass tracts. In *Elsevier eBooks* (pp. 599–676). DOI: 10.1016/b978-0-323-52356-1.00018-9

Jellis, C. (2015). Mitral Valve Nomenclature. *An Atlas of Mitral Valve Imaging*, 1-16. DOI:10.1007/978-1-4471-6672-6_1

Jiang, L., Owais, K., Matyal, R., Khabbaz, K. R., Liu, D. C., Montealegre-Gallegos, M., ... Mahmood, F. (2014). Dynamism of the mitral annulus: a spatial and temporal analysis. *Journal of Cardiothoracic and Vascular Anesthesia*, *28*(5), 1191-1197. DOI: 10.1053/j.jvca.2014.03.020

Jolley, M. A., Ghelani, S. J., Adar, A., & Harrild, D. M. (2017). Three-dimensional mitral valve morphology and age-related trends in children and young adults with structurally normal hearts using transthoracic echocardiography. *Journal of the American Society of Echocardiography*, *30*(6), 561-571. DOI: 10.1016/j.echo.2017.01.018

Kaiser, A. D., McQueen, D. M., & Peskin, C. S. (2019). Modeling the mitral valve. *International journal for numerical methods in biomedical engineering*, *35*(11), e3240. DOI: 10.1002/cnm.3240

Kalyanasundaram, A., Qureshi, A., Nassef, L. A., & Shirani, J. (2010). Functional anatomy of normal mitral valve-left ventricular complex by real-time, three-dimensional echocardiography. *J Heart Valve Dis*, *19*(1), 28-34.

Kapadia, S. Dimensions and geometry of the mitral and tricuspid valves in normal and diseased states. University School 2785 Som Center Rd, Chagrin Falls, OH 44022

Karagodin, I., Singh, A., & Lang, R. M. (2020). Pathoanatomy of mitral regurgitation. *Structural Heart*, *4*(4), 254-263. doi: 10.1080/24748706.2020.1765055

Krawczyk-Ożóg, A., Hołda, M. K., Bolechała, F., Siudak, Z., Sorysz, D., Dudek, D., & Klimek-Piotrowska, W. (2018). Anatomy of the mitral subvalvular apparatus. *The Journal of thoracic and cardiovascular surgery*, *155*(5), 2002-2010. DOI: 10.1016/j.jtcvs.2017.12.061

Krawczyk-Ożóg, A., Hołda, M. K., Sorysz, D., Koziej, M., Siudak, Z., Dudek, D., & Klimek-Piotrowska, W. (2017). Morphologic variability of the mitral valve leaflets. *The Journal of Thoracic and Cardiovascular Surgery*, *154*(6), 1927-1935. DOI: 10.1016/j.jtcvs.2017.12.061

Kumar, M., Khokhar, N. A., Bano, S., Shah, S. A., Abrar, M., & Kalhoro, M. A. (2022). Prevalence of rheumatic heart disease in Pakistan: a meta-analysis study. *J Res Med Dent Sci*, *10*(2), 79-81.

Kunzelman, K. S., Cochran, R. P., Verrier, E. D., & Eberhart, R. C. (1994). Anatomic basis for mitral valve modelling. J Heart Valve Dis, 3(5), 491-496.

Lama, C. P., Pradhan, A., Chalise, U., Dhungel, S., & Ghosh, S. K. (2018). Measurement of the tricuspid and the mitral valve in adult human heart: a cadaveric study. *Nepal Medical College Journal*, *20*(4), 121-127. DOI: 10.3126/nmcj.v20i4.25128

Le Tourneau, T., Mérot, J., Rimbert, A., Le Scouarnec, S., Probst, V., Le Marec, H., ... Schott, J. J. (2018). Genetics of syndromic and non-syndromic mitral valve prolapse. *Heart*, *104*(12), 978-984. DOI: 10.1136/heartjnl-2017-312420

Leo, L. A., Paiocchi, V. L., Schlossbauer, S. A., Gherbesi, E., & Faletra, F. F. (2020). Anatomy of mitral valve complex as revealed by non-invasive imaging: pathological, surgical and interventional implications. *Journal of cardiovascular development and disease*, *7*(4), 49. DOI: 10.3390/jcdd7040049

Levine, R. A., Hagége, A. A., Judge, D. P., Padala, M., Dal-Bianco, J. P., Aikawa, E., ... Leducq Mitral Transatlantic Network. (2015). Mitral valve disease—morphology and mechanisms. *Nature reviews cardiology*, *12*(12), 689-710. DOI: 10.1038/nrcardio.2015.161

Litviňuková, M., Talavera-López, C., Maatz, H., Reichart, D., Worth, C. L., Lindberg, E. L., ... Teichmann, S. A. (2020). Cells of the adult human heart. *Nature*, *588*(7838), 466-472. DOI: 10.1038/s41586-020-2797-4

Loukas, M., Youssef, P., Gielecki, J., Walocha, J., Natsis, K., & Tubbs, R. S. (2016). History of cardiac anatomy: a comprehensive review from the Egyptians to today. *Clinical Anatomy*, *29*(3), 270-284. DOI: 10.1002/ca.22705

Maggiore, P., Anastasius, M., Huang, A. L., Blanke, P., & Leipsic, J. (2020). Transcatheter Mitral Valve Repair and Replacement: Current Evidence for Intervention and the Role of CT in Preprocedural Planning—A Review for Radiologists and Cardiologists Alike. *Radiology: Cardiothoracic Imaging*, *2*(1), e190106. DOI: 10.1148/ryct.2020190106

Mahadevan, V. (2018). Anatomy of the heart. *Surgery (Oxford)*, *36*(2), 43-47. DOI: 10.1016/j.mpsur.2008.09.022

Majonga, E. D., Norrish, G., Rehman, A. M., Kranzer, K., Mujuru, H. A., Nathoo, K., ... Ferrand, R. A. (2018). Racial variation in echocardiographic reference ranges for left chamber dimensions in children and adolescents: a systematic review. *Pediatric cardiology*, *39*, 859-868. DOI: 10.1007/s00246-018-1873-0

Makaryus, A. N., Ismail, H., Makaryus, J. N., & Fan, D. (2017). Geometric comparison of the mitral and tricuspid valve annulus: Insights from three-dimensional transesophageal echocardiography. *World Journal of Cardiology*, *9*(9), 757. DOI: 10.4330/wjc.v9.i9.757

Maken, Z. H., Ahmed, F., Ferogh, E., & Arumghan, A. (2016). An epidemiological analysis of socioeconomic risk factors among patients of rheumatic heart disease, Islamabad, Pakistan. *Pakistan Journal of Public Health*, *6*(4), 41-43. DOI: 10.32413/pjph.v6i4.13

Makhija, N., Magoon, R., Balakrishnan, I., Das, S., Malik, V., & Gharde, P. (2019). Left ventricular outflow tract obstruction following aortic valve replacement: A review of risk factors, mechanism, and management. Annals of Cardiac Anaesthesia, 22(1), 1. DOI: 10.4103/aca.ACA_226_17

Maréchaux, S., Illman, J. E., Huynh, J., Michelena, H. I., Nkomo, V. T., & Tribouilloy, C. (2017). Functional anatomy and pathophysiologic principles in mitral regurgitation: Non-invasive assessment. *Progress in cardiovascular diseases*, *60*(3), 289–304. DOI: 10.1016/j.pcad.2017.11.008

Marsit, O., Clavel, M. A., Côté-Laroche, C., Hadjadj, S., Bouchard, M. A., Handschumacher, M. D., ... Beaudoin, J. (2020). Attenuated mitral leaflet enlargement contributes to functional mitral regurgitation after myocardial infarction. *Journal of the American College of Cardiology*, *75*(4), 395-405. DOI: 10.1016/j.jacc.2019.11.039

Meschini, V., De Tullio, M. D., Querzoli, G., & Verzicco, R. (2018). Flow structure in healthy and pathological left ventricles with natural and prosthetic mitral valves. *Journal of fluid mechanics*, *834*, 271-307. DOI: 10.1017/jfm.2017.725

Mihăilă, S., Muraru, D., Piasentini, E., Miglioranza, M. H., Peluso, D., Cucchini, U., ... Badano, L. P. (2014). Quantitative analysis of mitral annular geometry and function in healthy volunteers using transthoracic three-dimensional echocardiography. Journal of the American Society of Echocardiography, 27(8), 846-857. DOI: 10.1016/j.echo.2014.04.017

Millington, S. (2014). Cardiac Ultrasound Technique. *Point of Care Ultrasound E-book*, 89.

Mishra, P. P., Rao, M. P., Paranjape, V., & Kulkarni, J. P. (2014). Morphometry of mitral valve. *Medical Journal of Dr. DY Patil University*, *7*(5), 625-630. DOI:10.4103/0975-2870.140453

Mohan, J. C. (2014). *A practical approach to clinical echocardiography*. JP Medical Ltd.

Mohtaj, T., Aazami, M. H., Sazegar, G., Poorzand, H., Hedjazi, A., Morovatdar, N., & Toorabi, A. (2018). Morphometric study of mitral valve annulus in Iran. *Galen Medical Journal*, *7*, e1078. DOI: 10.22086/gmj.v0i0.1078

Moorjani, N., Rana, B. S., Wells, F. C. (2018). Anatomy and physiology of the mitral valve. *Operative Mitral and Tricuspid Valve Surgery*, 1-20. DOI:10.1007/978-1-4471-4204-1

Morris, M. F., Maleszewski, J. J., Suri, R. M., Burkhart, H. M., Foley, T. A., Bonnichsen, C. R., ... Araoz, P. A. (2010). CT and MR imaging of the mitral valve: radiologic-pathologic correlation. *Radiographics*, *30*(6), 1603-1620. DOI: 10.1148/rg.306105518

Mujtaba, S. S., & Clark, S. (2018). Quadruple valve replacement for carcinoid heart disease. *Brazilian Journal of Cardiovascular Surgery*, *33*, 398-403. doi: 10.21470/1678-9741-2017-0224

Munafò, R., Saitta, S., Ingallina, G., Denti, P., Maisano, F., Agricola, E., ... Votta, E. (2024). A Deep Learning-Based Fully Automated Pipeline for Regurgitant Mitral Valve Anatomy Analysis From 3D Echocardiography. *IEEE Access*. DOI: 10.48550/arXiv.2302.10634

Muresian H. The clinical anatomy of the mitral valve. Clin Anat 2009; 22: 85e98. DOI: 10.1002/ca.20692

Naoum, C., Leipsic, J., Cheung, A., Ye, J., Bilbey, N., Mak, G., ... Blanke, P. (2016). Mitral annular dimensions and geometry in patients with functional mitral regurgitation and mitral valve prolapse: implications for transcatheter mitral valve implantation. JACC: Cardiovascular Imaging, 9(3), 269-280. DOI: 10.1016/j.jcmg.2015.08.022

Nemes, A., Kormányos, Á., Domsik, P., Kalapos, A., Ambrus, N., & Lengyel, C. (2020). Normal reference values of three-dimensional speckle-tracking echocardiography-derived right atrial volumes and volume-based functional properties in healthy adults (Insights from the MAGYAR-Healthy Study). *Journal of Clinical Ultrasound*, *48*(5), 263-268. DOI: 10.1002/jcu.22795

Nemes, A., Piros, G. Á., Domsik, P., Kalapos, A., Lengyel, C., Várkonyi, T. T., ... Forster, T. (2015). Changes in mitral annular morphology and function in young patients with type 1 diabetes mellitus—results from the three-dimensional speckle tracking echocardiographic MAGYAR-Path Study. *Quantitative Imaging in Medicine and Surgery*, *5*(6), 815. DOI: 10.3978/j.issn.2223-4292.2015.12.02

Netter, F. H. (2022). *Netter atlas of human anatomy: classic regional approach*. Elsevier Health Sciences.

Nordblom, P., & Bech-Hanssen, O. (2007). Reference values describing the normal mitral valve and the position of the papillary muscles. Echocardiography, 24(7), 665-672. DOI: 10.1111/j.1540-8175.2007.00474.x

Oehler, A. C., Sullivan, P. D., & Mansoor, A. M. (2017). Mitral Stenosis. *BMJ case reports*, *2017*, bcr2017220120. DOI: 10.1136/bcr-2017-220120

Oliveira, D., Srinivasan, J., Espino, D., Buchan, K., Dawson, D., & Shepherd, D. (2020). Geometric description for the anatomy of the mitral valve: a review. *Journal of Anatomy*, *237*(2), 209-224. DOI: 10.1111/joa.13196

Omran, A. S., Arifi, A. A., & Mohamed, A. A. (2010). Echocardiography of the mitral valve. *Journal of the Saudi Heart Association*, *22*(3), 165–170. DOI: 10.1016/j.jsha.2010.04.001

Pozzoli, A., Zuber, M., Reisman, M., Maisano, F., & Taramasso, M. (2018). Comparative anatomy of mitral and tricuspid valve: what can the interventionlist learn from the surgeon. *Frontiers in cardiovascular medicine*, *5*, 80. doi: 10.3389/fcvm.2018.00080

Rajiah, P., Fulton, N. L., & Bolen, M. (2019). Magnetic resonance imaging of the papillary muscles of the left ventricle: normal anatomy, variants, and abnormalities. *Insights into imaging*, *10*, 1-17.

Rajila Rajendran, H. S., Seshayyan, S., Victor, A., Murugesan, N., & Sundaramurthi, I. (2011). The study of mitral valve annular dimension in relation to the body surface area in the Indian population. *European journal of cardio-thoracic surgery*, *39*(5), 653-656. DOI: 10.1016/j.ejcts.2010.08.052

Rana, B., & Robinson, S. (2020). Transthoracic anatomy and pathology: valves. Oxford Specialist Handbooks in Cardiology: Echcardiography, 3, 287-324.

Rehman, I., & Rehman, A. (2023). Anatomy, Thorax, Heart. In *StatPearls*. StatPearls Publishing.

Rehman, I., Nassereddin, A., & Rehman, A. (2023). Anatomy, Thorax, Pericardium. In *StatPearls*. StatPearls Publishing.

Ricci, F., Aung, N., Gallina, S., Zemrak, F., Fung, K., Bisaccia, G., ... Petersen, S. E. (2021). Cardiovascular magnetic resonance reference values of mitral and tricuspid annular dimensions: the UK Biobank cohort. Journal of Cardiovascular Magnetic Resonance, 23, 1-13.

Rich, N. L., & Khan, Y. S. (2020). Anatomy, thorax, heart papillary muscles.

Ring, L., Dutka, D. P., Boyd, J., Parker, K., Wendler, O., Monaghan, M. J., & Rana, B. S. (2018). The normal mitral valve annulus in humans defined using 3-dimensional transesophageal echocardiography. JACC: Cardiovascular Imaging, 11(3), 510-512. DOI: 10.1016/j.jcmg.2017.05.017

Ripa, R., George, T., Shumway, K. R., & Sattar, Y. (2023). Physiology, Cardiac Muscle. In *StatPearls*. StatPearls Publishing.

Roberts, W., Salandy, S., Mandal, G., Holda, M. K., Tomaszewksi, K. A., Gielecki, J., ... Loukas, M. (2019). Across the centuries: Piecing together the anatomy of the heart. *Translational Research in Anatomy*, *17*, 100051. DOI: 10.1016/j.tria.2019.100051

Rostagno, C. (2019). Heart valve disease in the elderly. World journal of cardiology, 11(2), 71. DOI: 10.4330/wjc.v11.i2.71

Sadeghpour, A., Abtahi, F., Kiavar, M., Esmaeilzadeh, M., Samiei, N., Ojaghi, S. Z., ... Mohebbi, A. (2008). Echocardiographic evaluation of mitral geometry in functional mitral regurgitation. *Journal of cardiothoracic surgery*, *3*, 1-7. DOI: 10.1186/1749-8090-3-54

Saha, A., & Roy, S. (2018). Papillary muscles of left ventricle-Morphological variations and it's clinical relevance. *Indian heart journal*, *70*(6), 894–900. DOI:10.1016/j.ihj.2017.12.003

Salahuddin, S., Ramakrishnan, S., Seth, S., & Bhargava, B. (2012). "Smoking" Mitral Valve. Journal of the American College of Cardiology, 60(11), e19. DOI: 10.1016/j.jacc.2012.01.081

Saremi, F., Sánchez-Quintana, D., Mori, S., Muresian, H., Spicer, D. E., Hassani, C., & Anderson, R. H. (2017). Fibrous skeleton of the heart: anatomic overview and evaluation of pathologic conditions with CT and MR imaging. *Radiographics*, *37*(5), 1330-1351. DOI: 10.1148/rg.2017170004

Savalgi, G., Jayanthi, V., Shruthi, J., & Kumar, H. M. (2022). Morphometry of mitral valve leaflet for reconstructive surgery in human cadaveric hearts of South Indian population. *International Journal of Anatomy Radiology and Surgery*, *11*, 9-13. DOI:10.7860/IJARS/2022/52827.2754

Saxena, A. (2013). Echocardiographic diagnosis of chronic rheumatic valvular lesions. *Global heart*, *8*(3), 203-212. DOI: 10.1016/j.gheart.2013.08.007

Schmidt, C. W. P., & Schmidt, C. W. P. (2019). Body Surface Area (BSA). *Pediatric Oncologic Pharmacy: A Complete Guide to Practice*, 141-141. DOI:10.1007/978-3-030-10988-2

Schubert, S. A., Mehaffey, J. H., Charles, E. J., & Kron, I. L. (2017). Mitral Valve Repair: The French Correction Versus the American Correction. *The Surgical clinics of North America*, *97*(4), 867–888. DOI: 10.1016/j.suc.2017.03.009

Séguéla, P. E., Houyel, L., & Acar, P. (2011). Congenital malformations of the mitral valve. *Archives of cardiovascular diseases*, *104*(8-9), 465-479. DOI: 10.1016/j.acvd.2011.06.004

Shah, P. M. (2010). Current concepts in mitral valve prolapse—diagnosis and management. *Journal of cardiology*, *56*(2), 125-133. DOI: 10.1016/j.jjcc.2010.06.004

Soliyeva M.Y. (2022). In The Anatomy of the Heart, Its Specific Characteristics Are. *Global Scientific Review*, *9*, 13–20. Retrieved from https://scienticreview.com/index.php/gsr/article/view/76

Sonne, C., Sugeng, L., Watanabe, N., Weinert, L., Saito, K., Tsukiji, M., ... Lang, R. M. (2009). Age and body surface area dependency of mitral valve and papillary apparatus parameters: assessment by real-time three-dimensional echocardiography. European Journal of Echocardiography, 10(2), 287-294. DOI: 10.1093/ejechocard/jen237

Spicer, D. E., Bridgeman, J. M., Brown, N. A., Mohun, T. J., & Anderson, R. H. (2014). The anatomy and development of the cardiac valves. *Cardiology in the Young*, *24*(6), 1008-1022. DOI: 10.1017/S1047951114001942

Spicer, D. E., Mill, M. R., & Anderson, R. H. (2023). Cardiac Anatomy. In Baumgartner, W., Jacobs, J., & Darling, G. (Eds.), *Adult and Pediatric Cardiac Surgery. STS Cardiothoracic Surgery E-Book*. Chicago: Society of Thoracic Surgeons. ebook.sts.org

Sriambika, K., Nim, V. K., & Bage, N. N. (2018). Morphological and morphometric study of mitral valve with reference to anatomical variability in south indian subjects. *Int J Anat Res*, *6*(4.3), 5994-97. DOI:10.16965/ijar.2018.392

Standring, S. (Ed.). (2021). *Gray's Anatomy E-Book: Gray's Anatomy E-Book.* Elsevier Health Sciences.

Topilsky, Y. (2020). Mitral regurgitation: anatomy, physiology, and pathophysiology—lessons learned from surgery and cardiac imaging. *Frontiers in Cardiovascular Medicine, 7,* 84. DOI: 10.3389/fcvm.2020.00084

TORRES, V., MUNÍN, M. A., THIERER, J., RAGGIO, I. M., GOERNER, M. S., LOMBARDERO, M., ... Ortega, J. (2014). Three-dimensional echocardiographic analysis of mitral valve characteristics. *Revista Argentina de Cardiología*, *82*(4), 279-284.

Tortora, G. J., & Derrickson, B. H. (2018). *Principles of anatomy and physiology*. John Wiley & Sons.

Tran, D. B., Weber, C., & Lopez, R. A. (2019). Anatomy, thorax, heart muscles.

Tsang, W., Freed, B. H., & Lang, R. M. (2020). Three-dimensional anatomy of the aortic and mitral valves. *Valvular Heart Disease: A Companion to Braunwald's Heart Disease E-Book,* 22.

Tumenas, A., Tamkeviciute, L., Arzanauskiene, R., & Arzanauskaite, M. (2021). Multimodality imaging of the mitral valve: morphology, function, and disease. *Current Problems in Diagnostic Radiology*, *50*(6), 905-924. DOI: 10.1067/j.cpradiol.2020.09.013

Ugwuanyi, D. C., Eze, J. C., Uche, C. H., Thaddeus, N. C., & Eze, C. U. (2020). Echocardiographic evaluation of normal adult left Ventricular geometry in a Nigerian population. *bioRxiv*, 2020-04. DOI: 10.1101/2020.04.09.033993

Vaca, F. S., & Bordoni, B. (2023). Anatomy, Thorax, Mitral Valve. In *StatPearls [Internet]*. StatPearls Publishing.

van Wijngaarden, S. E., Kamperidis, V., Regeer, M. V., Palmen, M., Schalij, M. J., Klautz, R. J., ... & Delgado, V. (2018). Three-dimensional assessment of mitral valve annulus dynamics and impact on quantification of mitral regurgitation. European Heart Journal-Cardiovascular Imaging, 19(2), 176-184. DOI: 10.1093/ehjci/jex001

Walsh, E. P., Mayer, J. E., Teele, S. A., & Brown, D. W. (Eds.). (2023). *Nadas' Pediatric Cardiology-E-Book*. Elsevier Health Sciences.

Watkins, D. A., Johnson, C. O., Colquhoun, S. M., Karthikeyan, G., Beaton, A., Bukhman, G., ... Roth, G. A. (2017). Global, regional, and national burden of rheumatic heart disease, 1990–2015. *New England Journal of Medicine*, *377*(8), 713-722. DOI: 10.1056/NEJMoa1603693

Webb, R. H., Culliford-Semmens, N., Sidhu, K., & Wilson, N. J. (2017). Normal echocardiographic mitral and aortic valve thickness in children. *Heart Asia*, *9*(1), 70-75. DOI: 10.1136/heartasia-2016-010872

Weir-McCall, J. R., Blanke, P., Naoum, C., Delgado, V., Bax, J. J., & Leipsic, J. (2018). Mitral valve imaging with CT: relationship with transcatheter mitral valve interventions. *Radiology*, *288*(3), 638-655. DOI: 10.1148/radiol.2018172758

Whitaker, R. H. (2010). Anatomy of the heart. *Medicine*, *38*(7), 333-335. DOI: 10.1016/j.mpmed.2010.04.005

Whiteman, S., Alimi, Y., Carrasco, M., Gielecki, J., Zurada, A., & Loukas, M. (2021). Anatomy of the cardiac chambers: A review of the left ventricle. *Translational Research in Anatomy*, *23*, 100095. DOI: 10.1016/j.tria.2020.100095

Wineski, L. E. (2024). *Snell's clinical anatomy by regions*. Lippincott Williams & Wilkins.

Xu, B., Daimon, M., Kawata, T., Nakao, T., Hirokawa, M., Sawada, N., ... Yatomi, Y. (2021). Relationship Between Mitral Leaflet Size and Coaptation and Their Associated Factors in Patients with Normal Left Ventricular Size and Systolic Function Real-Time 3D Echocardiographic Analysis. *International Heart Journal*, *62*(1), 95-103. DOI: 10.1536/ihj.20-148

Yandrapalli, S., Biswas, M., & Kaplan, J. (2021). Mitral Valve Minimally Invasive Surgical Treatment. In StatPearls [Internet]. StatPearls Publishing.

Yu, M., Tcheandjieu, C., Georges, A., Xiao, K., Tejeda, H., Dina, C., ... Priest, J. R. (2022). Computational estimates of annular diameter reveal genetic determinants of mitral valve function and disease. *JCI insight*, *7*(3). DOI: 10.1172/jci.insight.146580

ANNEXURES

FACULTY RESEARCH COMMITTEE
FACULTY OF HEALTH SCIENCES
(FRC-FoHS)

LETTER OF APPROVAL

Date: 02-01-2024

To,
Dr. Mahail Khan
MPhil – Student
Department of Anatomy
BUHSCK

Subject: **Faculty Research Committee**
FRC-BUHSCK Approval of Research Study

Title of Study: Evaluation of mitral valve dimensions in the tertiary cardiac center of Karachi.

Name of Student: **Dr. Mahail Khan**
Reference No: **FRC-BUHS 03/2024**

Dear Dr. Mahail Khan

Thank you for submitting research proposal to FRC-BUHSCK. The committee has approved your project.
Regards

PROF. DR. Shehla M. Baqai HI (M)
Maj. Gen (R)
Chairperson FRC-BUHSCK

Cc:
Registrar
Director PGP
Director QA
Director DRC
Dean HS
Secretary FRC
HOD Concerned
Student Concerned

Dean HS & Principal Secretariat, BUHSC Karachi, DHA Phase – II Adjacent PNS SHIFA Karachi
Office No. +92-21-99332688 Ext: 1026 |Tel: +92-21-35319491-9 | Web: www.bahria.edu.pk/bumdc/

Bahria University
Health Sciences Campus, Karachi

IRB
No one left behind for research.

Institutional Review Board

BUHS-IRB # 032/23-new-24

Date: 02-02-24
Name of PI: Dr. Mahail Khan.
Affiliation & Department: MPhil Candidate Anatomy
Address-BUHS, C Sailor Street, DHA Phase 2, Karachi

Subject: **APPROVAL OF YOUR RESEARCH PROPOSAL WITH A CHANGED TITLE:**

Old Title of the research
Analysis of mitral valve geometry in the Pakistani population

New Title of the research
EVALUATION OF MITRAL VALVE DIMENSION IN THE TERTIARY CARDIAC CENTRE OF KARACHI

Dear Dr. Mahail Khan.

I am writing this letter at your request to confirm that we support the research project **"EVALUATION OF MITRAL VALVE DIMENSION IN THE TERTIARY CARDIAC CENTRE OF KARACHI" (with a new title).** I know the research will determine the normal values of mitral valve geometry parameters and the association of variations in mitral valve geometry parameters with age, gender, body surface area, and ethnicity in the Pakistani population by Transthoracic 2D Echocardiography. The IRB will support the project under the proposed guidelines in the IRB application for twelve *months.*

Suppose any unanticipated problems or adverse advents occur. In that case, it is up to Dr. Mahail Khan to report these events to the IRB as promptly as possible. This research will provide the foundation for future research for developing specific guidelines and interventional strategies tailored to patients with mitral valve conditions within the Pakistani population. We will be happy tosupport this endeavor.

Sincerely,

Prof Dr. Inayat H. Thaver
FCPS (Community Medicine); PhD (Public Health)
Chairperson, Institutional Review Board (IRB)
Bahria University Health Sciences Campus
Karachi

Prof. Dr. Inayat H. Thaver
Chair, Institutional Review Board.

IRB Office, BUHSC(K) Adjacent PNS SHIFA, Sailor Street, DHA Phase – II Karachi
Office No. +92-21-35319491-6 Ext: 1080 | Fax: +92-21-99332689

EVALUATION OF MITRAL VALVE DIMENSIONS IN THE TERTIARY CARDIAC CENTRE OF KARACHI

CONSENT FORM

This is a questionnaire-based study, the objective of which is to the normal values of mitral valve geometry parameters in the Pakistani population by Transthoracic 2D Echocardiography and its association with age, gender, body surface area, and ethnicity and also to evaluate the impact of variations of mitral valve geometry on left ventricular dimensions and wall thickness. You will be required to answer questions related to demography and your health status. All the data provided by you will be used only for research purposes. Data will remain highly confidential and will be saved in a password protected file accessible only to the principal investigator.

Risks Involved:

You have been informed that there are no risks involved to you during the study

Benefits of the Study:

Based on the study results, cardiologist will be able provide more tailored treatment options based on their mitral valve variations and leading to improve patient outcomes.

Compensation:

You are aware that there will be no reward, monetary or otherwise in return of your participation in the study.

Confidentiality:

Any information that you provide regarding your health will be kept thoroughly confidential. All data will be coded and saved in a password protected folder accessible only to the principal investigator.

Referral:

You have been informed that you will be referred for counselling/medical help if required

Withdrawal from the Study:

You are free to withdraw from the study at any point. No repercussions or consequences will be followed in any form if you decide to do so.

Contact:

You can contact Dr. Mahail Khan at Bahira University Medical and Dental College, adjacent to PNS Shifa Hospital, Sailor Street, Phase II DHA, Karachi. (8:30 am – 4:00 pm) if you have any queries regarding your participation.

I hereby confirm that I have read and understood everything that has been stated above and based on the same I voluntarily consent to participate in the study with my free will.

Participant's Signature: ___________ **Witness' Signature:** ____________

Participant's Name: _______________ **Witness' Name:** ____________

Participant's Number: ______________

Participant's Address: ____________________

Date: _______________ **S. No.:** ____________

باخبر رضامندی۔

یہ ایک سوالنامے پر مبنی مطالعہ ہے، جس کا مقصد پاکستانی آبادی میں Transthoracic 2D ایکوکارڈیوگرافی کے ذریعے مائٹرل والو جیومیٹری کے پیرامیٹرز کی نارمل اقدار اور عمر، جنس، جسم کی سطح کے رقبے اور نسل کے ساتھ اس کا تعلق اور اس کے اثرات کا جائزہ لینا ہے۔ بائیں وینٹرکولر طول و عرض اور دیوار کی موٹائی پر مائٹرل والو جیومیٹری کے تغیرات۔ آپ کو ڈیموگرافی اور آپ کی صحت کی حیثیت سے متعلق سوالات کے جوابات دینے کی ضرورت ہوگی۔ آپ کے ذریعہ فراہم کردہ تمام ڈیٹا صرف تحقیقی مقاصد کے لیے استعمال کیا جائے گا۔ ڈیٹا انتہائی خفیہ رہے گا اور پاس ورڈ سے محفوظ فائل میں محفوظ کیا جائے گا جو صرف پرنسپل تفتیش کار کے لیے قابل رسائی ہے۔

<u>شامل خطرات</u>

آپ کو مطلع کیا گیا ہے کہ مطالعہ کے دوران آپ کو کوئی خطرہ نہیں ہے۔

<u>مطالعہ کے فوائد</u>

مطالعہ کے نتائج کی بنیاد پر، ماہر امراض قلب اپنے مائٹرل والو کی مختلف حالتوں کی بنیاد پر مزید موزوں علاج کے اختیارات فراہم کر سکیں گے اور اس کے نتیجے میں مریض کے نتائج بہتر ہوں گے۔

معاوضہ

آپ کو معلوم ہے کہ مطالعہ میں آپ کی شرکت کے بدلے کوئی انعام، مالی یا دوسری صورت میں نہیں ملے گا۔

رازداری

آپ اپنی صحت سے متعلق جو بھی معلومات فراہم کرتے ہیں اسے مکمل طور پر خفیہ رکھا جائے گا۔ تمام ڈیٹا کوڈ کیا جائے گا اور پاس ورڈ سے محفوظ فولڈر میں محفوظ کیا جائے گا جو صرف پرنسپل تفتیش کار کے لیے قابل رسائی ہے۔

حوالہ

آپ کو مطلع کیا گیا ہے کہ اگر ضرورت ہو تو آپ کو مشاورت/طبی مدد کے لیے بھیجا جائے گا۔

مطالعہ سے دستبرداری

آپ کسی بھی وقت مطالعہ سے دستبردار ہونے کے لیے آزاد ہیں۔ اگر آپ ایسا کرنے کا فیصلہ کرتے ہیں تو کسی بھی شکل میں کوئی اثر یا نتائج نہیں ہوں گے

رابطہ

آپ ڈاکٹر ماہیل خان سے بحیرہ یونیورسٹی میڈیکل اینڈ ڈینٹل کالج، پی این ایس شفا اسپتال سے ملحق، سیلر اگر آپ کو اپنی شرکت سے متعلق کوئی سوالات ہیں۔ اسٹریٹ، فیز

میں اس کے ذریعے اس بات کی تصدیق کرتا ہوں کہ میں نے اوپر بیان کی گئی ہر چیز کو پڑھ اور سمجھ لیا ہے اور اسی کی بنیاد پر میں رضاکارانہ طور پر اپنی آزاد مرضی سے مطالعہ میں حصہ لینے کی رضامندی دیتا ہوں۔

: دستخط گواہ کے ______________ شرکت کنندہ کے دستخط**:** __________________

:گواہ کا نام ______________ حصہ لینے والے کا نام**:** __________________

شرکت کنندہ کا نمبر **:** ________________

شرکت کنندہ کا پتہ **:** _______________________

تاریخ**:** __________________

SUBJECT EVALUATION FORM

Date: ___________ Verbal consent: YES NO

Age: ________________ Gender: ______________________

Medical record #: _________________ Occupation: ___________________

Address: _________________ No. of family members: ______________

Height: ________________ Weight: ______________ Body surface area: _________________

Socio-economic background: ____

Ethnicity: ☐ Sindhi ☐ Punjabi ☐ Balochi ☐ Pashtun ☐ Urdu speaking ☐ Other

Family history of cardiac disease(s): YES NO

If yes, then which disease(s): ____

Smoking: YES NO

Any co-morbidity: ____

Current medication (if any with name & dose) ____

Past medical history (hospitalization/surgeries/transfusion): ________________________________

S. no	Parameters	Measurement 1	Measurement 2	Measurement 3	Average
1.	Annular diameter (long axis view)				
2.	Annular diameter (4-chamber view)				
3.	Annular area				
4.	Anterior leaflet length				
5.	Anterior leaflet thickness				
6.	Posterior leaflet length				
7.	Posterior leaflet thickness				
8.	Intercommissural distance				
9.	C-septal distance				
10.	Interpapillary distance				
11.	Systolic dimensions of left ventricle				
12.	Diastolic dimensions of left ventricle				
13.	Septal thickness				
14.	Posterior wall thickness of left ventricle				

NICVD

NATIONAL INSTITUTE OF CARDIOVASCULAR DISEASES

RAFIQUI (H.J.) SHAHEED ROAD, KARACHI-75510, PAKISTAN
PHONE: 99201271-10 Lines

Dated: February 28, 2024 **Ref #: IRB-18/2024**

To,
Dr. Sabha Bhatti,
Principal Investigator and Professor of Cardiology,
NICVD, Karachi, Pakistan.

Subject: Approval for the study titled: "Evaluation of mitral Valve Dimensions in the Tertiary Cardiac Centre of Karachi."

Dear Investigator,

The Institutional Review Board (IRB) meeting was held on February 28, 2024, to review your application dated: January 29, 2024 for the above mentioned study. We would like to inform you that the IRB has approved this study for being conducted as described in your last submitted protocol (IRB-18/2024).

The following documents were reviewed and approved:

- Study Protocol (version 1.0, submission date: January 29, 2024)
- CRF: Case Report Form (version 1.0, submission date: January 29, 2024)

As per the guidelines, the IRB approves this study from an ethical point of view. Any update or amendments to the study documents need to be forwarded to IRB.

The study can be initiated at National Institute of Cardiovascular Diseases, Karachi. The duration of the IRB approval is for 06 months only from the date of this letter. Kindly submit progress report before expiry of this approval period for any extension in this IRB approval or submit project closure report if the study gets concluded.

Best Regards

(Professor Tahir Saghir)
MBBS, FCPS (Card), FSCAI, FACC
Director Clinical Research
Executive Director &
Chairman Institutional Review Board
Chairman Academic Faculty

Copy to: All co-investigators namely: Dr. Mahail Khan, Dr. Aneel Ahmed, Dr. Aisha Qamar

ORIGINALITY REPORT

14%	6%	12%	1%
SIMILARITY INDEX	INTERNET SOURCES	PUBLICATIONS	STUDENT PAPERS

PRIMARY SOURCES

1	justmed.eu Internet Source	<1%
2	journal.waocp.org Internet Source	<1%
3	"Cardiac Surgery", Springer Science and Business Media LLC, 2017 Publication	<1%
4	Andrew R Houghton. "Making Sense of Echocardiography - A Hands-on Guide", CRC Press, 2023 Publication	<1%
5	Joseph G. Murphy. "Mayo Clinic Cardiology - Concise Textbook", CRC Press, 2018 Publication	<1%
6	"Percutaneous Treatment of Left Side Cardiac Valves", Springer Science and Business Media LLC, 2018 Publication	<1%
7	Simcha Yagel, Norman H. Silverman, Ulrich Gembruch. "Fetal Cardiology - Embryology,	<1%